UNIVERSITY OF CALIFORNIA,
IRVINE

Delivery strategies for the chaperonin subunit domain ApiCCT1 in Huntington's disease

DISSERTATION

submitted in partial satisfaction of the requirements
for the degree of

DOCTOR OF PHILOSOPHY

in Biological Sciences

by

Julia Overman

Dissertation Committee:
Professor Leslie Michels Thompson, Chair
Associate Professor Mathew Blurton-Jones
Professor Charles Glabe

2017

DEDICATION

To my parents: Bill and Rita

You have given me unconditional love and encouragement to further my education. You taught me the value of knowledge and critical thinking and helped mold me into the person I am today. Special thanks to my Dad who meticulously proof read this dissertation.

To my siblings: Justine and Brian

You have serves as role models for me throughout my life and career. I especially thank my sister, Justine, who has provided invaluable career and life advice through every transition.

To my loving and supportive partner: Armin

You have given me the strength and courage to persevere. Thank you for providing words of encouragement, acts of kindness, and for being my pillar of strength as I completed this dissertation.

TABLE OF CONTENTS

LIST OF ABBREVIATIONS

AAV	Adeno-associated virus
AGE	Agarose Gel Electrophoresis
ApiCCT1	Apical domain of the first subunit of CCT
hApiCCT1	Human ApiCCT1
yApiCCT1	Yeast ApiCCT1
BACHD	A full length model of HD
BDNF	Brain-derived neurotrophic factor
CAG	Nucleotide codon encoding the amino acid glutamine
CAGG	A chicken β-Actin promoter coupled with CMV early enhancer
CCT	Chaperonin containing TCP-1 (also called TRiC)
CryoEM	Cryo-electron microscopy
E17	Embryonic day 17
HA	Human influenza hemagglutinin tag
HD	Huntington's disease
His	Polyhistidine tag
Hsp	Heat shock protein, a family of chaperone proteins
HTT	Human huntingtin protein
HTT	The gene encoding human huntingtin protein
IL2ss	Human interleukin 2 secretion signal
mHTT	Mutant human huntingtin protein
mNSCs	Mouse neural stem cells

mNSC-sApiCCT1	Mouse neural stem cells expressing secreted human ApiCCT1
NSCs	Neural stem cells
NT	Non-transgenic
PAGE	Polyacrylamide Gel Electrophoresis
PC12	An immortalized cell lin derived from rat adrenal medulla
PCNs	Primary cortical neurons
PK	Proteinase K
PolyQ	Polyglutamine repeat expansion
PonA	Ponasterone A, induction ligand for 14A2.6 cells
R6/1	An HD transgenic mouse line containing exon1 of the human HD gene with approximately 115 CAG repeats
R6/2	An HD transgenic mouse line containing exon1 of the human HD gene with approximately 150 CAG repeats and showing a more severe phenotype compared to R6/1
TRiC	TCP-1 ring complex (also called CCT)
14A2.6	PC12 cells expressing inducible Httex1
97QP	A GFP-tagged truncated mHTT exon 1 construct containing 97Qs

LIST OF FIGURES

Chapter 3 **Page**

Chapter 4 **Page**

ACKNOWLEDGMENTS

I whole-heartedly thank my advisor, Dr. Leslie Thompson, for her dedicated mentorship, support, advice, and guidance. She gave me the skills to become an effective scientist and the opportunity to grow in ways I never imagined. Leslie's advice, connections, colleagues, and positions opened the door for many professional and training opportunities that have set the stage for a thriving career.

I would also like to thank Dr. Jack Reidling for his mentorship, guidance and assistance in planning and executing many of the experiments in the present dissertation. I would also like to thank Dr. Joan Steffan for her advice, support, and vast knowledge of the HD field, particularly the history of HD research. A conversation with Joan is arguably more valuable than any PubMed search and her vast knowledge will be missed. Thank you to all of the other graduate students, technicians, and undergraduates in our lab. I'd especially like to thank Austin Weld, who worked with me throughout his time as an undergraduate. Thanks to Alice Lau and Sylvia Yeung who worked with my on the mNSC project and helped many times with transplantations. Thanks to Lexi Kopan, who helped with much of the western blot analysis. I'd also like to acknowledge Isabella Sanchez, who I had the pleasure of mentoring during the beginning of her graduate career and has been heavily involved with the CCT project.

This work would not have been possible without input from our many collaborators. I'd like to thank the CCT consortium, especially the Frydman, Housman, and Mobley groups. Thanks to Dr. Ben Deverman for providing virus and his input on Chapter 3 of

this dissertation, Dr. Zhiquin Tan for providing DNA constructs, the Blurton-Jones for providing mouse neural stem cells, and the Green group for advice on histology and microglial morphology.

This work was funded by multiple awards from the National Institutes of Health, including NIH Program Project Grant, NIH nanomedicine Program- CPFM, NIH NRSA, and NIH T32 Training Grant.

CURRICULUM VITAE

JULIA OVERMAN

EDUCATION

2017	Ph.D.	University of California, Irvine School of Biological Sciences Dept. of Neurobiology and Behavior Advisor: Dr. Leslie Thompson
2015	M.S.	University of California, Irvine School of Biological Sciences Dept. of Neurobiology and Behavior Advisor: Dr. Leslie Thompson
2009	B.S.	University of California, Davis Major: Biochemistry and Molecular Biology, with honors

PROFESSIONAL EXPERIENCE

2011-2017 Graduate Student Researcher
University of California, Irvine
Department of Neurobiology and Behavior
Advisor: Dr. Leslie Thompson

2016 Adjunct Instructor
Golden West College
Courses taught: G225, G225L Human Physiology

2009-2011 Staff Research Associate
University of California, Los Angeles
Department of Neurology
Advisor: Dr. Melissa Spencer

2008-2009 Undergraduate Student Researcher
University of California, Los Angeles
Department of Molecular Biosciences
Advisor: Dr. Cecilia Giulivi

HONORS AND AWARDS

2016	Pedagogical Fellowship, Center for Engaged Instruction, UC Irvine, $2,000
2015	Lightning Talk Award, Stem Cell Translational Medicine Training Grant Retreat, UC Irvine
2015	Edward Steinhaus Teaching Award, School of Biological Sciences, UC Irvine, $750
2015	Poster Award, GRC conference for GAG triplet repeat disorders, Italy, $265
2014-2017	National Research Service Award (NRSA), National Institutes of Health (NIH), National Institute of Neurological Disorders and Stroke (NINDS), $33,300 annual
2013-2014	NIH Training Fellowship in Stem Cell Translational Medicine for Neurological Disorders, $30,300 annual
2011	NIH Training Fellowship, UCLA MCIP Graduate Program, $32,000, *Declined*
2009	Outstanding Academic and Research Achievements in Biochemistry and Molecular Biology, UC Davis

SELECTED RESEARCH PRESENTATIONS

2012-2016	Annual Presentation, Neuroblitz, Graduate Research Departmental Symposium, UC Irvine
2015	Selected Speaker, GRC conference for CAG triplet repeat disorders, Lucca (Barga), Italy
2015	Selected Speaker, Regional ABLE (Association for Biology Lab Education) Conference, UC Irvine
2014	Selected Speaker, Orange County Graduate Women in Science, 25th Science Conference, UC Irvine
2014	Invited Speaker, ReMIND 5th Annual Emerging Scientist Symposium, UC Irvine
2010	Selected Speaker, Osteopontin Biology FASEB Conference, Steamboat Springs, CO

PUBLICATIONS

Zhao X, Han E, Hu Y, Chen X, Paik P, Ding Z, **Overman J**, Lau A, Shahmoradian S, Chiu W, Thompson L, Mobley W. TRiC subunits enhance BDNF axonal transport and rescue striatal atrophy in Huntington's disease. *Proc. Natl. Acad. Sci.* **113 ,** E5655–E5664 (2016).

Tan Z., Dai W., van Erp T. G. M., **Overman J**., Demuro A, Digman M., … Potkin, S. G. Huntington's disease cerebrospinal fluid seeds aggregation of mutant huntingtin. *Mol. Psychiatry* 1–8 (2015). doi:10.1038/mp.2015.81

TEACHING EXPERIENCE

2016	**Instructor**, Human Physiology (G225), 96 students, Golden West Community College
2016	**Instructor**, Human Physiology (G225L), 2 sections, 32-34 students, Golden West Community College
2015	**Guest Lecturer**, Anatomy and Physiology (A221), Cherryl Baker, 176 students, Orange Coast College
2015	**Guest Lab Instructor,** Anatomy and Physiology (A221), Cherryl Baker, 32 students, Orange Coast College
2015-2016	**Course Coordinator**, Neurobiology Lab (N113L), 3 quarters, UC Irvine
2015	**Guest Instructor**, Neurodegeneration (N150), Dr. Leslie Thompson, 25 students, UC Irvine
2014	**Guest Lecturer**, Drugs and the Brain (Bio 36), Dr. Andrea Nicholas, 300 students, UC Irvine
2013-2015	**Lab Leader**, Neurobiology Lab (N113L), Behavioral Neuroscience, 4 quarters, UC Irvine
2013-2014	**Instructor/Teaching Assistant**, Neurobiology Lab (N113L), 2 quarters, UC Irvine, 20-24 students
2013	**Teaching Assistant,** Neurobiology and Behavior (N110), 1 quarter, UC Irvine

COMMUNITY AND UNIVERSITY SERVICE

University Service, University of California, Irvine

2017	Graduate Student Representative, Assistant Professor of Teaching Hiring Committee
2016	Pedagogical Fellow and Instructor, TA Professional Development Program (TAPDP)
2015	Invited panelist, Career Exploration Graduate Student Panel, UC Irvine
2015	Invited panelist, Campus-wide New Graduate Student Orientation, UC Irvine
2015	Peer Mentor for Competitive Edge Research Program
2015	Science Fair Judge, Intel ISEF qualifying competition, UC Irvine
2015	Science Fair Abstract Reviewer, Intel ISEF qualifying competition, UC Irvine
2014-2015	Graduate Student Representative, Interdepartmental Neuroscience Doctoral Program, UC Irvine

Community Service

2015	Mentor, H.O.P.E. Mentoring Program, KidWorks, Santa Ana, CA
2014	Tutor, University Starts Now (USN) Program, KidWorks, Santa Ana, CA
2014	Volunteer, Judge, 6th Grade Science Fair, St. Joachim School, Costa Mesa, CA
2011	Volunteer, 7th and 8th Grade Science Student Instructor, Costa Mesa High School, Costa Mesa, CA

MEETINGS ATTENDED

1. Federation of American Societies for Experimental Biology (FASEB) Conference on Osteopontin Biology. Steamboat Springs, CO. (2010)
2. Gordon Research Conference (GRC) for CAG triplet repeat disorders. Waterville Valey, NH. (2013)
3. CHDI HD Therapeutics Conference. Palm Springs, CA. (2014)

4. Regional Association for Biology Lab Endication (RABLE) Conference. Irvine, CA. (2015)
5. Gordon Research Conference (GRC) for CAG triplet repeat disorders. Lucca (Barga), Italy. (2015)
6. Neuroscience 2016. Society for Neuroscience Annual Meeting. San Diego, CA (2016)
7. Drug Information Association (DIA) Medical Affairs and Scientific Communications Forum. Tuscon, AZ. (2017)

ABSTRACTS PRESENTED

1. **Overman J**, Tan Z, Lau A, Joachimiak L, Crook Z, Tomlinson A, Zhao X, Reidling J, Frydman J, Wu C, Mobley W, Housman D, and Thompson L (2016) Therapeutic delivery strategies for the apical domain of CCT1 in Huntington's disease. Society for Neuroscience Annual Meeting.

2. **Overman J**, Sontag E, Lau A, Tran A, Joachimiak L, Tan Z, Tomlinson A, Reidling J, Housman D, Glabe C, Potkin S, Frydman J, and Thompson L (2015) Therapeutic delivery strategies for the apical domain of CCT1 in Huntington's disease. Gordon Research Conference (GRC) for GAG triplet repeat disorders

3. **Overman J**, Javier L, Goldberg N, White A, Boucquey V, Nicholas A (2015) Flipping a Course: Behavioral neurobiology in C. elegans. Regional ABLE (Association for Biology Lab Education) Conference

4. Goldberg N, White A, Boucquey V, **Overman J**, Javier L, Nicholas A (2015) Neurophysiology: Electrical Activity of Neurons. Regional ABLE Conference (RABLE)

5. **Overman J**, Sontag E, Lau A, Tran A, Joachimiak L, Tan Z, Tomlinson A, Reidling J, Housman D, Glabe C, Potkin S, Frydman J, and Thompson L (2014) Chaperonin subunit fragment ApiCCT1 as a novel therapeutic peptide to treat Huntington’s disease. CHDI HD Therapeutics Conference

6. **Overman J**, Sontag E, Lau A, Tran A, Joachimiak L, Tan Z, Tomlinson A, Reidling J, Housman D, Glabe C, Potkin S, Frydman J, and Thompson L (2013) Chaperonin subunit fragment ApiCCT1 as a novel therapeutic peptide to treat

Huntington’s disease. Gordon Research Conference (GRC) for GAG triplet repeat disorders

7. **Overman J**, Kramerova I, Martinez L, Vetrone S, Kudryshova E, Silva O, Miceli C, Spencer M (2010) Osteopontin as a therapeutic target for Duchenne muscular dystrophy. Osteopontin Biology Federation of American Societies for Experimental Biology (FASEB) Conference

ABSTRACT OF THE DISSERTATION

Delivery strategies for the chaperonin subunit domain ApiCCT1 in Huntington's disease

By

Julia Overman

Doctor of Philosophy in Biological Sciences

University of California, Irvine, 2017

Professor Leslie Michels Thompson, Chair

Huntington's disease (HD) is a genetic neurodegenerative disease caused by a polyglutamine (PolyQ) repeat expansion within the Huntingtin (HTT) protein. One of the hallmarks of Huntington's disease is aberrant accumulation and aggregation of misfolded mutant HTT (mHTT), leading to production of large inclusion bodies within cells. While the precise impact of aggregation in HD is not clear, studies suggest that smaller, soluble forms of mHTT accumulation may confer toxicity. The chaperone protein CCT (chaperonin containing TCP-1/TCP-1 ring) binds and folds proteins during *de novo* protein synthesis. Previous studies demonstrated that exogenous delivery of the substrate-binding apical domain of subunit 1 of CCT (ApiCCT1) is sufficient to decrease mHTT aggregation and rescue mHTT-mediated toxicity in multiple cell models of HD, making ApiCCT1 a promising therapeutic for HD. The goal of this dissertation is to evaluate delivery methods of a novel modifier of mHTT accumulation in mouse models of Huntington's disease (HD).

Here, we compare local, striatal viral delivery with global, systemic viral delivery and provide a proof of concept for mouse neural stem cells (mNSCs) as a delivery vehicle. Striatal *in vivo* delivery of ApiCCT1 with a secretion signal (sAiCCT1) targets multiple cell types, likely due to its ability to penetrate the cell membrane in multiple cell types. We find that viral delivery of sApiCCT1 to striatum provides robust expression and can modulate mHTT accumulation and motor phenotypes; however, the *in vivo* studies reported here were complicated by confounding factors. Further, systemic delivery of ApiCCT1 did not appear to ameliorate behavioral or biochemical outcomes in HD mice under the conditions tested. Data from viral studies suggests that ApiCCT1 is not sufficient to overcome disease phenotypes in the presence of additional stressors. Finally, we provide evidence suggesting the mNSCs engineered to secrete ApiCCT1 modulate mHTT accumulation after striatal transplantation, supporting the ability of ApiCCT1 to impact protein accumulation and aggregation. Data presented here provides support for mNSC-mediated delivery of sApiCCT1 as a therapeutic approach for Huntington's disease and elicits important caveats and considerations for future study design involving viral delivery.

CHAPTER 1

INTRODUCTION

Huntington's disease

The focus of this dissertation is to evaluate delivery methods of a novel modifier of mHTT accumulation *in vivo* in mouse models of Huntington's disease (HD). HD is a hereditary neurodegenerative disease that is caused by a polyglutamine (polyQ) repeat expansion in the N-terminal region of the Huntingtin (HTT) protein [4]. HTT is a 350 kDa protein involved in a plethora of cellular functions, including embryonic development, protein homeostasis, axonal and vesicle transport, and BDNF production [5]. Wild type HTT contains 6-35 polyQ repeats [5] whereas expansions above 40 appear to be fully penetrant [6, 7] . PolyQ expansions between 35-39 may lead to development of Huntington's disease with incomplete penetrance.

The HD gene was identified by the HD Collaborative Research Group in 1993 [4]. This study was aided by the large population of HD patients living near Lake Maracaibo, Venezuela. In the rural Venezuelan villages Barranquitas and Laguneta, residents are at an unusually high risk of developing HD [8]. Researchers gathered genetic and clinical data from these patients and others to map the HD gene to chromosome 4 in 1983 [9] and identify the gene itself in 1993 [4]. While the global prevalence of HD is difficult to estimate, studies have suggested that at least 1 in every 10,000 individuals have HD [10, 11], with approximately 16% of all cases being juvenile forms, characterized by polyQ repeat lengths above 60 and onset before the age of 20 [12]. HD manifests in an age-dependent manner, with symptoms typically appearing around mid-life [13].

HD is transmitted in an autosomal dominant manner and results in pervasive neuronal dysfunction and cell death, particularly of the medium spiny neurons within the striatum [8]. HD patients exhibit smaller whole-brain volume, differences in regional grey and white matter, and shrinkage of the cortex [14]. The clinical features of HD are progressive motor dysfunction, cognitive decline, personality changes, psychiatric disturbances, and invariably death, which occurs approximately 15–20 years after disease onset [8, 15]. Characteristic symptoms include chorea, dystonia, bradykinesia, slowed saccadic eye movements, and a lack of coordination. Premanifest HD carriers exhibit significant changes in whole-brain volume, with striatal atrophy detected up to 15 years prior to disease onset [16-18]. HD patients often show cognitive and personality changes as a first sign of disease onset [19]. HD patients are at an increased risk for depression and are 5–10 times more likely to commit suicide, regardless of HD status awareness [20]. Patients often show some, but not all of these symptoms, therefore the manifestation of disease phenotypes can vary between patients [21].

Although the gene was discovered over 2 decades ago, there are currently no disease-modifying treatments for HD. Current treatment strategies alieve symptoms of the disease rather than the disease pathology itself. Commonly prescribed treatments are tetrabenazine, antipsychotic drugs, and dietary and lifestyle changes. Tetrabenine (Xenazine) and it's isomer Deutetrabenazine (Austedo), used for the treatment of chorea symptoms, are reversible inhibitor of vesicle monoamine transporter type 2 (VMAT2), inhibiting the uptake of monoamines including serotonin, norepinephrine, and dopamine [22]. Tetrabenazine was approved by the FDA in 2008 and Deutetrabenazine was approved earlier this year. Tetrabenazine is reported to reduce symptoms of

chorea by approximately 25% and is widely prescribed and while it is generally well tolerated, it is associated with increased fatigue, nausea, and can even aggravate suicidal and depressive behaviors [23]. Antipsychotics, or dopamine antagonists, are frequently prescribed to treat both psychological and motor symptoms of HD. Treatment approaches using antipsychotics are varied and adverse effects range from dry mouth to depression. The adverse effects of these drugs often lead patients to manage their symptoms with lifestyle changes, including dietary changes and stress management. While these approaches may improve quality of life for HD patients, therapies that change or reverse the course of the disease are essential.

Protein misfolding and accumulation in neurodegenerative diseases

A pathological hallmark of HD is accumulation and aggregation of misfolded mutant huntingtin protein (mHTT), ultimately resulting in intranuclear and cytoplasmic inclusions within neurons and neurite processes [24, 25]. Nucleation-dependent polymerization of misfolded peptides leads to formation of intermediate soluble oligomers, fibrils, and eventually large, insoluble inclusion bodies [26]. Amyloid fibrils are one of the defining characteristics of protein misfolding neurodegenerative diseases and contain a highly ordered, cross-β structure with a series of repeating β-sheets organized ‘in register’ that are arranged perpendicular to the fibril axis [27, 28]. Misfolded mHTT assembles into soluble conformations, or oligomers, before becoming fibrils. Oligomeric conformations are heterogeneous in both structure and size. This heterogeneity has presented a challenge in characterizing oligomeric species and much research focuses on defining the structural and functional characteristics of oligomeric species [29]. Several

oligomeric mHTT species are found to be immunologically distinct and can be distinguished by conformation-specific antibodies [1]. Figure 1 represents a schematic of the aggregation pathway representing some of the detected mHTT conformations.

Protein misfolding and accumulation is often viewed as a driver of toxicity as formation of visible mHTT aggregates correlates with timing of pathogenesis and occurrence of toxic cellular events [24, 25, 30, 31]. One of the early findings linking aggregation to toxicity was in 1999, when the Wanker group [32] found that the rate of insoluble aggregate formation correlates with polyQ length and also disease severity. It was subsequently found that visible mHTT aggregates are not tightly correlated with cell death. For example, YAC72 mice, a full-length mHTT model of HD, show degeneration of medium spiny neurons prior to appearance of visible mHTT aggregates [33]. Most notably, neuronal cell death in cultured striatal neurons expressing mHTT is inversely proportional to inclusion body formation. Arrasate et al. [30] showed that, when tracking a single neuron over time, cell death is more highly correlated with diffuse intracellular mHTT expression than with insoluble aggregates, suggesting that inclusion body formation may serve as a compensatory mechanism [30]. Indeed, several studies have linked soluble accumulated species to cytotoxicity [34-37]. Because oligomers are structurally heterogeneous, some hypothesize that their heterogeneous nature enables exposure of interaction-prone hydrophobic surfaces, a feature that may contribute to toxicity [38, 39]. Furthermore, oligomers are shown to engage in aberrant interactions that interfere with multiple cellular processes, including synaptic plasticity, RNA binding, and signaling pathways [39, 40].

All of the known polyglutamine (polyQ) disorders, including HD, spinal bulbar muscular atrophy (SBMA), dentatorubral-pallidolutsian atrophy (DRPLA), and the spinocelebellar ataxias (SCA), are characterized by a toxic gain of function from the mutated protein [31]. More recent work suggests that for each disease, there is also a contribution derived from some loss of normal protein function. Each, except SCA6, show the same pathological threshold of 36-40Qs [41] and the length of polyQ expansion correlates with the propensity of aggregate formation in HD patients [42]. The various polyQ disorders affect different specific subtypes of neurons, resulting in distinct patterns of neurodegeneration and different clinical features for each disorder [43]. Further, other neurodegenerative diseases such as Alzheimer's disease (AD), Parkinson's disease (PD), and Amylotrophic Lateral Sclerosis (ALS) also exhibit accumulation of misfolded, amyloid proteins [44]. Amyloid fibril aggregates are characterized by highly ordered, β-sheet rich fibrils that form a ribbon-like structure [5] and emerging evidence suggest that these amyloid aggregates potentially propagate via a prion-like mechanism [45-48]. Although all these diseases manifest phenotypes differently, the similarities between them, in terms of amyloid accumulation, suggest that misfolding and accumulation of the mutated protein may be an important contributor to neurodegeneration.

Indeed, many studies suggest that interfering with protein accumulation and aggregation, resulting in readouts of reduced protein aggregation, is neuroprotective. For instance, several small molecules that inhibit polyQ aggregation in cells showed a significant protection against polyQ-dependent toxicity in drosophila models [49]. Given that reduction of mHTT expression in HD mice results in disappearance of inclusions and reversal of behavioral phenotypes, strategies to increase degradation of mHTT are

likely to inhibit or reverse disease progression [50]. A handful of studies have shown that molecules that target mHTT or mHTT accumulation improve behavioral outcomes in HD models. Results from the Thompson group indicate that intrastriatal knockdown of PIAS1, an E3 ligase that also regulates mHTT accumulation, ameliorates behavioral phenotypes and mHTT accumulation in a rapidly progressing, R6/2 HD mouse model [51]. Congo red, a dye that binds to amyloid β-sheets, inhibits polyQ oligomerization and improves behavioral outcomes in R6/2 mice, even when given *after* symptom onset [52]. Perhaps the most convincing evidence supporting therapeutics targeting mHTT is the recent developments in HTT lowering studies [53]. Both antisense oligonucleotide (ASO) [54, 55] and RNA interference (RNAi) [56] mediated knockdown of HTT rescue disease phenotypes in animal models. These therapies reduce HTT expression at the level of mRNA [57], and thus prevent mHTT expression and accumulation. An ASO developed by the pharmaceutical companies Ionis and Roche, termed IONIS-HTTRx, is currently in Phase 1/2a clinical trials for safety and tolerability in HD patients (clinical study ISIS-443139-CS1). Toxicology studies performed in rodents and non-human primates suggest that intrathecal infusion of IONIS-HTTRx is well tolerated [54], and this therapy has the potential to become the first approved disease-modifying therapy for HD. Together with evidence linking mHTT accumulation to toxicity, these studies indicate that targeting the mHTT protein itself may be a valuable approach to treating HD.

Models of Huntington's disease

Because HD is a genetic disorder, it is possible to generate model systems by mutating the *HTT* gene. The polyQ expansion is contained in exon1 of HTT and studies show that truncated exon1 aggregates more readily and produces a more rapidly progressing disease phenotype than full length HTT [58]. Researchers have generated cell, mouse, and invertebrate models that express full length mHTT or mHTT fragments and mimic various aspects of HD pathology. This dissertation utilizes mammalian neuronal cell and mouse models to recapitulate HD biology in neuronal settings.

Cell Models

Many HD cell models have been developed since the discovery of the HD gene. Cell models can be used to evaluate therapeutic targets as well as identify specific pathways or pathogenic mechanisms on a cellular level. Engineered cell lines can produce disease phenotypes that range in severity depending on the length of the repeat, length of mHTT construct, and cell type. A variety of cell lines of neuronal lineage or that can be differentiated to neurons have been developed to express stable, transient, or inducible forms of mHTT and allow researchers to study HD phenotypes in a neuronal context [59, 60]. Inducible mHTT expression offers the added benefit of being able to turn on expression of mHTT at specified time points. The Thompson group has developed one such inducible cell line in rat phaeochromocytoma (PC12) cells, a neuronal-like cell model, expressing a truncated mHTT exon1 with 103Qs in a hybrid ecdysone inducible system [61]. This cell line, 14A2.6, shows robust aggregation upon mHTT induction and offers an effective method to study mHTT accumulation. Primary

cortical neurons (PCNs) or striatal neurons (PSNs), isolated from embryonic mice, offer alternative methods to study mechanisms in an *ex vivo* context. For the purposes of studying mHTT accumulation, primary neurons from wild-type mice can be transduced with GFP tagged, truncated mHTT exon1, which accumulates readily *in vitro* [62]. Both 14A2.6 cells and PCNs have been used to characterize modifiers of mHTT accumulation [62-64].

The use of induced pluripotent stem cells (iPSCs) is an emerging resource for a variety of fields. iPSCs offer a clinically relevant model as these cells are derived from human fibroblasts and recapitulate the endogenous genomic context [65, 66]. The technology to induce pluripotency in fibroblasts was first reported in 2006 [67]. Over the last decade, much research has focused on utilizing this technology to develop models for a variety of diseases, including HD [68], using patient-derived lines. Neuronally differentiated iPSCs from HD patients are found to have transcriptional changes in genes associated with neuronal development, axonal guidance, and electrophysiology, among others [69, 70]. Furthermore, the Thompson group recently described the use of differentiated iPSCs as a model for blood brain barrier (BBB) dysfunction in HD [66]. Together with data from a number of other laboratories, iPSCs are quickly becoming an effective and efficient method of studying HD in a dish.

Mouse Models

Mouse models are a critical part of preclinical therapeutic research. HD mouse models can generally be divided into three categories: N-terminal fragment transgenic models, full-length transgenic, and knockin models (Fig 2) [3]. R6/1 and R6/2 mice (both

fragment models) express exon 1 of the human HTT gene with an expansion of approximately 115 and 150 CAG, respectively, on a C57BL/6 background [71]. Fragment models tend to have the earliest disease onset and show robust HD phenotypes, including mHTT accumulation [3]. Fragment models are used in the following described studies to evaluate a modifier of HD accumulation.

R6/2 HD transgenic mice are a widely used model in HD research. These mice show a very rapid and reproducible disease progression, with intranuclear inclusions developing very early on (4 weeks) and behavioral deficits and transcriptional changes as early as 6 weeks of age. R6/2 show decreased expression of disease-associated genes including DARPP-32, a marker of medium spiny neurons, and DRD2, a dopamine receptor that is highly expressed in the striatum [72, 73]. Mice eventually develop resting tremors, dystonic attacks, gait abnormalities, metabolic irregularities, an inability to coordinate locomotor movement, lack of coordination, and excessive weight loss, leading to death at a very early age (~12–14 weeks). R6/1 mice show a slightly less severe phenotype, with lifespans up to a year [71]. Motor abnormalities begin around 3–4 months; however, these mice show downregulation of caudate-specific genes beginning at 10 weeks of age [74]. Both R6/1 and R6/2 are used in the following studies. The benefit of using the R6/1 mouse is that it has a slower progression relative to the R6/2 mouse and therefore allows us to deliver therapeutics earlier in the disease progression as well as over a longer period of time. However, R6/2 mice are arguably the best characterized and allow for rapid testing of therapeutics due to their rapidly progressing phenotypes [75].

Full-length transgenic models (e.g. BACHD and YACHD), which express the entire HTT

protein as a transgene, showed delayed motor symptoms and reduced pathology compared to fragment models [33, 76], and have also been widely used.. Knockin models (e.g. Hdh150), where a CAG expansion is introduced into the endogenous *HTT* gene, tend to show the slowest-progressing phenotypes [3], but arguably model the human condition most accurately. Fragment models are often used as a first step in investigating a new therapy due to their rapid disease onset and severe phenotype. Full-length and knockin models can be used as a later step in preclinical validation of therapeutic targets. All of these models have individual benefits that are well suited to model a variety of aspects of the human HD condition [3]. This dissertation will use the R6/1 and R6/2 strains to as they are well-characterized and serve to model mHTT accumulation in an *in vivo* context.

Chaperone proteins in protein misfolding diseases

Chaperone proteins are potential targets for protein misfolding diseases [77, 78] due to their ability to facilitate the folding of newly synthesized or misfolded proteins, prevent protein aggregation, and facilitate degradation [44]. Molecular chaperones are defined as ‘any protein that interacts with and aids in the folding or assembly of another protein without being part of its final structure’ [38]. Figure 3 shows a schematic representation of the role of chaperone proteins in native state folding and prevention of protein accumulation. Molecular chaperones work to both prevent misfolding, by facilitating normal protein folding, and to prevent protein accumulation by preventing aberrant intermolecular contacts [2, 44]. Many chaperons are stress proteins, or heat shock proteins (Hsp), which are up-regulated under conditions of stress presumably to refold

proteins affected by stress-induced structural instability [38]. There is evidence that chaperone protein levels are decreased with normal aging, which may explain the age-related component of many neurodegenerative diseases [79, 80]. In HD, protein levels of molecular chaperones, including Hsp70, are reduced by up to 40% at the end stage of disease in R6/2 [81]. For this reason, a variety of chaperone proteins have been investigated as potential therapeutic targets for multiple neurodegenerative diseases, including HD.

Chaperone proteins Hsp 40, 70, and 90, which are named according to their molecular weight [38], have been extensively studied in relation to polyQ disorders. For example, treatment of polyQ expressing cells with geldanomycin, a potent inducer of Hsp40 and Hsp70 led to a significant decrease in polyQ aggregation [82]. Several groups have shown that over-expression of Hsp70 [83-85] or Hsp40 [83-89] suppresses polyQ aggregation in cell cultures and that overexpression of both proteins is cumulative in aggregate suppression. Increased cell survival with overexpression of chaperones has been reported by several groups [83, 90, 91]. Importantly, mouse models of the polyQ diseases SCA1 and SBMA showed behavioral and pathological improvements when mice were bred to overexpress Hsp70 [78, 92]. Overexpression of Hsp70 in R6/2 delays the formation of nuclear inclusions by 1 week; however, there is no difference in mHTT aggregation at 4 weeks and no improvement in behavioral tasks [81]. While overexpression of Hsp 40, 70, and 90 may provide generalized support for the proteome, this dissertation focuses on the chaperone protein CCT (chaperone containing TCP1), which interacts directly with HTT [93], to target the disease-causing protein.

CCT, also known as TRiC (TCP1 ring complex), is an ATP-dependent hetero-oligomeric chaperonin that binds and folds proteins during *de novo* protein synthesis [94]. CCT is a member of the chaperonin family of molecular chaperones, which is defined by a characteristic double-ring structure [38]. ATP-dependent conformation changes create a barrel-shaped hydrophilic central cavity where non-native proteins are able to refold into native conformations while in a protected environment [95]. Each CCT subunit consists of three distinct domains. the equatorial domain, which binds and hydrolyses ATP, the apical domain, which contains the substrate binding site, and the intermediate or hinge domain, which connects the equatorial and apical domains [96]. The majority of sequence variation between the subunits is within the apical domains, which are important for substrate recognition [97]. CCT differs from other chaperonins in that it does not require a co-factor to act as a 'lid', but has a built-in lid to encapsulate proteins [98]. ATP-induced conformational changes allow CCT to encapsulate proteins within the folding chamber via an iris-like lid closure. Flexible protrusions from each of the subunits acts as a lid, closing in an ATP-dependent and iris-like manner. The size limit of the folding chamber is ~70kDa, but this unique lid closure allows CCT to partially encapsulate proteins [38], which is likely what enables CCT to refold many large, cytosolic, and structural proteins including actin, tubulin, and HTT.

The hetero-oligomeric nature of CCT allows it to promote folding in a very broad range of protein substrates. Indeed, CCT interacts with 5-10% of all cytosolic proteins, one of which is HTT [93, 99, 100]. Recently published studies also indicate a role for CCT in autophagy [101]. Pavel, et al. [101] showed that CCT function is required for autophagosome degradation. Additionally, their results suggest that protein

accumulation is a consequence of autophagy inhibition more so than a loss of anti-aggregation activity of CCT [101]. This is particularly relevant as autophagy is reduced in HD and protein clearance is directly impaired by mHTT expression [102]. The role of CCT in autophagy is just beginning to be elucidated, but this study suggests a dual role for CCT in protein misfolding disease.

In 2004, six of the eight CCT subunits were identified as regulators of mHTT aggregation in a genome-wide RNAi screen in C. elegans [103]. Subsequent studies found that over-expression of the first subunit of CCT (CCT1) prevent mHTT aggregation in models of HD [90, 93, 104, 105], making CCT components a promising therapeutic target.

ApiCCT1 in Huntington's disease

Because the apical domains contain the binding substrate site, researchers purified the apical domain of CCT1 to determine if the HTT binding domain alone could affect mHTT accumulation [105]. The apical domain of CCT1 (ApiCCT1) binds directly to the first 17 amino acids of HTT, a domain that is critical to mHTT aggregation [93, 106, 107]. Previous studies demonstrated that over-expression of ApiCCT1 is sufficient to suppress mHTT aggregation in *in vitro* aggregation assays [93, 105]. Our group and collaborators showed that exogenous delivery of recombinant, purified ApiCCT1 ($ApiCCT1_r$) protein is sufficient to reduce the formation of potentially toxic fibrillar oligomers and insoluble mHTT in PC12 cells and suppress mHTT-mediated toxicity in a knockin cell model of HD [63]. Surprisingly, exogenous delivery of $ApiCCT1_r$ not only

enters the cells, but is also detected in the nucleus following cell fractionation. This finding is particularly relevant as accumulation of nuclear mHTT contributes significantly to mHTT toxicity [108]. The ability of ApiCCT1 to penetrate cell membranes circumvents complex methods to express the protein intracellularly, and suggests that introducing ApiCCT1 to the extracellular environment will be sufficient to modulate intracellular phenotypes.

CryoEM studies reveal that in the presence of the CCT complex, mHTT fibril formation is delayed and fibrils that do appear are smaller. CryoEM visibly confirms that CCT both interacts with soluble mHTT and binds to the tips of mHTT fibrils to prevent elongation, effectively capping mHTT fibrils [100]. Because the apical domain of CCT1 binds mHTT, it is likely that at least one mechanism of ApiCCT1 action is to prevent aggregation through capping mHTT fibrils and also sequestering monomeric or soluble mHTT, both preventing further aberrant interactions. This is supported by the observation that we find a reduction in the size and quantity of fibrillar oligomers and reduced inclusions when ApiCCT1$_r$ is delivered *in vitro* [63].

These observations lead to the hypothesis that delivery of ApiCCT1 may be an effective therapeutic strategy to reduce accumulation of misfolded and aggregated mHTT. Furthermore, because ApiCCT1 can enter cells, secreting ApiCCT1 into the extracellular space may enable ApiCCT1 to modulate intracellular phenotypes in neighboring cell populations. We have generated a construct encoding ApiCCT1 with a human interleukin 2 secretion signal peptide (IL2ss). This enables partial secretion of ApiCCT1. When this construct is transcribed, a portion of the mRNA should be directed to membrane-bound polysomes (MBP) for translation. The nascent signal peptide can

be recognized by the signal recognition particle (SRP) and translocated to the endoplasmic reticulum (ER) and enter the secretory pathway [109]. The IL2ss directs approximately 37% of the translated protein to the secretory pathway [109].

One of the challenges of treating neurodegenerative diseases is delivering therapeutics to the brain as many molecules are not able to cross the blood brain barrier. This dissertation first investigates two viral delivery approaches to supply secreted ApiCCT1 (sApiCCT1) to the brain in HD mouse models. We subsequently investigate engineered stem cells as a delivery mechanism. Stem cells can be engineered to secrete proteins and therefore provide continuous delivery of sApiCCT1.

Stem cells as a therapy for neurodegenerative diseases

Stem cell-based transplantation is emerging as a potentially effective therapeutic strategy for neurodegenerative diseases, including AD [110, 111] and HD [112]. In AD mouse models, mouse neural stem cell (NSC) transplantation improves cognition without affecting Aβ plaque and neurofibrillary tangle pathology [110] and neural stem cell transplantation rescues cognitive and motor impairments in PD mouse models [113]. Human neural progenitor cells engineered to secrete the neurotrophic factors BDNF, IGF-1 or GDNF provide protection against Aβ toxicity in cell culture [111]. Importantly, one study found that human neural stem cell transplantation in a lesion model of HD produced significant behavioral improvements and provided protection against striatal loss caused by quinolinic acid (QA) lesion [112]. Our lab has tested non-engineered stem cells for therapeutic effects in HD and we find that striatal

transplantation of mouse neural stem cells (mNSCs) and human NSCs can each provide neuroprotection in R6/2 HD mice, ameliorating motor deficits altering biochemical changes elicited by mHTT [manuscript submitted]. The effects by the human NSCs appear to be mediated through increased neurotrophic signaling pathways (e.g. BDNF), but there is also a significant decrease in accumulated mHTT.

Clinical use of fetal stem cells to treat neurodegeneration to date has shown limited success. Fetal nerve cell transplants show short term success in both PD and HD patients [91, 114], with transplants developing disease-like pathology years after engraftment within a patient's host brain. While there is some initial improvement, many PD patients experience motor dysfunction five or more years after transplantation, with some patients exhibiting PD pathology in transplanted tissue [91]. HD patients that received neural transplants show marginal clinical improvements lasting approximately 2 to 4 years; however, there is at least one reported case of long term clinical improvement [115]. Autopsy results from a handful of HD patients who had undergone fetal cell transplantation a decade earlier reveal that grafts appear to undergo neuronal degeneration in a disease-like manner [114]. Further research by the same group characterized the spread of mHTT from the host tissue to the genetically normal material and found that mHTT is primarily localized to the extracellular matrix in transplanted tissue [116]. In this dissertation, we provide a proof of concept for neural stem cells as a delivery vehicle for sApiCCT1. One of the benefits of this approach is that it may prevent transplanted stem cells from acquiring HD phenotypes as ApiCCT1 is shown to prevent mHTT accumulation and other HD phenotypes in multiple models [63, 93, 100, 105].

Stem and fetal cell transplants like those described above were initially intended as a cell replacement therapy. It has since been discovered that the primary beneficial effect may likely be through secretion of neurotrophic factors [110], versus neuronal replacement. This neuroprotective effect may be negated once the tissue develops pathology as mHTT alters transcription and trafficking of the neurotrophic factor BDNF [5]. This could explain why patients may not experience long-term improvements in clinical outcomes upon transplantation. Therefore, combining the therapeutic effects of stem cell transplantation with a molecule to target disease pathology (e.g. ApiCCT1) may prevent or delay injected stem cells, as well as surrounding host tissue, from developing disease phenotypes. Using stem cells to deliver therapeutic molecules may offer an improvement over stem cell transplantation alone and serve as a promising combination therapy.

Data presented in this dissertation serves to characterize a novel modifier of mHTT accumulation *in vivo* and supports *in vivo* efficacy of sApiCCT1 as a potential disease-modifying therapeutic target for Huntington's disease. We provide evidence that ApiCCT1 can improve behavioral and biochemical readouts of disease when locally delivered to the striatum depending on the delivery paradigm. Our data is consistent with the hypothesis that ApiCCT1, when injected into the striatum, may act to prevent accumulation of mHTT and therefore delay onset of HD phenotypes. We also investigated systemic delivery of ApiCCT1. To our surprise, systemic delivery of ApiCCT1 did not modify mHTT accumulation. It is not yet clear whether this is due to systemic expression of ApiCCT1 itself or whether due to the high levels of virus, in this case a modified AAV9. Finally, we provide a proof of concept for stem cell mediated

delivery of sApiCCT1 and find that mice transplanted with mNSCs expressing secreted ApiCCT1 (mNSC-sApiCCT1) exhibit reduced mHTT accumulation compared to mNSCs alone.

CHAPTER 1

FIGURES

Figure 1.1

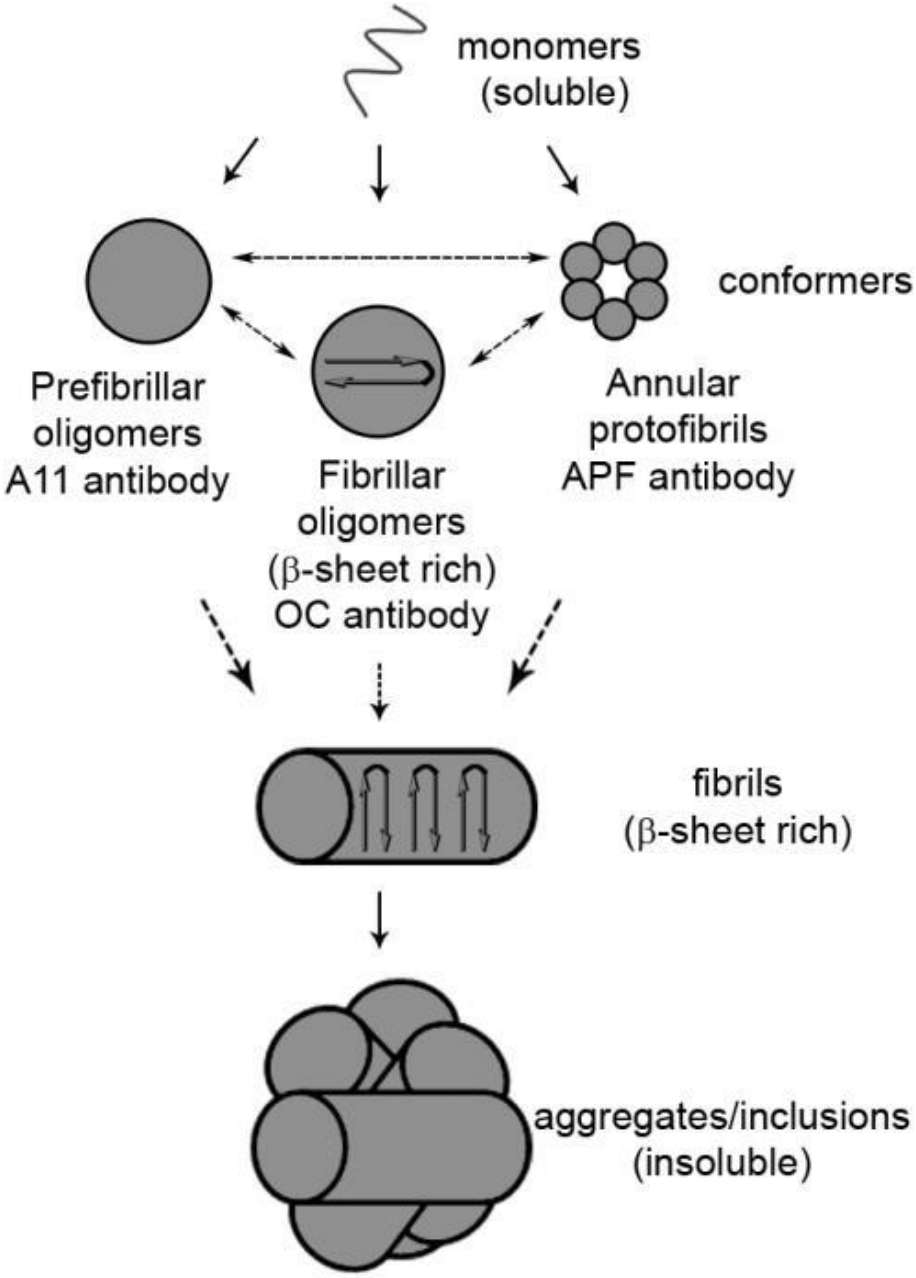

Figure 1. Schematic illustration of the possible conformations of accumulated mHTT. Misfolded mHTT proteins can accumulate into various conformations. Prefibrillar oligomers, fibrillar oligomers, and annular protofibrils are found to be immunologically distinct. The precise interaction between all of these conformations is not yet known; however, it is clear that soluble oligomers precede fibril and inclusion formation. Dashed arrows indicate unknown interactions between conformations. Figure adapted from [1].

Figure 1.2

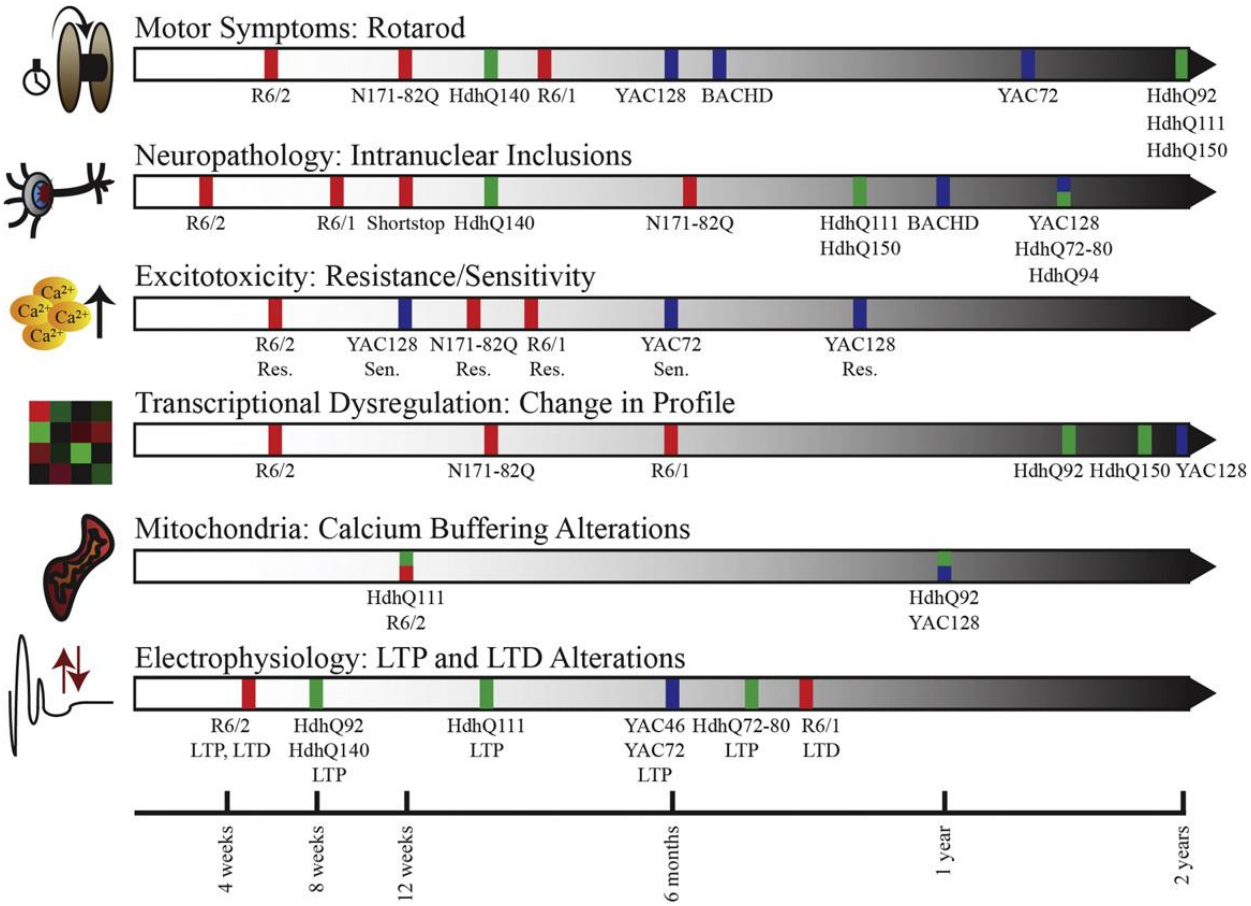

Figure 2. Timeline of Behavioral and Neuropathological Symptoms in Selected HD Model Mice. Strains are categorized by color: red indicates N-terminal transgenic, blue indicates full-length transgenic, and green indicates knockin. Figure adapted from [3].

Figure 1.3

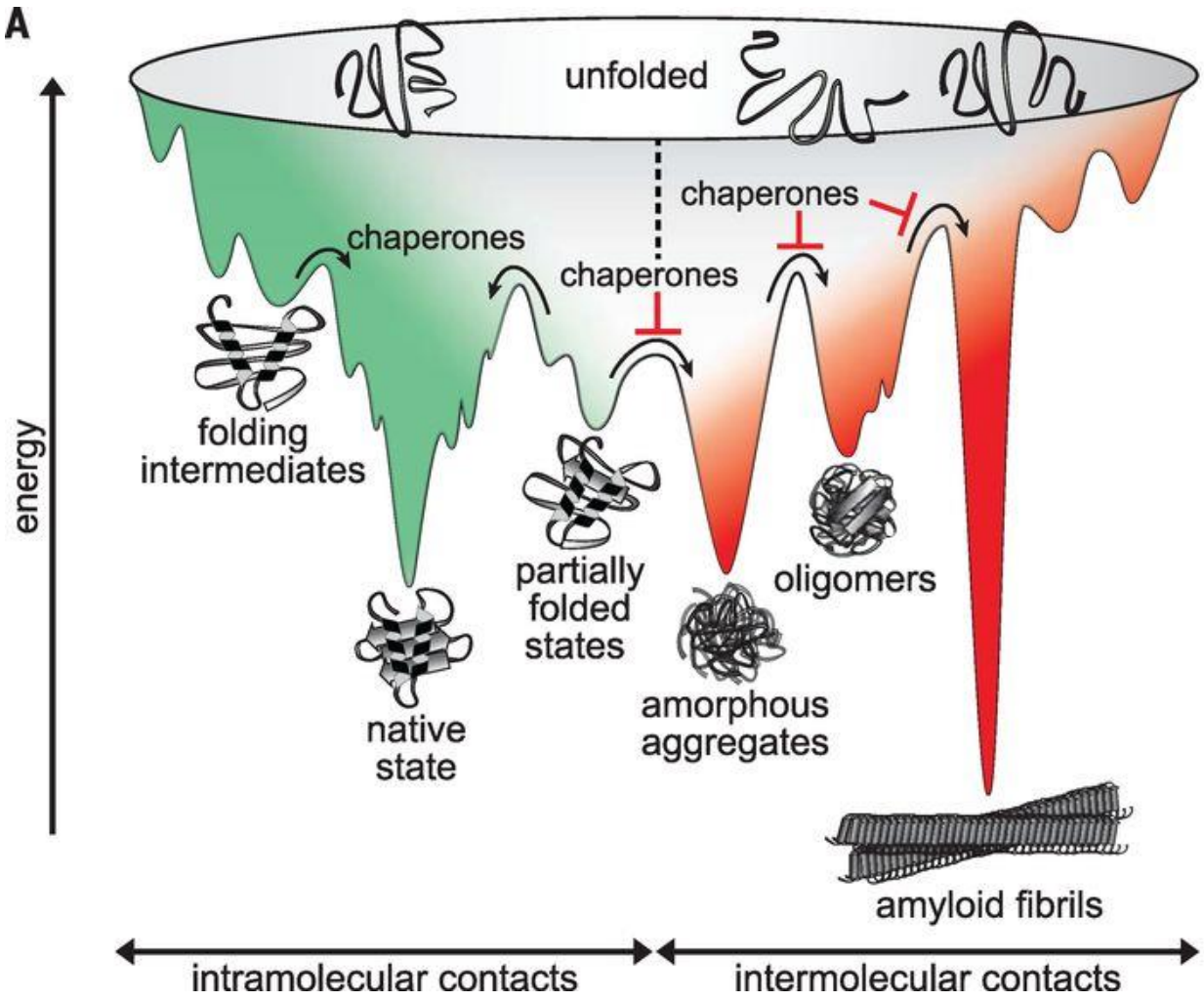

Figure 3. Energy landscape of protein misfolding, aggregation, and chaperone interactions. During folding, protein molecules travel downhill to lower energy states. Thermodynamic favorability of conformations is represented by the depth of the well. Green represents conformations facilitated by intramolecular contacts and red represents conformations characterized by intermolecular contacts (aka accumulation of proteins). Chaperones facilitate native state folding and prevent aberrant intermolecular interactions. Figure adapted from [2].

CHAPTER 2

Evaluation of striatal delivery of the chaperonin subunit domain ApiCCT1

Summary

Chaperone proteins are potential therapeutic targets for protein misfolding diseases, in part, due to their ability to modulate protein misfolding and prevent protein aggregation. The apical domain of the first subunit of the chaperonin CCT (ApiCCT1) binds to the N-terminal region of Huntingtin (HTT) and reduces accumulation. Here, we evaluate AAV2/1 viral-mediated and purified protein delivery of ApiCCT1 in the striatum of HD mice. We find that ApiCCT1 with a secretion signal can be taken up by multiple cell types, likely due to its ability to penetrate the cell membrane of neighboring cells. We find that sApiCCT1 can modulate mHTT accumulation in one viral study. However, in the second larger cohort with viral delivery, no effect on accumulation was observed, likely due to confounding factors including a different inflammatory response. Data presented here shows that delivery of sApiCCT1 is promising as a potential therapeutic for HD; however, additional testing and development is necessary.

Introduction

Huntington's disease (HD) is a progressive neurodegenerative disease characterized by protein misfolding, leading to aggregation and the accumulation of insoluble protein aggregates [5]. HD is caused by a polyglutamine (PolyQ) expansion in exon 1 of the Huntington protein (HTT) and results in neuronal dysfunction with extensive tissue loss, particularly affecting the medium spiny neurons in the striatum. HD leads to motor impairments, cognitive deficits, personality changes, and invariably death [15]. Misfolding of mutant HTT (mHTT), resulting in protein accumulation and subsequent

neurodegeneration, is a key feature of the disease. While the consequences of aggregated mHTT are not clearly defined, the formation of mHTT accumulation temporally correlates with occurrence of toxic cellular events [24, 25, 30, 35, 36]. More specifically, several studies have linked accumulation of soluble species to cytotoxicity [34-37] and provide evidence that oligomeric forms engage in aberrant interactions that interfere with cellular processes, including synaptic plasticity, RNA binding, and signaling pathways [39, 40]. This study seeks to evaluate a potential therapy that targets this mHTT accumulation.

Chaperone proteins, which facilitate the folding of newly synthesized proteins and refolding of misfolded proteins, are candidate molecules for altering mHTT aggregation due to their ability to prevent protein aggregation and facilitate degradation [44, 77, 78]. CCT, also known as TRiC (TCP1 ring complex), is an ATP-dependent hetero-oligomeric chaperonin that binds and folds proteins during *de novo* protein synthesis [94]. CCT is a member of the chaperonin family of molecular chaperones, and consists of 8 subunits [38]. Each CCT subunit consists of three distinct domains. The equatorial domain, which binds and hydrolyses ATP, the apical domain, which contains the substrate binding site, and the intermediate or hinge domain, which connects the equatorial and apical domains [96]. The present study focuses on the apical domain of one of the subunits.

CCT interacts with 5-10% of all cytosolic proteins, one of which is HTT [93, 99, 100]. Previous studies show that overexpression of the first subunit of CCT (CCT1) prevents mHTT aggregation in models of HD [90, 93, 104, 105], making CCT1 a promising therapeutic target. The apical domain of CCT1 binds directly to mHTT [93] and addition of just the apical domain of a single subunit of CCT (ApiCCT1) decreases aggregation

of mHTT in *in vitro* aggregation assays [93, 105]. ApiCCT1 binds the N-terminal region of mHTT, a region that is critical for mHTT aggregation [93, 100, 105-107]. In microfluidic chamber co-cultures, exogenous addition of recombinant, purified ApiCCT1 ($ApiCCT1_r$) restored BDNF transport and prevented striatal neuronal atrophy in cultured striatal neurons from BACHD mice [64]. Our group and collaborators showed that exogenous delivery of $ApiCCT1_r$ protein also is sufficient to reduce the formation of potentially toxic fibrillar oligomers and insoluble mHTT in PC12 cells and suppress mHTT-mediated toxicity in a knockin cell model of HD [63]. Sontag, et al. [63] showed that $ApiCCT1_r$ not only penetrates the cell membrane of PC12 cells, but can also enter the nucleus following cell fractionation. This finding is particularly relevant as accumulation of nuclear mHTT contributes significantly to mHTT toxicity [117, 118]. Because ApiCCT1 can penetrate the plasma and nuclear membranes, this circumvents the need to express the protein within each affected cell. We can instead express ApiCCT1 within a subset of cells and subsequently affect a larger population. For the present study, we utilized a secreted form of ApiCCT1 (sApiCCT1) to enable secretion into the extracellular space and uptake by neighboring cells. We chose to use human interleukin 2 (IL2ss). This secretion is partial [119] (exhibiting 37% activity relative luciferase control [109]), thus the protein is both secreted by the cell and expressed within the cell .

Previous studies show that ApiCCT1 is protective against mHTT toxicty and reduces mHTT accumulation in multiple cell models [63, 93, 100, 105]; however, it has not yet been studied *in vivo*. CryoEM studies indicate that CCT binds to both monomeric and fibrillar mHTT, effectively targeting both early and late stage mHTT accumulation [100].

In this dissertation, we find that ApiCCT1 can modulate mHTT accumulation and improve behavioral outcomes in HD mice; however, confounding factors in one study lead to inconsistencies between biochemical readouts. Therefore, the results are promising that delivery *in vivo* may be efficacious; however, additional experimentation will be needed in future studies.

RESULTS

ApiCCT1$_r$ is Taken Up by Primary Cortical Neurons Following Exogenous Delivery. CCT interacts directly with mHTT and can modulate protein misfolding and accumulation [100]. Previous work has shown that purified, recombinant ApiCCT1 (ApiCCT1$_r$) is taken up by PC12 cells, an immortalized cell line derived from rat medulla [120], following exogenous delivery [63]. Here, we find that ApiCCT1$_r$ is also taken up by primary cortical neurons (PCNs), an important consideration when transitioning to *in vivo* studies as the *ex vivo* PCNs more accurately mimic the *in vivo* environment.

PCNs were isolated from E17 mice and treated exogenously with either yeast or human ApiCCT1$_r$. Lysates were fractionated into total, cytoplasmic, and nuclear fractions. Fractionated samples were analyzed by SDS-PAGE followed by western blot (Fig 1). Blots were probed with anti-His antibody (ApiCCT1$_r$), anti-GAPDH (cytoplasmic marker), and anti-p84 (nuclear marker). Consistent with previous findings, a large portion of ApiCCT1$_r$ remains in the media. Each of the intact fractions was treated with proteinase K (PK) prior to lysis to degrade any proteins outside of the membrane in order to only detect proteins that have crossed the plasma or nuclear membrane (Fig. 1, red box).

ApiCCT1$_r$ is found in all three fractions for both yeast and human in both PK- and non-PK-treated samples. It is noteworthy that our nuclear marker is absent from PK-treated groups, which may be due to overtreatment with PK. Even with high PK treatment, ApiCCT1 is still found within the nuclear fraction. This may indicate that P84 is more easily degraded compared to ApiCCT1. Regardless, this result suggests that ApiCCT1 is able to penetrate plasma and nuclear membranes in neurons. Here, we show that both yeast and human ApiCCT1$_r$ are able to enter PCNs when added exogenously to the media. These findings support the rationale that extracellular ApiCCT1$_r$ could be taken up by neuronal cells *in vivo*. The finding that human ApiCCT1$_r$ (hApiCCT1) enters PCNs (Fig. 1B) was published by us and collaborators last year in PNAS, where Zhao, et al. report that exogenous hApiCCT1$_r$ enters cells and rescues BDNF transport in BACHD cortical neurons [64]. The studies presented in this dissertation utilize human ApiCCT1$_r$ as the human protein may be more compatible for use in patients.

<u>Study 1:</u> Direct injection of ApiCCT1$_r$ transiently reduces mHTT accumulation in R6/2 mice.

ApiCCT1$_r$, when directly injected in the striatum, transiently reduces mHTT accumulation *in vivo.* As a first step to evaluate whether cell-based effects of ApiCCT1 translate *in vivo*, we asked whether a single injection of ApiCCT1$_r$ could modify mHTT accumulation *in vivo* in R6/2 mice. R6/2 mice are a fragment model of HD, expressing exon 1 of human mHTT with ~150 repeats [75]. R6/2 are well-characterized and have been used by our group and many others to test therapeutics

and modifiers of mHTT accumulation [51, 62, 75], and offer a good first step to evaluate *in vivo* delivery of ApiCCT1. 5 week old HD or non-transgenic (NT) R6/2 mice were given intrastriatal injections of ApiCCT1$_r$ and tissue harvested at 3 days (n=1HD, 1NT), 2 weeks (n=2HD, 2NT), or 3 weeks (n=2NT, 2HD). We find that ApiCCT1$_r$ protein is present in the striatum 3 days after injection, begins to disappear 2 weeks after injection, and is completely degraded by 3 weeks after injection. Whole cell lysates were analyzed by Agarose Gel Electrophoresis (AGE), which preferentially resolves fibrillar oligomeric mHTT species [62, 63], followed by Western blot to visualize accumulated oligomeric mHTT species. At 2 weeks, HD animals exhibit almost 40% reduction in oligomeric mHTT (Fig. 2 D, F). This effect is gone by 3 weeks (Fig. 2 E, F), presumably due to degradation of the injected protein.

<u>Study 2:</u> AAV2/1-mediated delivery of secreted ApiCCT1 can reduce mHTT accumulation 12 weeks after injection in R6/1 mice.

Viral delivery of ApiCCT1 to the striatum can reduce mHTT accumulation *in vivo.*

To test whether the biochemical effect of ApiCCT1 persists long term *in vivo*, we tested viral delivery in R6/1 mice. R6/1 mice are also a fragment model of HD, expressing exon 1 of human mHTT with ~115 repeats [75, 121]. However, compared to R6/2, R6/1 have a slower onset and progression phenotype, with lifespans up to a year [71]. We chose this model to evaluate ApiCCT1 over a longer time course. Adeno-associated viruses (AAV's) were engineered that express HA-tagged sApiCCT1 to allow biochemical identification (Fig. 3A). R6/1 mice were given intrastriatal injections of

AAV2/1 expressing sApiCCT1 at 5 weeks of age and tissues harvested at 17 weeks of age. The four groups injected are as follows: (1) NT treated with AAV2/1-mCherry control virus (n= 8 males). (2) NT treated with AAV2/1-sApiCCT1 (n=8 males). (3) HD treated with AAV2/1-mCherry (n= 6 males). (4) HD treated with AAV2/1-sApiCCT1 (n= 6 males). This study served as a proof-of-concept study to investigate biochemical changes with ApiCCT1 *in vivo* as the number of animals were not powered sufficiently for adequate behavioral analysis.

Whole cell lysates of microdissected striatum were analyzed by AGE, followed by Western blot analysis to visualize accumulated oligomeric mHTT species. AAV2/1-sApiCCT1-treated animals show a significant reduction in oligomeric mHTT, with sApiCCT1 bands appearing both narrower and shorter (Fig. 3B, C). Studies have shown that smaller, soluble oligomeric species may represent a more toxic aggregation species [39, 122], so this finding is particularly noteworthy. Expression of the virus was confirmed by PAGE followed by western blot analysis (Fig. 3D). Although there is some variability in the expression of sApiCCT1, presumably due to clearance of the foreign protein or technical differences in injections, most animals show high expression of sApiCCT1 or mCherry control.

To further analyze insoluble mHTT species, brain tissue was fixed and stereology was performed on DAB stained sections to visualize insoluble, visible inclusions (n=4). In animals treated with AAV2/1-sApiCCT1 approximately 28% of cells contained visible inclusions. In animals treated with AAV2/1-mCherry control approximately 39% of cells contained visible inclusions; however, this result is not significant (p=0.33) (Fig 4).

Previous studies indicate that CCT interacts with both soluble mHTT and mHTT fibrils and that ApiCCT1 has an effect on insoluble and visible inclusions in addition to soluble forms of mHTT [63]. CryoEM studies show that CCT binds to the tips of mHTT fibrils and prevents elongation of the aggregated protein [100]. In the present study, we find a reduction in oligomeric mHTT but not visible mHTT inclusions. It is possible that ApiCCT1 affects different species when delivered *in vivo* and there is not a direct path from soluble oligomers to inclusion formation. More likely, it may be that, in the present experimental design, our treatment began after onset of mHTT accumulation and that pathology already existed in these mice. Visible inclusions are apparent as early as 9 weeks of age in R6/1 [123]; however, it is likely that soluble forms of accumulated mHTT are present at earlier timepoints. If true, then we may only observe prevention of newly formed oligomeric mHTT without clearing the pathology that was already established prior to virus injection and expression.

<u>Study 3:</u> AAV2/1-sApiCCT1 treatment does not fully rescue HD phenotypes in R6/1 HD mice.

AAV2/1-sApiCCT1-treated mice show significant improvements in rotarod performance at 14 weeks of age. To determine if the observed biochemical effect translates to behavioral outcomes, a larger cohort of R6/1 mice were given intrastriatal injections of AAV2/1-sApiCCT1 as in the previous experiment at 5 weeks of age and subject to behavioral assays. The six groups injected are as follows: (1) Vehicle-treated NT mice (n=2 males, 5 females) (2) NT treated with AAV2/1-mCherry control virus (n= 8

males, 10 females). (3) NT treated with AAV2/1-sApiCCT1 (n=10 males, 10 females). (4) Vehicle-treated HD animals (n=2 males, 4 females) (5) HD treated with AAV2/1-mCherry (n= 9 males, 10 females). (6) HD treated with AAV2/1-sApiCCT1 (n= 9 males, 10 females).

One of the evident markers of disease progression in R6/1 mice is progressive loss of motor coordination and balance [124], abnormally splayed limbs when held by the tail (clasping) [121], and a decrease in performance when climbing down a vertical pole [125]. Animals were assessed in rotarod, pole test, and clasping behavior. The rotarod test measures the amount of time an animal is able to remain balanced on an accelerating, rotating rod. A genotype effect on rotarod performance begins to appear at 12 weeks of age (Fig. 5A) and at 13 weeks on pole test (Fig. 5G). At 14 weeks, sApiCCT1-treated animals show significant improvements in rotarod performance (Fig. 5C, red bars), with no significant improvement at earlier timepoints. NT animals get progressively better at this task, with most animals remaining balanced for the maximum measured time, 300 seconds, at the 14 week time point (Fig. 5C). ApiCCT1-treated HD animals show improved rotarod performance at 10, 12 and 14 weeks compared to mCherry and Vehicle control groups, which becomes significant at the 14 week time point (Fig. 5 A-C). Behavioral analysis reflects both male and female animals; however when analyzed separately, only males exhibit a significant improvement at the 14 week timepoint on rotarod (data not shown). Pole test measures the amount of time for an animal to descend a vertical pole. A genotype effect on this task begins to appear at 13 weeks of age (Fig. 5G). sApiCCT1 animals show slight improvements in pole test, although the change is not significant. ApiCCT1-treated mice show a delay in the onset

of clasping behavior compared to mCherry, but not Vehicle-treated animals (Fig. 5 D, F). Clasping measures the percentage of animals exhibiting clasping behavior (see Fig. 5F for visual).

sApiCCT1 is found in both neurons and astrocytes *in vivo*. One of the benefits of using the apical domain is that ApiCCT1 has the ability to penetrate the cell and nuclear membranes. Therefore ApiCCT1 can affect both directly transduced cells and neighboring populations. Mouse tissue was harvested 12 weeks after injection as in the previous study. Brain tissue was fixed and stained by immunohistochemistry. Tissues were stained with βIII-tubulin (cytoplasm), HA (treatment), and synaptophysin (synapse). We find viral expression in the striatum, along the white matter tract, and in the ventral portion of the cortex in some animals (Fig. 6A). sApiCCT1 appears to show higher expression in the cell body and nucleus compared to mCherry, which is apparently from the relative co-localization with βIII-tubulin (Fig. 6B).

AAV2/1 transduces neurons [51, 126]; however, we find sApiCCT1 expression in both neurons and astrocytes (Fig. 7 A-C), an indication that secreted ApiCCT1 is likely being taken up by neighboring astrocytes as predicted. Tissue was stained with NeuN (red, neurons), GFAP (blue, astrocytes), and HA (green, treatment). NeuN is a neuronal marker that is primarily found in the nucleus [127], whereas GFAP is a marker of astrocyte cytoplasm and processes [128]. mCherry-treated animals show expression in some NeuN+ cells; however, most mCherry expression appears to be outside of the nucleus, and no transduced GFAP+ cells were found (Fig. 7E). This is consistent in all tissues stained (Fig. 6, 7, 11). sApiCCT1-treated animals show high amounts of co-localization with NeuN+ cells (Fig. 7B) and some co-localization with GFAP+ cells (Fig.

7C). This finding may indicate that secreted ApiCT1 is taken up by neighboring astrocytes and neurons and localizes to the nucleus.

AAV2/1-sApiCCT1 treatment does not significantly reduce most mHTT accumulated species in HD mice. Whole cell lysates of microdisssected striatum were subject to biochemical analysis to visualize virus expression and accumulated oligomeric species. PAGE analysis followed by western blot confirms expression of both sApiCCT1 and mCherry control (Fig 8E). As with the previous study, there is some variability in virus expression between animals; however, most treated animals show high expression of virus (Fig. 8E).

mHTT accumulation was analyzed using multiple methods as each method resolves different aggregated species. AGE analysis shows that sApiCCT1 does not significant reduce oligomeric mHTT (Fig. 8A, B). AGE analysis resolves oligomeric species above ~400kDa; however, there are accumulated species below this size that may not be detectable on an AGE gel. To this end, we ran the same whole cell lysate samples on a 3-8% Tris-acetate gel, which can resolve species that cannot be detected on an AGE gel (40-500kDa) (Fig. 8C). The band near to top of the gel likely corresponds to mHTT species that did not run into the gel and this band was not included in quantitation. Using this method, we see a significant reduction in mHTT species between ~200-500kDa (Fig. 8D). While it is unclear which specific mHTT species this corresponds to, it is possible that we are visualizing a soluble species of accumulated mHTT.

mHTT accumulation was also analyzed by fractionation, separating detergent-soluble and detergent-insoluble fractions. The detergent soluble fraction contains most

cytoplasmic proteins, including monomeric and soluble oligomeric mHTT, while the detergent insoluble fraction contains nuclear protein, high MW mHTT, and other insoluble proteins [129, 130]. This method of analyzing accumulated mHTT is distinct from AGE analysis that primarily resolves soluble, oligomeric species [1]. The fractionation method indicates a 5% reduction in high MW insoluble mHTT in the striatum, which is not significant (p=0.68) (Fig. 9 A, B).

Visible, insoluble mHTT inclusions were analyzed by Imaris fluorescent staining. Brain sections were stained with anti-HA (ApiCCT1), Anti-EM48 (mHTT), and βIII-tubulin (cytoplasm). Visible inclusions were quantified by Imaris in the striatum. Only areas with virus were quantified. There was no significant difference in visible inclusions between treatment groups (Fig. 9C, D).

Analysis of mHTT accumulation from study 3 is not consistent with analysis from study 2, which found a significant reduction in oligomeric mHTT (Fig. 3). While we did find a significant reduction in soluble, high MW mHTT in this study (Fig. 8C), we found no significant change in oligomeric mHTT (Fig. 8A).

sApiCCT1 treatment does not significantly alter gene expression compared to control-treated animals. Because ApiCCT1 did not alter mHTT accumulation in this study, we sought to determine whether other disease readouts were altered in sApiCCT1-treated animals. If ApiCCT1 is reducing mHTT-mediated toxicity, as we have seen in *in vitro* studies [63], then ApiCCT1 should prevent disease-related changes in gene expression. To test whether ApiCCT1 treatment alters disease-related gene expression profiles, RNA was isolated from microdissected striatum (n=5). qPCR of

cDNA reveals no significant changes in gene expression with sApiCCT1 treatment (Fig. 10). Expression was analyzed for mHTT (transgene expression), DARPP-32 (a marker of medium spiny neurons), and dopamine receptor DRD-2. NT animals did not show any mHTT transgene expression (not shown). mHTT expression is not significantly different between HD animals (Fig. 10A). It is well-established that DARPP-32 and DRD-2 are downregulated in HD [72, 73], and we observe this same genotype effect. sApiCCT1 does not rescue this downregulation (Fig. 10B, C). This is further evidence that ApiCCT1 is not modulating disease phenotypes in this study.

Astrocytes and activated microglia are found near areas of high viral expression. Tissue was stained with Iba1 (red, microglia), GFAP (blue, astrocytes), and HA (green, treatment). We find abundant astrocytes near areas of transduced cells (Fig. 11A, C, D). We also find activated microglia in the same regions. Microglial activation can be identified by a change in morphology, including a swollen cell body and thicker processes [131]. One animal did not show viral expression (Fig. 11B), presumably due to clearance of the foreign virus; this animal shows normal microglia morphology and a minor increase in astrocyte expression near where the injection injury would be (Fig. 11B). This finding suggests that the increase in astrocytes and activated microglia is due to virus, with minimal contribution of the healed injection injury. It is possible that this aberrant immune response is contributing to the unexpected biochemical results observed in this study.

AAV2/1-mediated delivery of sApiCCT1 does not change cellular degeneration. We next sought to determine if AAV2/1-mediated delivery of sApiCCT1 alters degeneration. The purpose of this was to rule out any possible toxic effects of viral

delivery. To visualize degenerating cells, we stained brain sections with Fluoro-Jade, a stain used for the assessment of neurodegeneration [132]. Very few cells stained with Fluoro-Jade, with no obvious difference between HD and NT animals (Fig. 12), indicating that AAV2/1 virus does not elicit cell death.

Studies utilizing AAV2/1 may be confounded by an increased stress response. Because of the differences between the outcomes of the two studies, we sought to compare them directly to identify possible confounding factors. Striatal whole cell lysates from both studies were analyzed by western blot. In study 2, p- IRE1α is detected in HD animals, but not NT, which is consistent with published studies [133]. We find increased levels of p-IRE1α, a marker of ER stress [134], normalized to total IRE1α (Fig. 13A, B) in lysates from study 3. IRE1α is a transmembrane ER protein that is phosphorylated under ER stress and plays a role in initiation of the unfolded protein response (UPR) [134, 135]. All lysates from study 3 show detectable p- IRE1α, including NT. Most animals from study 3 show high levels of GFAP (Fig. 13, third row), which is consistent with the immunohistochemistry analysis (Fig. 11). Of the lysates analyzed from study 2, mCherry-treated HD mice show the highest levels of p-IRE1α relative to total IRE1α and increased GFAP staining. This could suggest that, in study 2, sApiCCT1 expression prevented an aberrant stress response triggered by the virus in HD animals. Alternatively, this could be due to toxicity from the mCherry protein.

The degree of ER stress is an important consideration as aberrant and chronic ER stress is associated with increased neurodegeneration and mHTT accumulation [133, 134] and ER stress may play an important role in mHTT-induced cell death [136, 137]. One study found that overexpression of IRE1α directly increased mHTT accumulation in

HEK293T cells, with an increase in both detergent-soluble and –insoluble species [133]. A separate study by the same group found that inducing ER stress with tunicamycin leads to increased mHTT accumulation in R6/2 [138]. Therefore, the conflicting data presented here may be explained by increased mHTT accumulation associated with ER stress. Further, this may suggest that ApiCCT1 is not sufficient to overcome the additional stress response found in study 3. Consequently, these studies cannot conclusively determine the potential efficacy of ApiCCT1 as a therapeutic target for Huntigton's disease. Further characterizations with alternative delivery methods are needed.

Discussion

Chaperone-based therapies for neurodegenerative diseases have been studied extensively due to their ability to modulate protein misfolding and subsequent accumulation. Here, we evaluate *in vivo*, striatal delivery of a fragment of a chaperone protein (ApiCCT1) that is known to modulate mHTT accumulation [63, 93, 100, 105]. ApiCCT1 can penetrate cellular membranes and localize to both the cytoplasm and nuclear compartments and appears to be able to target both transduced cells, as well as neighboring cell populations. Data presented here yield conflicting results. Studies 1 and 2 suggest that ApiCCT1 can modulate mHTT accumulation *in vivo*. Study 3 showed no significant change in most accumulated mHTT species; however, we did find a significant improvement in behavior at one timepoint. This study was confounded by an additional stress response which may have altered mHTT accumulation.

While it is unclear why there is a difference in stress response and mHTT accumulation between these studies, this may be explained by external factors or technical aspects of the experiments. While the two viruses were generated from the same DNA construct, they were generated by different sources and injected at different volumes. All animals received $12X10^9$ genome copies of virus in each hemisphere; however, the volume of injection differed. In study 2, we injected 4µl of virus at $3X10^{12}$vg/ml, but in study 3 the virus was more concentrated and we injected 2µl of virus at $6X10^{12}$vg/ml. While there was no obvious difference in expression (Fig. 13) between these two studies, small differences in injection volume may be enough to influence stress response or measurement of protein accumulation. Further, animals from study 3 may have been subjected to additional external stressors. During the entirety of study 3, construction was taking place in an adjacent building. Environmental factors can lead to great variability in mouse behavior [139] and it is possible that nearby construction caused an increased stress response or made the animals more susceptible to the potentially toxic effects of viral injection. Finally, mice were obtained through different sources, with study 2 being bred in house and study 3 purchased from Jackson Laboratory (JAX) directly. The differences in breeding location or the experience of being transported a long distance may explain the differences in stress response between these two cohorts.

Studies 1 and 2 suggest that ApiCCT1 may modulate mHTT accumulation *in vivo*. However, if the differences between all three studies are due to environmental factors, then ApiCCT1 alone may not be sufficient to overcome pathology that is exacerbated by external stressors. While we did find an improvement one behavioral task, ApiCCT1 did

not fully rescue HD phenotypes in study 3. Future studies will be carried out to more clearly define potential efficacy of ApiCCT1.

MATERIALS AND METHODS

Protein.

The 6×-his tagged ApiCCT1$_r$ was purified and added to cells as previously described [63].

Primary Cortical Neurons and Fractionation

Primary cortical neurons (PCNs) were isolated from embryonic day 17 FVB mice as previously described [62]. Cortical neurons were plated at 13×10^6 cells per dish, in poly-L-lysine (Sigma) coated 10cm dish (Corning) in Neurobasal medium supplemented with B27, N2, 2 mM glutamax, and streptomycin/amphotericin B (Life Technologies). Cells were treated with 1 μM exogenous, purified yeast or human ApiCCT1$_r$, or buffer control on DIV 9 and harvested on DIV 11. Cellular fractionated was performed as previously described [63] and the total (T), cytoplasmic (C), and nuclear (N) fractions were collected. Samples were run on a 15% Criterion gel (Bio-Rad) and wet-transferred to a nitrocellulose membrane and probed with anti-His (Sigma, 1:1,000), anti-GAPDH (Imgenex, 1:1,000) and anti-p84 (AbCam, 1:1,000).

Direct delivery of ApiCCT1 in R6/2 mice

5 week old R6/2 mice were given a single intrastriatal injection of yeast ApiCCT1$_r$. Bilateral intrastriatal injections were performed using a stereotax apparatus (coordinates 0.01mm caudal to bregma, 0.2mm right/left lateral, 0.345 pocket to 0.325mm ventral to pial surface). Mice were anesthetized with isofluorane, placed in stereotax, and injected with 4.6ug (Fig. 1A, B, D) or 10ug (Fig. 1 C, E) of yeast ApiCCT1$_r$ in each hemisphere with a Hamilton syringe. The needle was left in place for 2 minutes before slowly removing and the incision was sutured.

AAV2/1 transplants

AAV constructs were generated expressing ApiCCT1 with an IL2 secretion signal sequence or mCherry under a CAGG promoter. Virus was generated by Dr. David Housman's group (Fig. 3-4) or by the Research Vector Core at Children's Hospital of Philadelphia (Fig. 5-9). Mice were given bilateral intrastriatal injections using a stereotax apparatus (coordinates 0.01mm caudal to bregma, 0.2mm right/left lateral, 0.345 pocket to 0.325mm ventral to pial surface). Mice were anesthetized with isofluorane, placed in stereotax, and injected with $12X10^9$ genome copies of virus in the striatum of each hemisphere with a Hamilton syringe. In study 2, mice were injected with 4µl of virus at MOI $3X10^{12}$vg/ml. In study 3, mice were injected with 2µl of virus and MOI $6X10^{12}$vg/ml. The needle was left in place for 2 minutes before slowly removing and the incision was sutured.

Mouse Behavior and Tissue Harvest

Behavioral outcomes were analyzed using rotarod, pole test, and clasping. At 17 weeks of age (12 weeks after injection). Statistics were analyzed by one-way ANOVA followed by Tukey's post-hoc test. Mice were sacrificed by Euthasol followed by transcardinal perfusion. Cortex and striatum were microdissected from one hemisphere and flash frozen for biochemical analysis. The other hemisphere was fixed in paraformaldehyde overnight, transferred to 30% sucrose solution, and tissue was sectioned using a microtome.

Histology

Brain sections were analyzed by immunohistochemistry. Slices were stained with the following antibodies: anti-HA (Sigma H6908), anti-EM38 (Millipore MAB5374), anti-synaptophysin (Sigma-Aldrich S5768), anti-Iba1 (Wako Pure Chemicals Industries 27030), anti-βIII-tubulin (Covance PRB-435P-100), anti-GFAP (Abcam ab7260), anti-NeuN (Millipore) and ToPro3 nuclear stain. Visible aggregates quantified by either stereology (study 2) or Imaris (study 3). 4 animals were analyzed for each group. For each animal, 6 sections were stained taking every third section near the approximate injection site. Only sections with virus were analyzed, leaving 4-6 sections per animal to analyze. 4-6 images were counted per section, depending on spread of virus. Only images containing viral staining were analyzed. Stereological quantifications were performed using Stereo-Investigator software from Microbrightfield Bioscience (MBF Bioscience, Williston, VT, USA). The following antibodies were used: anti-HA (Sigma H6908) and anti-EM48 (Millipore). Alexa fluorescent-conjugated secondary antibodies

were used (Life Technologies). Stained tissue was mounted on slides and coverslipped with Fluoromount-G (SouthernBiotech). Images were acquired on a LeicaDM2500 confocal microscope.

RNA Isolation and Quantitative PCR (qPCR)

Microdissected striatum from animals in study 3 was homogenized in TRIzol (Invitrogen), and total RNA was isolated using RNEasy Mini kit (QIAGEN). DNase treatment was incorporated into the RNEasy procedure in order to remove residual DNA. Reverse transcription was performed using oligo (dT) primers and 1 µg of total RNA using SuperScript III First-Strand Synthesis System (Invitrogen). Quantitative PCR (qPCR) was performed and ddCt values were quantitated and analyzed against RPLPO and fold change was calculated compared to the lowest value in the control group (control group was mCherry HD animals for mHTT gene and mCherry NT animals for DRD2 and DARPP-32 genes). One way ANOVA followed by Tukey's post-hoc was performed on dCt values.

Soluble/Insoluble Fractionation

Fractionation protocol was modified from O-Rourke, et al [129]. Brain tissue was homogenized in lysis buffer (10mM Tris (pH 7.4), 1% Triton X-100, 150mM NaCl, 10% glycerol, and 0.2 mM PMSF) with Roche Complete Protease Mini and PhosphoStop pellets. Tissue was kept frozen on dry ice until immediately before homogenization. Homogenized tissue was incubated on ice for 60 minutes before centrifugation at 15,000xg for 20 minutes at 4°C. Supernatant represents the detergent-soluble fraction. The pellet was washed 3x with lysis buffer and centrifuged at 15,000xg for 5 minutes

each at 4°C. The pellet was then resuspended in lysis buffer supplemented with 4% SDS, sonicated 3 times, and boiled for 30 minutes. The resuspended pellet represents the detergent-insoluble fraction. Detergent-insoluble fractions samples were analyzed using a 3-8% Tris-Acetate polyacrylamide gel (Invitrogen), and detergent-soluble samples with NuPAGE 4-12% Bis-Tris polyacrylamide gel (Invitrogen), followed by western blot.

Polyacrylamide (PAGE) and Agarose (AGE) gel electrophoresis

Brain tissue was lysed in modified RIPA (radio immune precipitation) buffer containing 10mM Tris, pH7.2, 158mM NaCl, 1mM EDTA, 0.1% SDS, 1% Triton X-100, 1% sodium deoxycholate, and 1x Complete protease inhibitors (Roche) as described previously [62]. Samples were analyzed by both PAGE and AGE. SDS-AGE followed by Western blot analysis was performed a previously described [1, 62, 63, 140, 141]. Samples were analyzed with either NuPAGE 4-12% Bis-Tris polyacrylamide gel (Invitrogen), 3-8% Tris-Acetate polyacrylamide gel (Invitrogen), or 15% Criterion Bis-Tris polyacrylamide gel (Bio-Rad), followed by western blot analysis. Blots were quantified using ImageJ software. Membranes were probed with the following antibodies: anti-polyHistadine (Sigma), anti-5492 (Millipore), anti-GAPDH (Imgenex), anti-p84 (AbCam), anti-HA (Sigma), anti-α-tubulin (Sigma), anti-phospho-IRE1α (NovusBio), and anti-IRE1α (NovusBio).

Fluoro-JadeB

Brain sections were stained with Fluorojade B (Millipore AG310) to visualize cells undergoing degeneration. Mounted brain sections were dehydrated in 80% ethanol for two minutes then 70% ethanol for another two minutes. After a three minute rinse in H_2O, slides were immersed in 0.06% $KMnO_4$. Slides are again rinsed in H_2O and incubated in 0.0004% Fluoro-Jade B in 0.01% acetic acid for fifteen minutes with rotation. Slides are rinsed three times in H_2O and dried in the dark for 1 hour. Once dry, slides are immersed in three changes of xylene for one minute each and air dried for 10-20 minutes before coverslipping in DPX mounting media (Electron Microscopy Services 13512).

CHAPTER 2

FIGURES

Figure 2.1

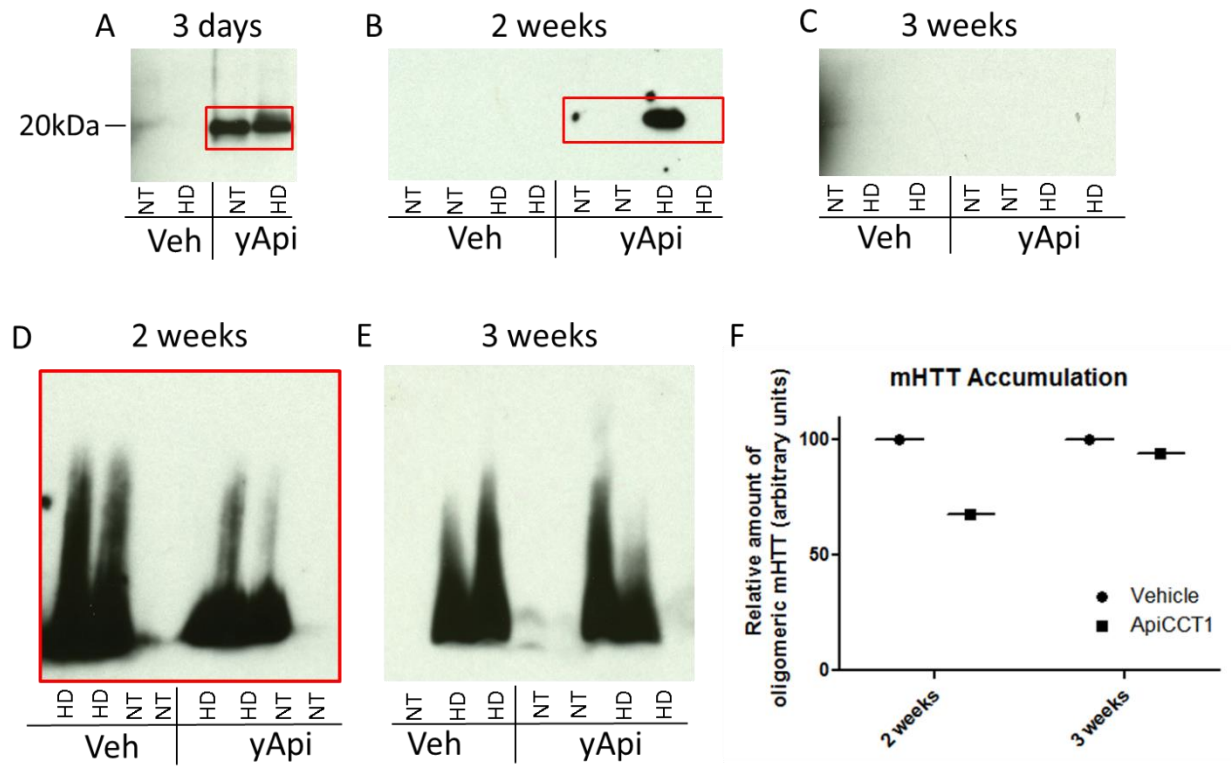

Figure 1: ApiCCT1$_r$ is present in R6/2 striatum 3 days after injection, but is not detectable at 3 weeks. 5 week old R6/2 mice were given intrastriatal injections of purified, recombinant yeast ApiCCT1$_r$. Mice were injected with either 4.6µg of protein (A,B,D) or 10µg of protein (C,E) and tissue harvested 3 days, 2 weeks, or 3 weeks after injection. Lysates were analyzed by SDS-PAGE followed by Western blot. (D,E). ApiCCT1$_r$ is present in both samples at 3 days, but begins to disappear at 2 weeks after injection. ApiCCT1$_r$ is not present in any samples 3 weeks after injection. Lanes are labeled as follows: NT, non-transgenic R6/2; HD, transgenic R6/2. Blots were probed with anti-His against ApiCCT1$_r$ (A-C) or anti-5492 against HTT N-terminal 82 amino acids. 30µg of total protein was loaded in each lane.

Figure 2.2

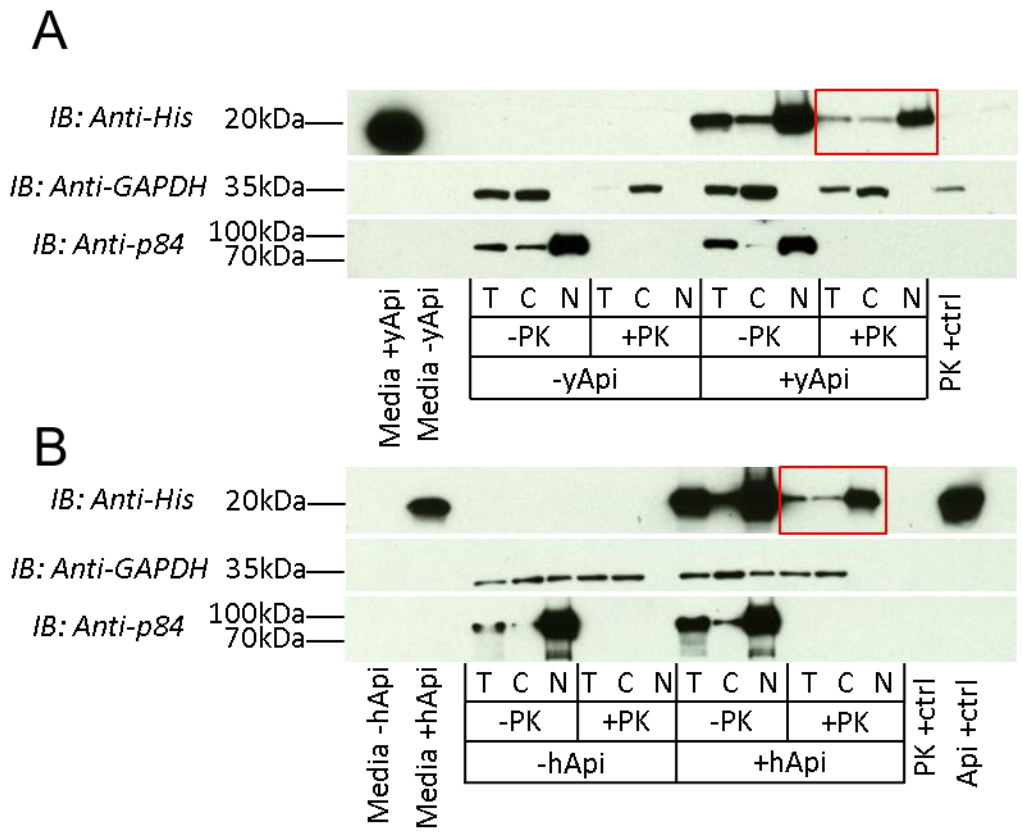

Figure 2: Both yeast and human ApiCCT1$_r$ enter primary cortical neurons. PCNs were isolated from E17 FVB mice and treated at DIV 5 with 1 µM exogenous, purified yeast (A) or human (B) ApiCCT1$_r$. Cells were subjected to fractionation and treated with proteinase K prior to lysis to degrade membrane-bound proteins. ApiCCT1$_r$ is detected inside the cytosol and nucleus (red box). Conditioned media was also analyzed for the presence of ApiCCT1$_r$. Lanes are labeled as follows: Total (T), cytoplasmic (C), and nuclear (N) fractions, -PK, no PK treatment; PK+ ctrl, 60µg of lysed nuclear fraction treated with PK. Samples were analyzed by western blot with anti-His antibody (ApiCCT1r), anti-GAPDH (cytoplasmic marker), and anti-p84 (nuclear marker).

Figure 2.3

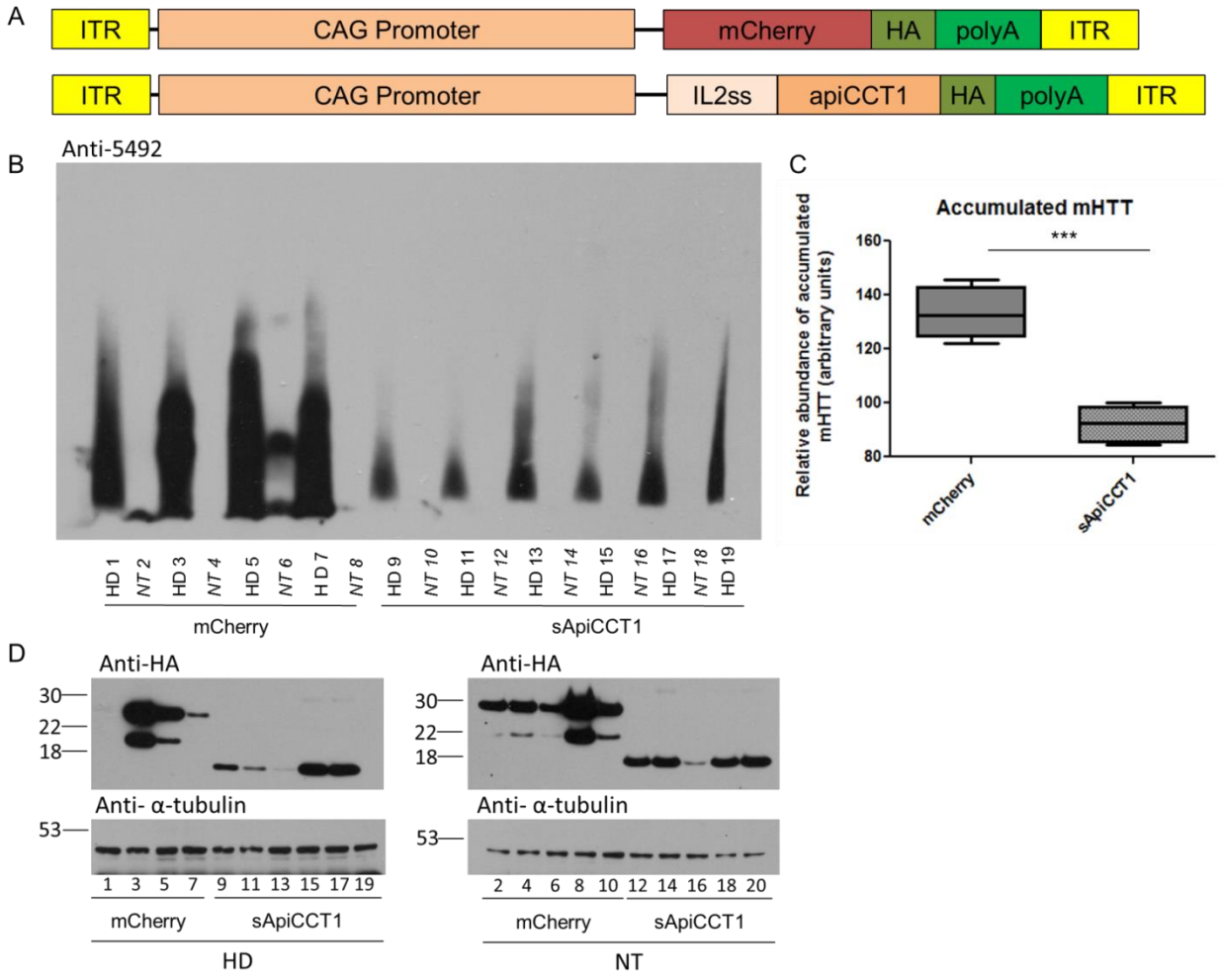

Figure 3: AAV2/1-sApiCCT1 delivery reduces fibrillar mHTT oligomers and visible inclusions *in vivo* 12 weeks after injection. R6/1 mice were given bilateral intrastriatal injections of AAV expressing sApiCCT1 or mCherry control at 5 weeks of age. Mice were injected with $12x10^{9}$ genome copies and harvested at 17 weeks of age. (A) Schematic of DNA constructs. (B,C) Agarose gel electrophoresis of lysed striatal tissue followed by western blot shows a significant reduction in oligomeric mHTT in animals injected with AAV2/1-sApiCCT1. (D) Western blot analysis confirms expression of virus in all but 2 animals. Blots probed with anti-HA (ApiCCT1), anti-5492 (anti-HTT), anti-α-tubulin. ***p<0.001.

Figure 2.4

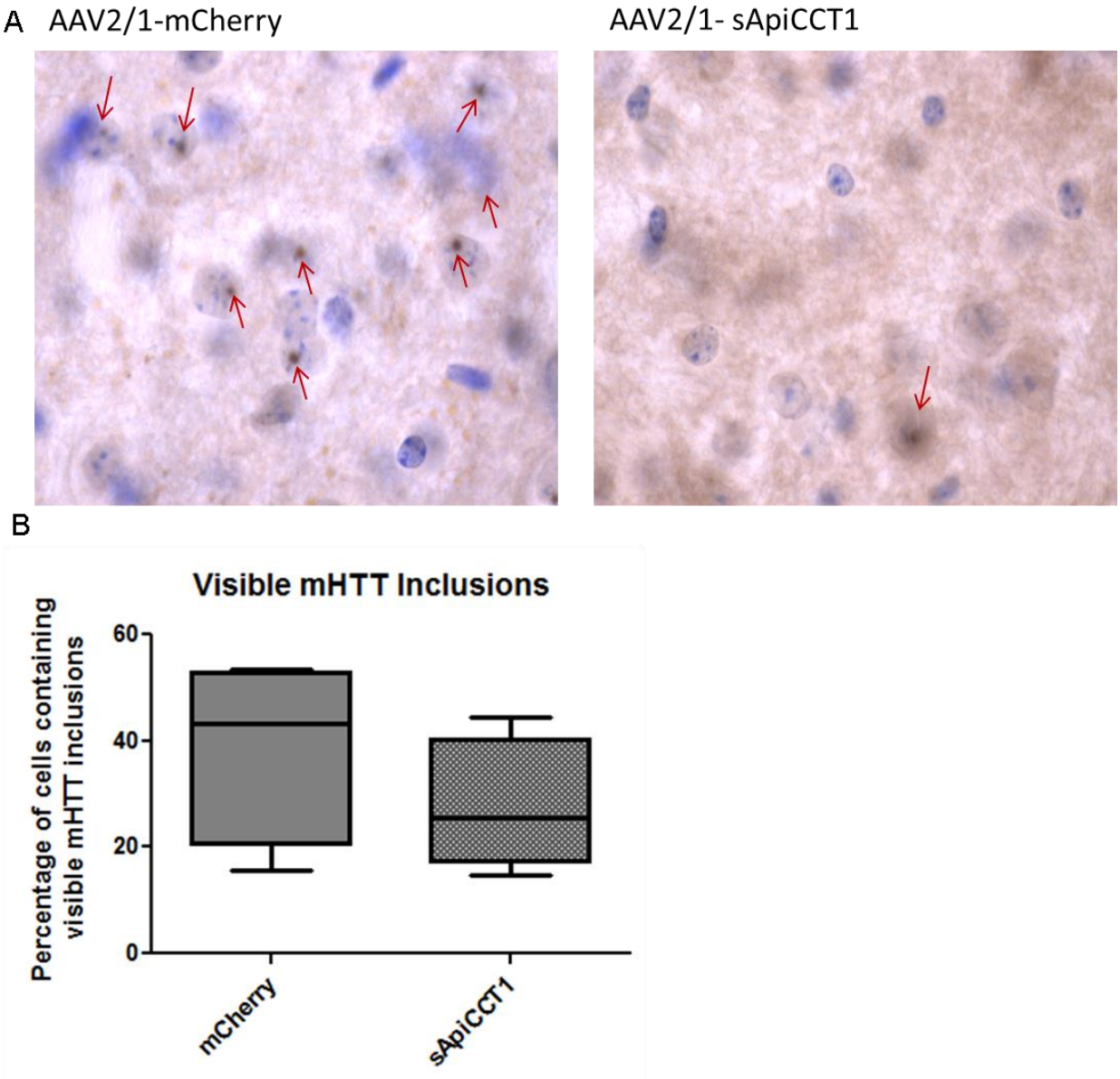

Figure 4: Visible inclusions are not significantly reduced in animals treated with AAV2/1-sApiCCT1 (A,B) Stereology shows a reduction in visible inclusion in the striatum of mice treated with AAV2/1-sApiCCT1, although the result is not statistically significant (A) Representative images of DAB stained sections showing mHTT visible aggregates (anti-EM48 and anti-HA). Puncta (mHTT aggregates) are indicated by red arrows. (B) There is not a significant change in visible mHTT aggregates between sApiCCT1 and mCherry control treated animals. (p=0.33)

Figure 2.5

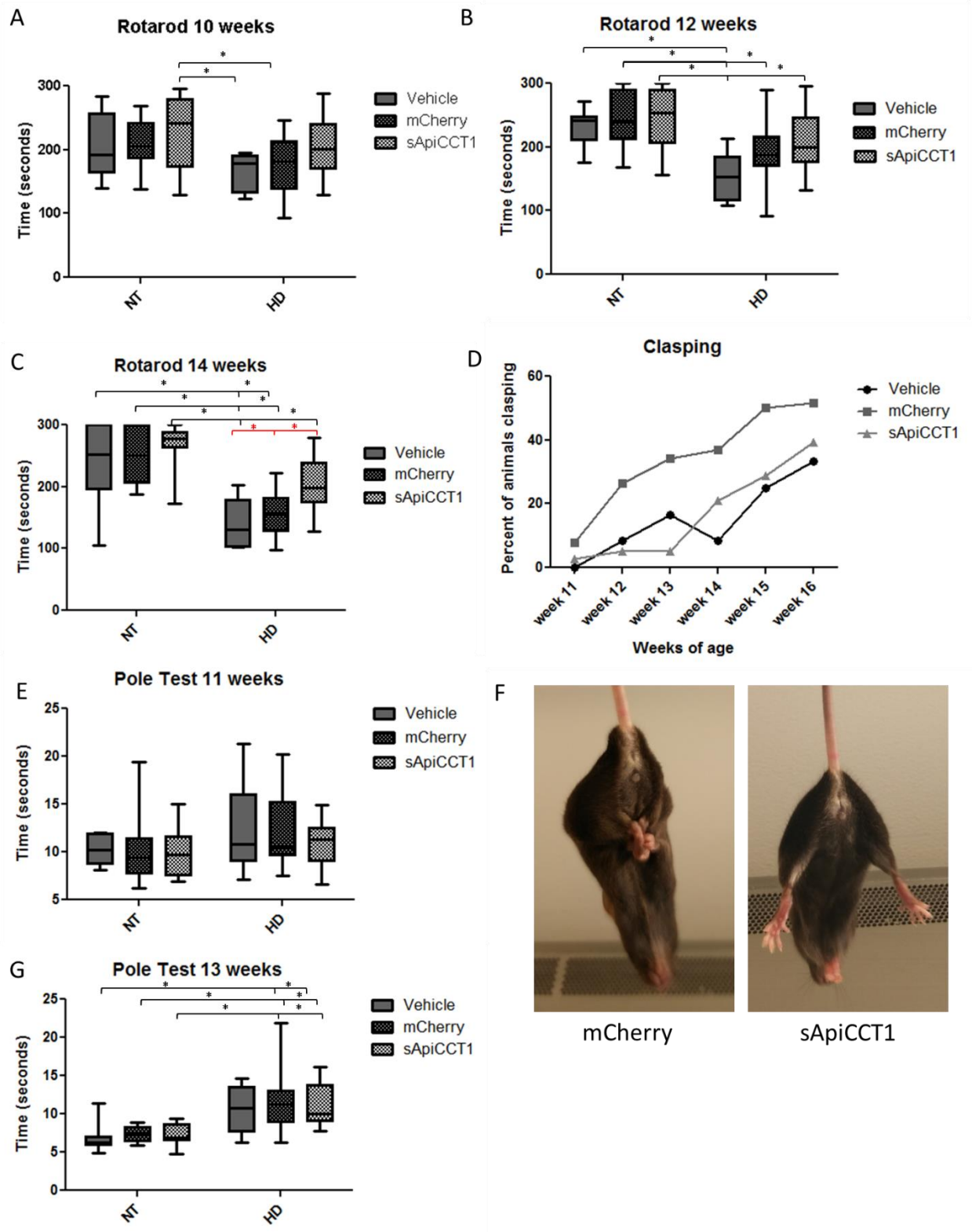
A
Rotarod 10 weeks
Time (seconds)
300
200
100
0
NT
HD
Vehicle
mCherry
sApiCCT1
B
Rotarod 12 weeks
Time (seconds)
300
200
100
0
NT
HD
Vehicle
mCherry
sApiCCT1
C
Rotarod 14 weeks
Time (seconds)
300
200
100
0
NT
HD
Vehicle
mCherry
sApiCCT1
D
Clasping
Percent of animals clasping
60
40
20
0
week 11
week 12
week 13
week 14
week 15
week 16
Weeks of age
Vehicle
mCherry
sApiCCT1
E
Pole Test 11 weeks
Time (seconds)
25
20
15
10
5
NT
HD
Vehicle
mCherry
sApiCCT1
F
mCherry
sApiCCT1
G
Pole Test 13 weeks
Time (seconds)
25
20
15
10
5
0
NT
HD
Vehicle
mCherry
sApiCCT1

Figure 5: AAV2/1-sApiCCT1 delivery improves performance on some motor tasks after striatal injection. R6/1 mice were given bilateral intrastriatal injections of AAV expressing sApiCCT1 or mCherry control at 5 weeks of age. Mice were injected with $12x10^9$ genome copies of virus. (A-C) Treated animals show improvements on a rotarod task at 10, 12 and 14 weeks of age. (D) Treated animals show a delay in onset of clasping behavior. (E,G) Pole test shows no significant differences between treatment groups. *p<0.05, **p<0.01**.** Vehicle n=6, mCh n=19, sApi n=19.

Figure 2.6

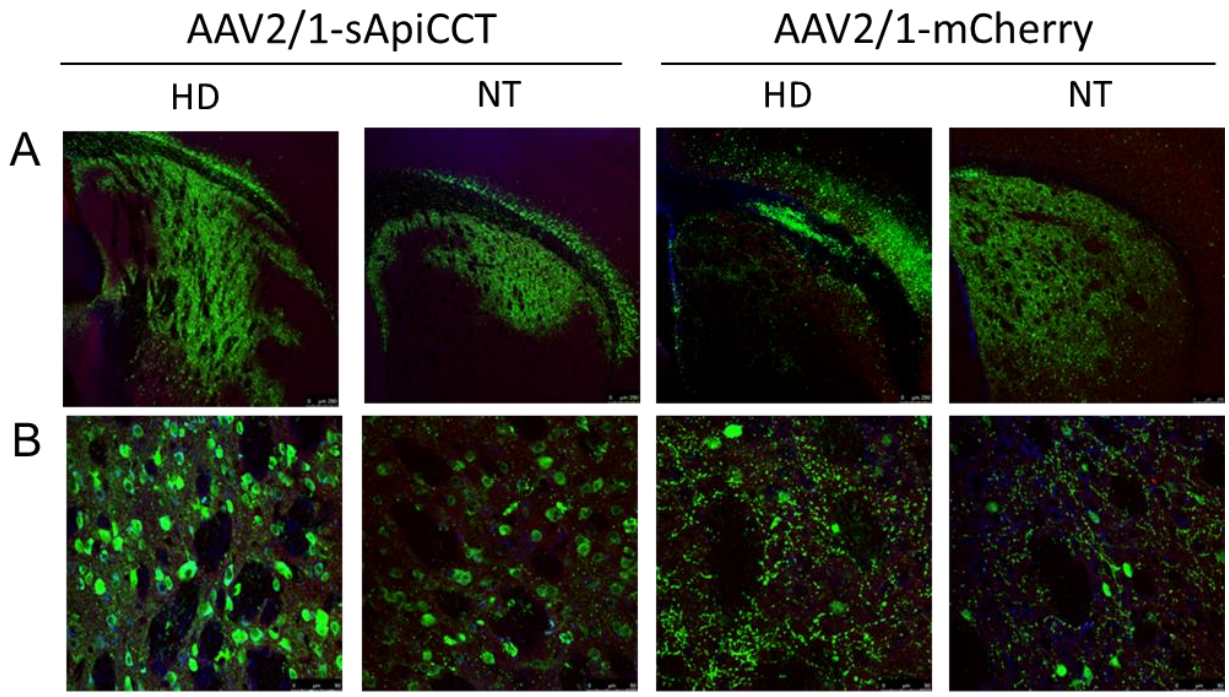

Figure 6: Protein is expressed in the striatum, along the white matter tract, and ventral region of cortex. Mice were injected with AAV2/1 expressing either sApiCCT1 or mCherry control into the striatum ($12x10^9$ genome copies). Tissue was harvested at 17 weeks of age. (A) 5X images. The virus transduces cells in the striatum, and also along the white matter tract between the striatum and cortex and in the ventral region of the cortex. (B) 40X images. sApiCCT1 appears to show higher expression inside of cells, whereas mCherry shows less co-localization with βIII-tubulin (anti-HA: green, anti-βIII-tubulin: blue, anti-synaptophysin: red).

Figure 2.7

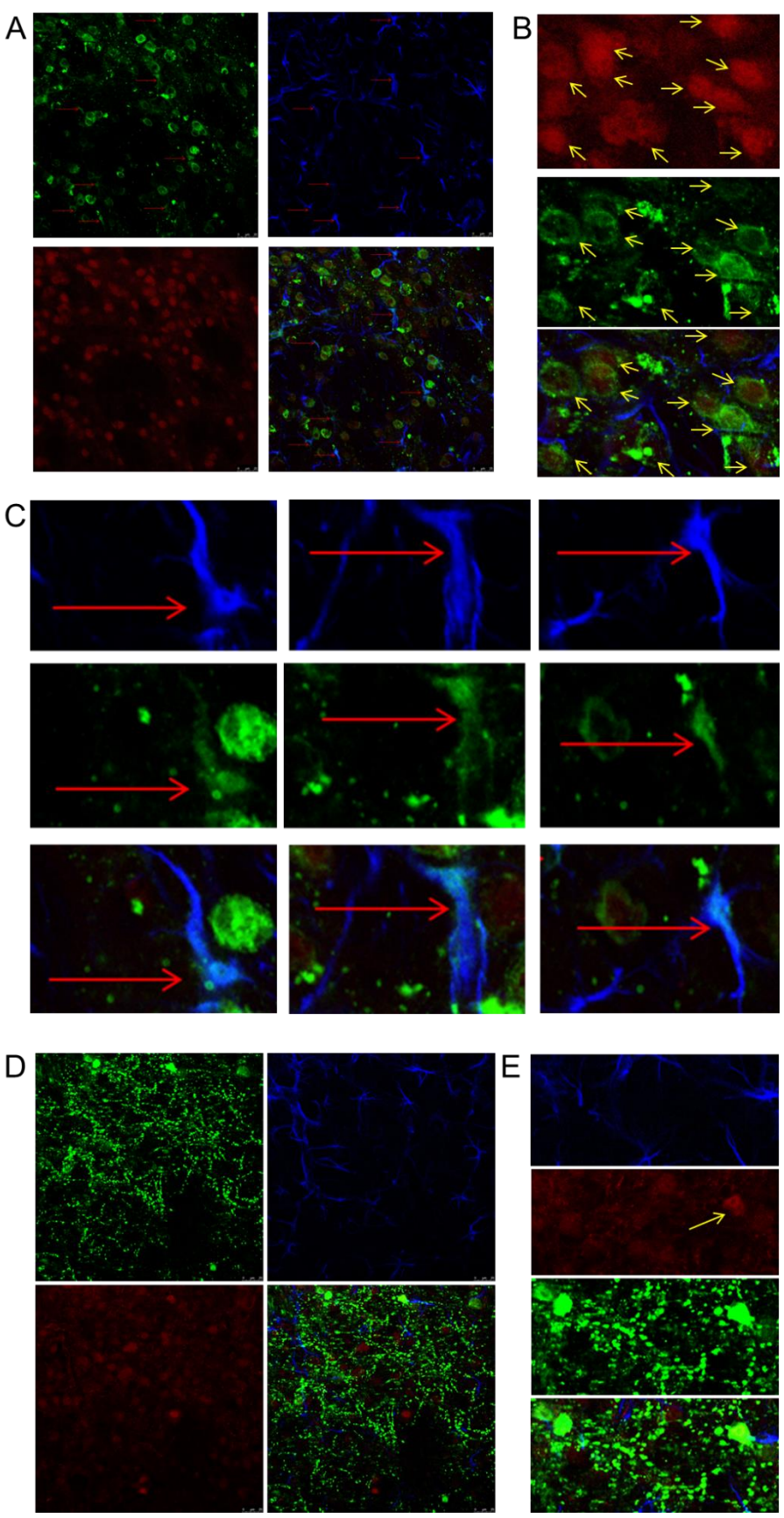

Figure 7: sApiCCT1 is found inside of both NeuN+ and GFAP+ cells. Tissue from sApiCCT1 and mCherry-treated mice were stained with anti-HA (green), anti-NeuN (red), and anti-GFAP (blue). (A-C) sApiCCT1 striatal tissue (40x Images) Red arrows indicate co-localization of GFAP and HA. (B) sApiCCT1 is found inside of neurons. Yellow arrows indicate co-localization of NeuN and HA. (C) sApiCCT1 is also found inside of astrocytes,. Red arrows indicate co-localization of GFAP and HA. (D, E) mCherry striatal tissue (40x Images) (E) mCherry is found to co-localize with some NeuN+ cells, but no GFAP+ cells.

Figure 2.8

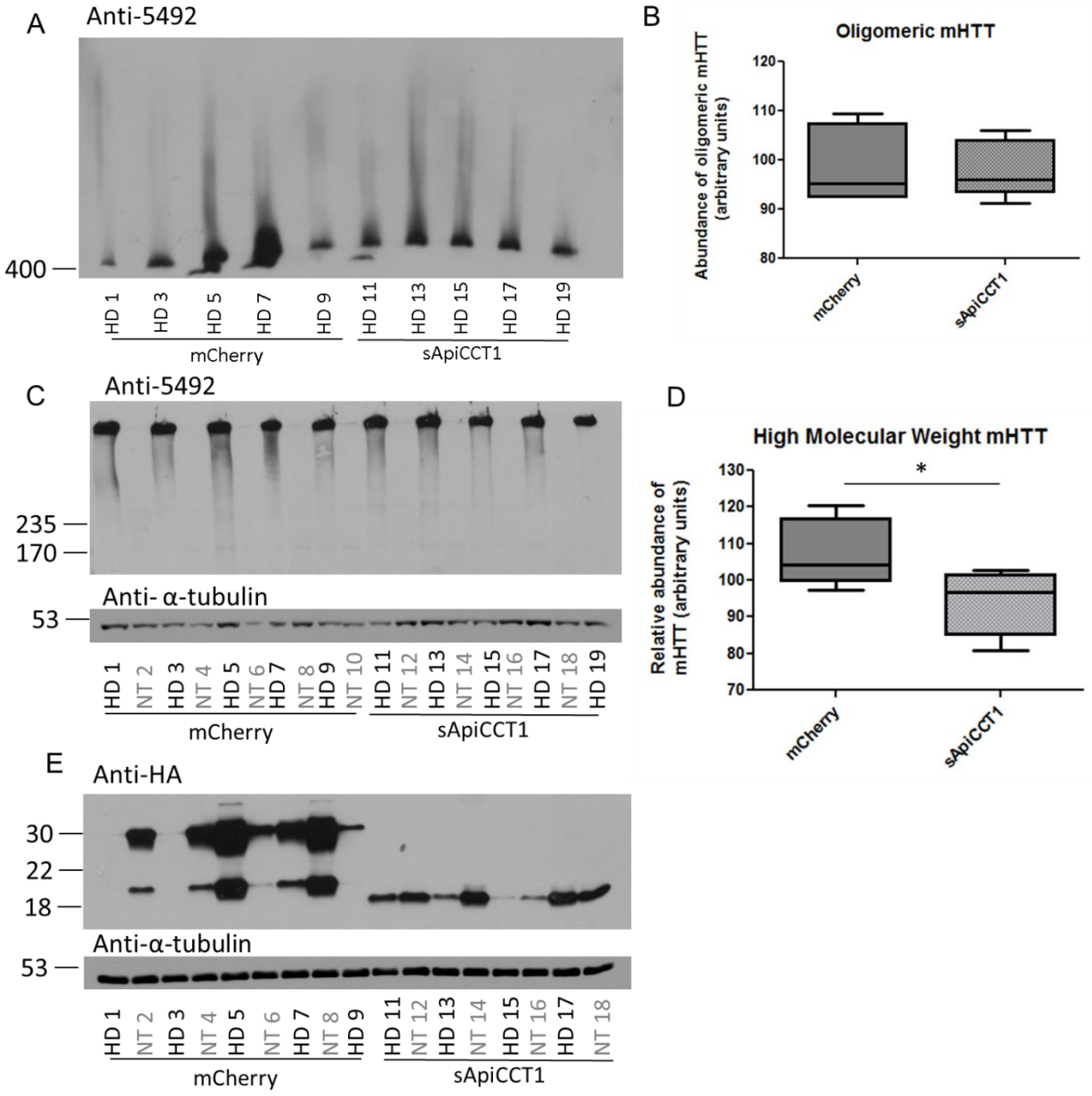

Figure 8: AAV2/1-sApiCCT1- treated mice show no changes in oligomeric mHTT. (A-E) Western blot analysis of striatal tissue whole cell lysate. (A, B) AAV2/1-sApiCCT1 treated animals show no significant change in mHTT accumulation. (c) AAV2/1-treated animals show a reduction in high MW soluble mHTT. Western blot analysis of protein expression (Anti-HA and Anti-α-tubulin). *p<0.05

Figure 2.9

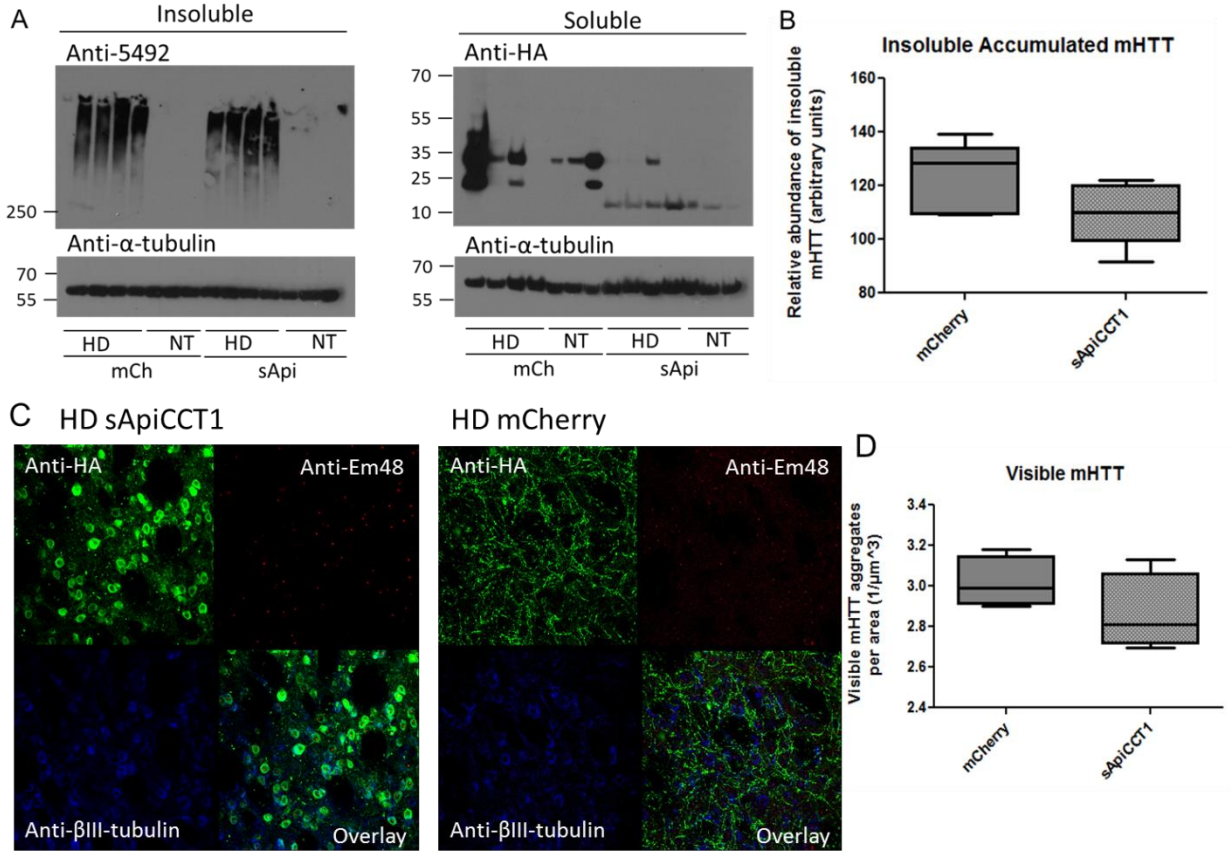

Figure 9: AAV2/1-sApiCCT1 does not alter insoluble or visible mHTT accumulation. (A,B) Western blot analysis of striatal mouse tissue separated into detergent-insoluble and detergent-soluble fractions. AAV2/1-sApiCCT1 does not modulated insoluble mHTT in HD animals. Analysis of soluble fractions confirm expression of protein in striatum. (C,D) Visible mHTT inclusions were analyzed by immunohistochemistry. Tissue was stained with anti-EM48 (red), anti-HA (green), and anti-βIII-tubulin (blue). mHTT inclusions are visualized as red puncta. AAV2/1-sApiCCT1 does not modify visible inclusion in R6/1 mice (p=0.68).

Figure 2.10

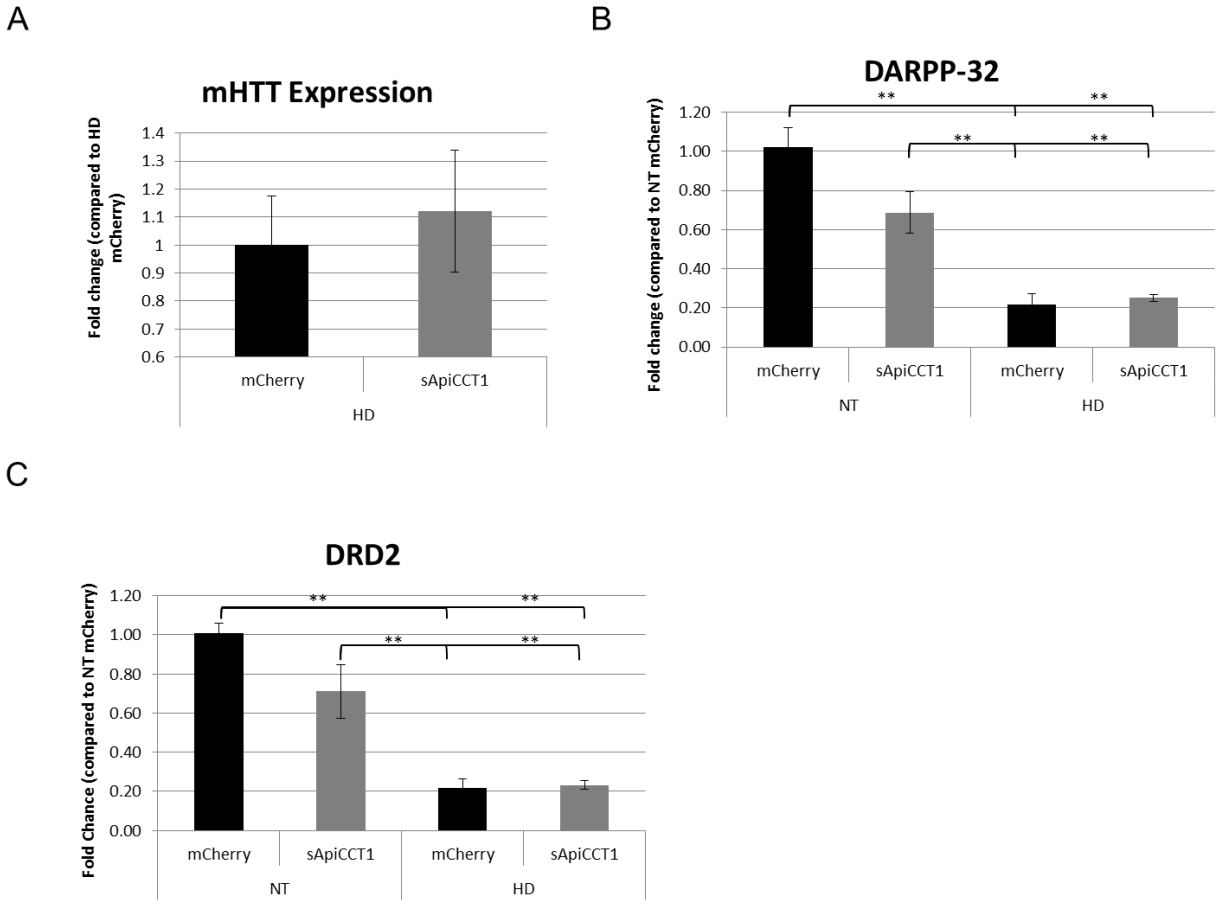

Figure 10: AAV2/1-sApiCCT1 transplanted mice do not exhibit significant changes in gene expression. Striatal tissue was analyzed by qPCR for changes in gene expression. (A) sApiCCT1 treatment does not alter mHTT expression. DARP-32 (B) and DRD2 (C) are downregulated in HD mice; however, there is no treatment effect. **p<0.01

Figure 2.11

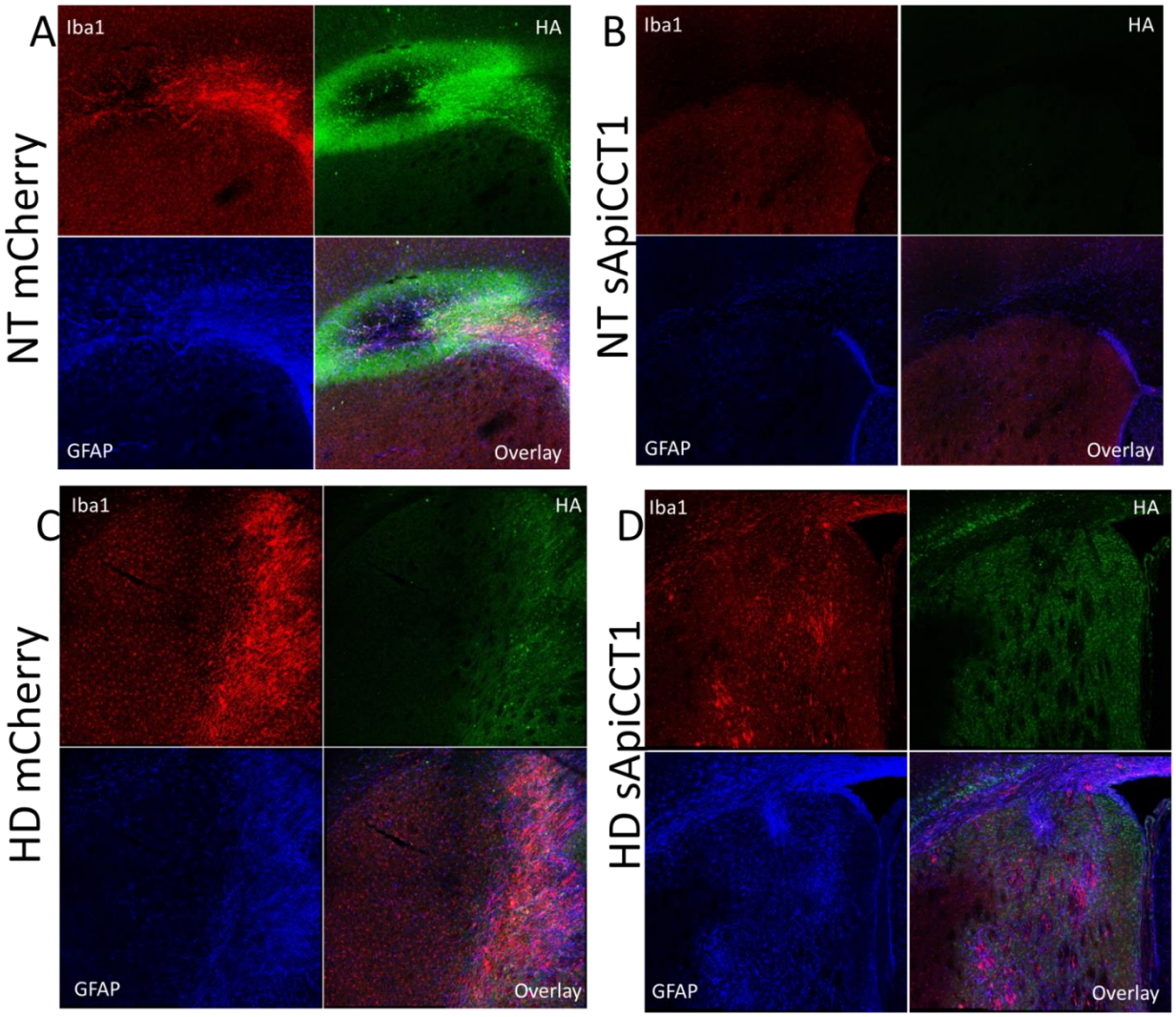

Figure 11: Activated microglia and astrocytes are found near areas of high virus expression. sApiCCT1 and mCherry tissue were stained with anti-HA (green), anti-Iba1 (red) and anti-GFAP (blue). (A-D) 10X images of areas transduced with virus. Activated microglia are found to co-localize with areas of high viral expression. (A, C, D) Virus expression is in the medial striatum (A,D) or along the white matter tract (A). Panels (A) and (B) show the cortex, striatum, and white matter tract. Panels (C) and (D) do not show cortex. (B) One animal did not show any apparent transduced cells, presumably due to clearance of the virus, and staining shows only normal, resting microglia.

Figure 2.12

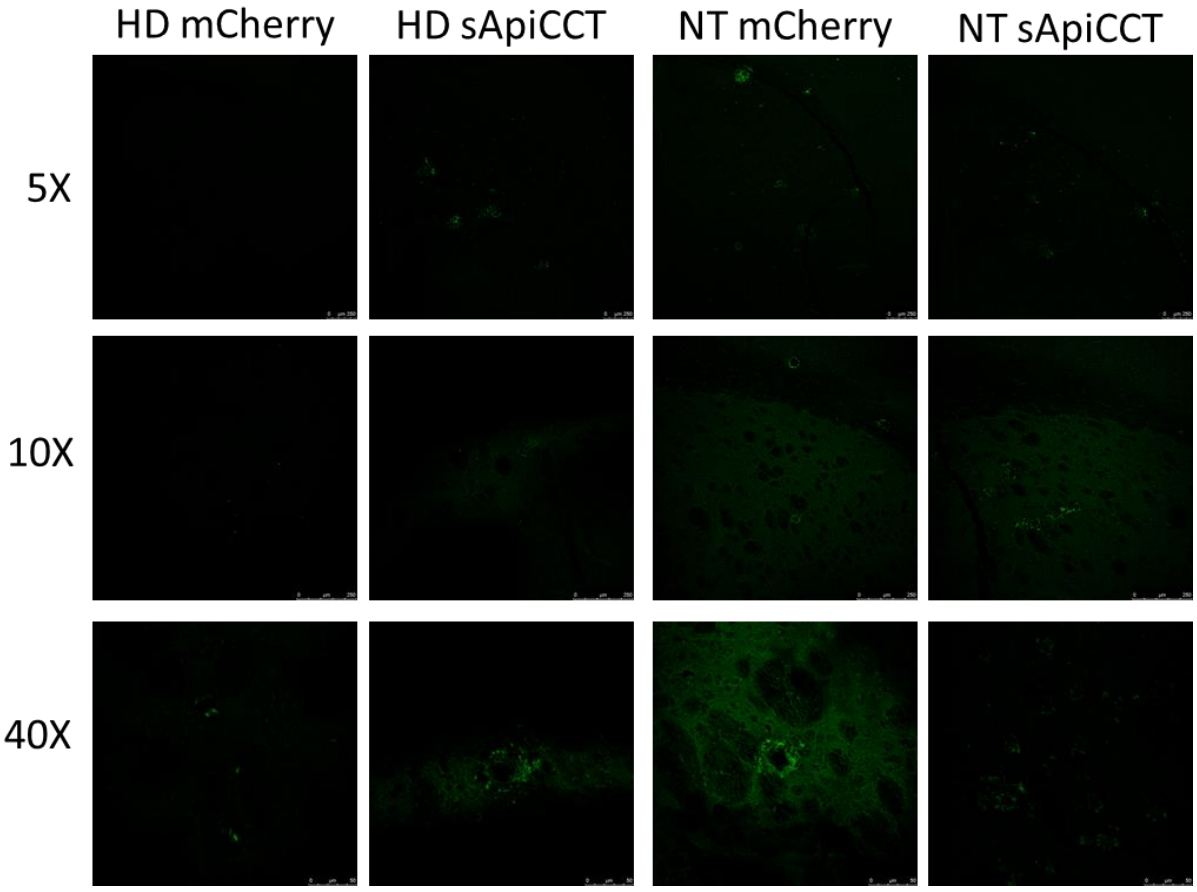

Figure 12: AAV2/1 viral injection does not induce cellular degeneration. Brain sections were stained with Fluoro-Jade neurodegeneration marker and visualized on a confocal microscope. Mice given AAV2/1 striatal injections show minimal cellular degeneration in both the striatum and cortex. 5x objective (top row), 10x (mid row), and 40x (bottom row) show very minor patches of degenerating cells spread throughout the striatum and cortex.

Figure 2.13

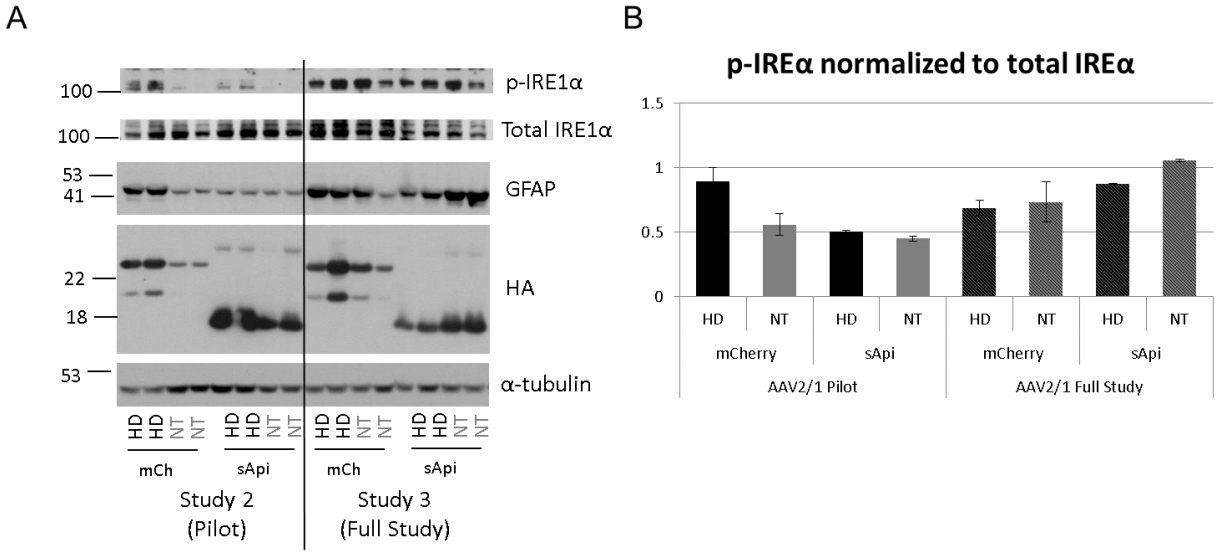

Figure 13: Studies may be confounded by an increase in ER stress. Striatal lysates from Study 2 and Study 3 were compared by western blot. (A top two panels, B) Animals from Study 3 show increased p-IRE1α, a marker of ER stress, compared to total IRE1α. (A) Animals from Study 3 also show increased GFAP in most animals. Both studies show similar levels of mCherry or sApiCCT1 expression. Membranes were probed with p-IRE1α (a marker of ER Stress), total IRE1α, GFAP (astrocytes), HA (treatment), and α-tubulin (loading control).

CHAPTER 3

Systemic delivery of secreted ApiCCT1 does not ameliorate disease phenotypes in HD mouse model

Summary

While Huntington's disease (HD) is characterized by overt degeneration of the striatum, other brain areas also exhibit pathology and cell death. Further, intrastriatal viral delivery does not broadly express throughout the striatum. Therefore, we sought to test global expression of sApiCCT1, an established modifier of mHTT accumulation. A recently created virus, PHP.B [142], exhibits high expression throughout the CNS and offers a method to study sApiCCT1 expression in the CNS via peripheral delivery versus injection into the brain. We find that PHP.B-sApiCCT1 systemic injection did not improve biochemical or motor readouts of HD phenotypes in this study. We also found microglial activation in areas of high virus expression and cell death in the striatum and cortex. Like the previously described study, this study may have been confounded by environmental factors or toxicity from the virus. Given the potential effects from virus delivery or the strong promoter used, it is not clear whether systemic delivery of sApiCCT1 could provide benefit in HD.

Introduction

HD results in massive degeneration of the medium spiny neurons of the striatum [5]. However, huntingtin (HTT) is ubiquitously expressed and pathology exists in other areas of the brain and the periphery. While medium spiny neurons of the striatum appear to be more susceptible to degeneration, the cerebral cortex actually shows the greatest mHTT aggregation and inclusion bodies are detected in the cortex, striatum, cerebellum and spinal cord [143]. Furthermore, one study shows that selective expression of mHTT

exon 1 in striatal neurons is not sufficient to cause locomotor deficits, although mice exhibit mHTT accumulation, and expression in both striatal and cortical cells is necessary to recapitulate all disease phenotypes [144]. Additionally, studies in BACHD mice indicate that it is necessary to target mHTT in both striatum and cortex together to ameliorate all behavioral deficits [145]. This suggests that therapeutics targeting multiple tissues and cell types may be more effective than targeting the striatum alone. The previous chapter provided evidence that AAV2/1-mediated delivery of sApiCCT1 in the striatum can ameliorate some motor and biochemical phenotypes in HD mice. However, a global approach to target pathology in other tissues may provide additional benefit. Finally, systemic delivery would ultimately be preferable to surgical intervention in the brain.

The present study examines the use of a modified AAV9 for global delivery of sApiCCT1. Until recently, intravenous administration of AAV9s offered widespread expression in the periphery with lower expression throughout the CNS [142]. One study found at least 20-fold lower expression in the brain compared to liver, heart, and skeletal muscle [146]. Deverman et al. [142] developed a modified AAV9 capsid that allowed for at least 40-fold greater expression throughout the CNS when injected systemically, providing a useful tool for non-invasive delivery of proteins to the brain [142]. This virus, PHP.B, can be administered intravenously and shows high expression in multiple tissues. Compared to traditional AAV9, PHP.B shows increased expression in cortex (40 fold), striatum (92 fold), thalamus (76 fold), cerebellum (41 fold), and spinal cord (75 fold). Remarkably, PHP.B shows approximately equivalent expression in brain

compared to liver [142]. We can utilize this delivery approach to not only express sApiCCT1 globally in the brain, but also in peripheral tissues.

To generate the PHP.B virus, a library of modified AAV9 capsid proteins was created containing various mutations within the first capsid protein (VP1). The AAV genome consists of two open reading frames, Rep and Cap, with Rep encoding proteins necessary for AAV life cycle, and Cap encoding capsid proteins. Cap encodes for expression of three different proteins (VP1, VP2, and VP3), which arise from alternative splicing of the Cap gene [147, 148]. VP1 is the largest, with the entire sequence of VP3 and VP2 contained within it. The AAV9 capsid library was generated by inserting randomized sequences of amino acids between amino acids 588 and 589 of the AAV9 VP1 capsid protein [142]. This domain is directly N-terminal to a region thought to facilitate binding to galactose on target cells, which allows for internalization of virus particles [149]. Therefore, all variants in the capsid library contain modified VP1 sequences that are likely to alter infection of target cells. Viruses were generated from this capsid library, intravenously introduced into mice, and sequences were selected based on the ability to cross the blood brain barrier (BBB) and infect CNS cells. AAV-PHP.B showed the highest CNS transduction efficiency and was therefore chosen for this study.

This study was designed to test the hypothesis that systemic delivery of sApiCCT1 improves rescue of HD phenotypes compared to the localized delivery discussed in the previous chapter. We found that PHP.B–sApiCCT1 treated animals showed no detectable improvements in HD phenotypes, increased activated microglia, and displayed an apparent increase in cellular degeneration in both HD and NT animals.

Results presented here suggest that systemic delivery of sApiCCT1 in this context did not rescue HD phenotypes and may exacerbate neurodegeneration.

Results

PHP.B injected mice show rapid expression of virus in the brain. The previous chapter of this dissertation utilized intrastriatal transplantation of AAV2/1. Traditional AAVs show minimal expression one week after transplantation with strong expression by three weeks after transplantation [150]. This delay in expression is not ideal as the rapidly progressing HD mice show mHTT accumulation early in disease progression and ApiCCT1 may work primarily to prevent accumulation of misfolded proteins [100]. One of the many benefits of the PHP.B virus is that it rapidly expresses protein, with cell transduction seen as early as 24 hours after injection [142]. To verify onset of expression, C57 mice were given retro-orbital injections of PHP.B-GFP (4e10 vg/g) (n=3). With this technique, a single bolus is injected into the retro-orbital sinus, a large area posterior to the orbital cavity that contains a substantial amount of blood flow. Retro-orbital injections were chosen over tail vein injections for systemic delivery as this technique is more humane, less technically challenging, and allows for injection of larger volumes (up to 150µl) [151]. Tissue was harvested 10 days after injection and mice show robust and widespread expression of GFP (Fig. 1). GFP expression is seen in both the striatum and cortex. These results indicate that PHP.B virus begins expressing rapidly and provides an opportunity to systemically express sApiCCT1 early in disease progression.

PHP.B-sApiCCT1 injected mice do not exhibit behavioral improvements. To test the *in vivo* efficacy of global delivery of sApiCCT1, HD mice were given retro-orbital injections of PHP.B-sApiCCT1 or GFP control. We chose to test this viral delivery approach in R6/2 mice as they have a rapidly progressive and highly consistent phenotype for preclinical analysis, thus taking advantage of the rapid expression of the PHP.B virus. Like R6/1 used in the previous study, R6/2 are a fragment model of HD, expressing exon 1 of human mHTT [3]. However, the R6/2 transgene contains an increased repeat length at ~150 Qs with a rapid onset and quickly progressing phenotype. R6/2 are well-characterized and have been used by our group and many others to test therapeutics and modifiers of mHTT accumulation [51, 62, 75]. The virus was again delivered systemically via retro-orbital injection.

R6/2 mice were given retro-orbital injections of PHP.B-sApiCCT1 or GFP control at 5 weeks of age (3E10 vg/g). The four groups injected are as follows: (1) Non-transgenic (NT) treated with PHP.B-GFP control virus (n=7 males, 5 females). (2) NT treated with PHP.B-sApiCCT1 (n=6 males, 6 females). (3) HD treated with PHP.B-GFP (n=8 males, 10 females). (4) HD treated with PHP.B-sApiCCT1 (n=8 males, 11 females). Behavioral phenotypes were analyzed by rotarod, pole test, or clasping as described in chapter 2 of this dissertation.

No treatment effect was observed for any of the assayed motor phenotypes (Fig 2). Animals treated with sApiCCT1 show no improvements on rotarod (Fig. 2A, B), pole test (Fig. 2C D), or clasping (Fig. 2E). Groups were analyzed by two-way ANOVA followed by Bonferroni post-testing. Significance is denoted by letters above bars; bars with different letters are significantly different from one another. Rotarod and pole test each

show a significant genotype at each timepoint as expected for this mouse model [3]; however, there is no treatment effect for any time point.

Retro-orbital injection of PHP.B shows widespread expression in striatum and cortex and co-localized with activated microglia. Mouse tissue was harvested at 10 weeks of age, 5 weeks after injection. Sections were co-stained with anti-HA (sApiCCT1), anti-Iba1 (microglia), and anti-GFAP (astrocytes). Immunohistochemistry confirms virus expression in both striatum and cortex (Fig. 3E). The choroid plexus is visible in one animal (Fig 3A) and PHP.B-sApiCCT1 appears to transduce the choroid plexus. This is not surprising as AAV9 has previously been shown to transduce choroid plexus cells [152]. Consistent with the previous study in this dissertation, viruses appear to co-localize with activated microglia. Microglia activation is identified by a change in morphology, including a swollen cell body and thicker processes [131].

Retro-orbital PHP.B-sApiCCT1 treatment does not reduce mHTT accumulation in R6/2 mice. Whole cell lysates were analyzed by AGE and PAGE followed by western blot. Western blot analysis confirms virus expression in striatum (Fig 4C) and cortex (Fig 5C) for most animals. While the amount of virus varies between animals, viral expression in an individual animal remains consistent between striatum (Fig 4C) and cortex (Fig 5C). Animals with high expression in the striatum also show high expression in the cortex. Three animals appear to have no virus expression in either striatum or cortex (animals 4, 6, and 13).

AGE analysis indicates that there is no change in oligomeric mHTT in the striatum (Fig. 4A). While there is a moderate decrease in oligomeric mHTT in the cortex, this effect is

not significant (Fig. 5). Because some animals show higher expression in the cortex compared to the striatum (Fig. 3E), it is possible that ApiCCT1 has some mHTT modulatory effect in the cortex. Even so, this result is consistent with study 3 of the previous chapter, both of which are in contrast with previous *in vitro* studies [63, 93, 105].

We next sought to examine any effect on insoluble mHTT given our previous data [51] showing that modulation of this species was associated with improved phenotypes. Lysates were fractionated into detergent-soluble and detergent-insoluble fractions as described in chapter 2, with the detergent-insoluble fraction containing nuclear proteins and high MW, insoluble mHTT. As with the other analyses, there is no change in insoluble mHTT accumulation with treatment of sApiCCT1 in either striatum (Fig 6A) or cortex (Fig 6B). This is not surprising given that the previous study presented in this dissertation also found a minimal impact on insoluble mHTT.

PHP.B injected mice show increased degeneration. Because immunohistochemistry indicates an immune response to the virus itself (Fig. 3), we asked whether viral delivery itself is toxic. To test this, we stained brain sections with Fluoro-Jade, a stain used for the assessment of neurodegeneration [132]. Widespread staining with Fluoro-Jade is apparent in all animals (Fig 7A). Degenerating cells are apparent in both HD and NT animals treated with either PHP.B-sApiCCT1 or PHP.B-GFP. Staining at the 5x and 10x images (top two rows) indicates that degeneration is widespread throughout the striatum and cortex. 40x images (bottom row) show detailed images of degenerating cells in the striatum. Compared to mice injected with AAV2/1 in the previous chapter (Fig 7B), PHP.B-injected mice exhibit an increase in degenerating cells. It is important

to note that these studies utilized different mouse models and are therefore not directly comparable. While these animals are from different studies and are different strains, the NT animals originate from the same strain (CBA x C57/BL6) and wild-type animals are not known to show this high level of staining with Fluoro-Jade. Therefore it is likely that the differences between them are due to viral treatment.

Because we see a considerable amount of degenerating cells even in the NT animals, this may be an indication that the virus itself might be causing cell death. Toxicity studies comparing viral serotypes show that AAV9 has lower toxicity compared to AAV1 and approximately equal toxicity compared to AAV2 in transduced PCNs [153]. This observation could be explained by a few scenarios. First, it is possible that a toxic effect may be due to the VP1 modification that allows PHP.B to infect the CNS with high efficiency. Alternatively, the mice from this cohort may have been more susceptible to toxic effects from viral expression. As with our previous study, these studies were performed while there was heavy construction on an adjacent building. Both studies performed during this time showed an unexpected response to the virus and it is possible that both cohorts were more susceptible to external stressors.

Discussion

Data presented here tested the systemic delivery of PHP.B expressing ApiCCT1 in the context of a neurodegenerative disease for high expression in the CNS. Systemic delivery did not ameliorate HD symptoms and, in fact, the PHP.B virus with the CAGG promoter used appears to induce cell death. AAV9 viruses have been shown to have

one of the lowest toxicity profiles compared to other commonly used AAV's [153]. It is unclear what is causing the increase in cellular degeneration and microglia activation; however, we have several hypotheses to explain our observations. The PHP.B virus offers the highest known expression in the CNS after intravenous injection. In chapter 2 of this dissertation, we found that activated microglia associate with areas of high AAV2/1 viral expression. The widespread and strong expression of PHP.B may cause toxicity and microglia activation in multiple cell types throughout the CNS. Thus, the abnormal microglia and Fluoro-Jade staining we see may simply be due to abnormally high virus expression. This may be exacerbated by environmental factors. Alternatively, the VP1 mutations that allow for efficient CNS transduction may confer toxicity. Use of this virus has not yet been published in the context of neurodegenerative disease. It is possible that the mutation within the VP1 capsid protein that increases CNS expression also causes cell death. The use of the relatively strong CAGG promoter in the context of this virus could also have overt effects. Finally, the selected mouse model R6/2, which shows a rapidly progressing phenotype vulnerability to exogenous stressors, may be more susceptible to any viral effects. The findings of the present study cannot directly evaluate these hypotheses. It will be helpful in future research to characterize the association between activated microglia, inflammatory responses, cell death, and viral expression in multiple cell types and also test the use of this virus in long-term HD mouse models.

Although we were not successful in eliciting a therapeutic effect with PHP.B, global expression of ApiCCT1 may still be a useful approach for delivering therapeutic proteins. HD is a disease resulting in neuronal death. For this reason, many therapies

have focused on delivering therapies to the brain. However, mHTT is ubiquitously expressed in all tissues [60]. Although peripheral pathology is less well understood, a number of studies have reported impairments in peripheral tissues, including fibroblasts [154], muscles [155], and liver [156]. Both R6/2 and *Hdh*Q150 have visible intranuclear mHTT inclusions in peripheral tissue [157]. Notably, HD patients have a number of peripheral symptoms, including abnormal skeletal muscle metabolism [158], insulin sensitivity [159], and mitochondrial abnormalities [160]. Therefore, it is possible that targeting mHTT systemically may offer additional benefits.

Conversely, if peripheral expression of sApiCCT1 is not protective, it is possible that the reason we were unable to detect a change in behavioral or biochemical outcomes in this study is due to the peripheral expression having a negative impact. By binding to mHTT in peripheral tissues, ApiCCT1 may be preventing endogenous function of HTT and exacerbating disease progression. Given the unclear effect of PHP.B expression on toxicity, we are unable to draw conclusions about global expression of sApiCCT1 from this study. Future studies should focus on characterizing systemic delivery of sApiCCT1 using alternative methods in addition to PHP.B as well as testing of this delivery method in the slower progressing R6/1 model and/or using alternative promoters. Traditional AAV9 would provide an opportunity to characterize the effect of sApiCCT1 on peripheral tissues.

MATERIALS AND METHODS

PHP.B retro-orbital injections

Constructs were generated expressing ApiCCT1 with an IL2 secretion signal or GFP under a CAG promoter and PHP.B virus was generated as previously described [142]. In the first experiment, 5 week old C57 mice were given retro-orbital injections of PHP.B-GFP (4E10 vg/g) (n=3). Retro-orbital injections were performed as previously described [151]. Tissue was harvested 10 days after injection (Fig. 1) and tissues analyzed by immunohistochemistry. In the subsequent experiment, R6/2 mice were given retro-orbital injections of PHP.B-sApiCCT1 or PHP.B-GFP (3E10 vg/g) at 5 weeks of age. The four groups injected are as follows: (1) Non-transgenic (NT) treated with PHP.B-GFP control virus (n= 7 males, 5 females). (2) NT treated with PHP.B-sApiCCT1 (n=6 males, 6 females). (3) HD treated with PHP.B-GFP (n= 8 males, 10 females). (4) HD treated with PHP.B-sApiCCT1 (n= 8 males, 11 females). Tissue was harvested 5 weeks after injection (Fig. 2-8). Mice were euthanized and tissue was harvested as described [130]. Mice were sacrificed by Euthasol followed by transcardinal perfusion. Cortex and striatum were microdissected from one hemisphere and flash frozen for biochemical analysis. The other hemisphere was fixed in paraformaldehyde overnight, transferred to 30% sucrose solution, and sectioned using a microtome.

Mouse Behavior and Tissue Harvest

Behavioral outcomes were analyzed using rotarod, pole test, and clasping. At 10 weeks of age (5 weeks after injection). Mice were sacrificed by Euthasol followed by transcardinal perfusion. Cortex and striatum were microdissected from one hemisphere and flash frozen for biochemical analysis. The other hemisphere was fixed in paraformaldehyde overnight, transferred to 30% sucrose solution, and sectioned using a microtome.

Histology

Brain sections were analyzed by immunohistochemistry. Slices were stained with the following antibodies: anti-HA (Sigma H6908), anti-EM38 (Millipore MAB5374), anti-Iba1 (Wako Pure Chemicals Industries 27030), anti-βIII-tubulin (Covance PRB-435P-100), anti-GFAP (Abcam ab7260), and ToPro3 nuclear stain. Alexa fluorescent-conjugated secondary antibodies were used (Life Technologies). Stained tissue was mounted on slides and coverslipped with Fluoromount-G (SouthernBiotech). Images were acquired on a LeicaDM2500 confocal microscope.

Soluble/Insoluble Fractionation

Fractionation protocol was modified from O-Rourke, et al [129]. Brain tissue was homogenized in lysis buffer (10mM Tris (pH 7.4), 1% Triton X-100, 150mM NaCl, 10% glycerol, and 0.2 mM PMSF) with Roche Complete Protease Mini and PhosphoStop pellets. Tissue was kept frozen on dry ice until immediately before homogenization. Homogenized tissue was incubated on ice for 60 minutes before centrifugation at 15,000xg for 20 minutes at 4°C. Supernatant represents the detergent-soluble fraction. The pellet was washed 3x with lysis buffer and centrifuged at 15,000xg for 5 minutes each at 4°C. The pellet was then resuspended in lysis buffer supplemented with 4% SDS, sonicated 3x, and boiled for 30 minutes. The resuspended pellet represents the detergent-insoluble fraction. Detergent-insoluble fractions samples were analyzed using a 3-8% Tris-Acetate polyacrylamide gel (Invitrogen),and detergent-soluble samples with NuPAGE 4-12% Bis-Tris polyacrylamide gel (Invitrogen), followed by western blot.

Polyacrylamide (PAGE) and Agarose (AGE) gel electrophoresis

Brain tissue was lysed in modified RIPA (radio immune precipitation) buffer containing 10mM Tris, pH7.2, 158mM NaCl, 1mM EDTA, 0.1% SDS, 1% Triton X-100, 1% sodium deoxycholate, and 1x Complete protease inhibitors (Roche) as described previously [62]. Samples were analyzed by both PAGE and AGE. SDS-AGE followed by Western blot analysis was performed a previously described [1, 62, 63, 140, 141]. Samples were analyzed with either NuPAGE 4-12% Bis-Tris polyacrylamide gel (Invitrogen), 3-8% Tris-Acetate polyacrylamide gel (Invitrogen), or 15% Criterion Bis-Tris polyacrylamide gel (Bio-Rad), followed by western blot. Blots were quantified using ImageJ software. Membranes were probed with the following antibodies used were: anti-5492 (Millipore), anti-HA (Sigma), anti-GFP (Living Colors), and anti-α-tubulin (Sigma).

Fluoro-JadeB

Brain sections were stained with Fluoro-Jade B (Millipore AG310) to visualize degenerating cells. Mounted brain sections were dehydrated in 80% then 70% ethanol for 2 minutes and 2 minutes, respectively. After a 3 minute rinse in H_2O, slides were immersed in 0.06% $KMnO_4$. Slides are rinsed in H_2O and incubated in 0.0004% Fluoro-Jade B in 0.01% acetic acid for 15 minutes with rotation. Slides are rinsed 3 times in H_2O and dried in the dark for 1 hour. Once dry, slides are immersed in 3 changes of xylene for 1 minute each and air dried for 10-20 minutes before coverslipping in DPX mounting media (Electron Microscopy Services 13512).

MSD (Meso Scale Discovery) Proinflammatory Assay

Proinflammatory cytokines were analyzed using the MSD Proinflammatory Palel 1 (mouse) kit (V-PLEX K15048D). 200µg of protein was analyzed in duplicates for each

sample. Samples were analyzed according to the manufacturer's instructions. Briefly, samples were diluted 2 fold in Diluent 41 before adding to the plate. Detection antibodies were diluted 50 fold in Diluent 45. Samples are added to the plate and incubated with shaking for 2 hours. The plate is washed 3 times with wash buffer and 25µl of the diluted detection antibody solution is added to each well and incubate with shaking overnight. The plate is washed 3 times with wash buffer and 150µl of 2x Read Buffer T and read on the MESO QuickPlex SQ 120.

CHAPTER 3

FIGURES

Figure 3.1

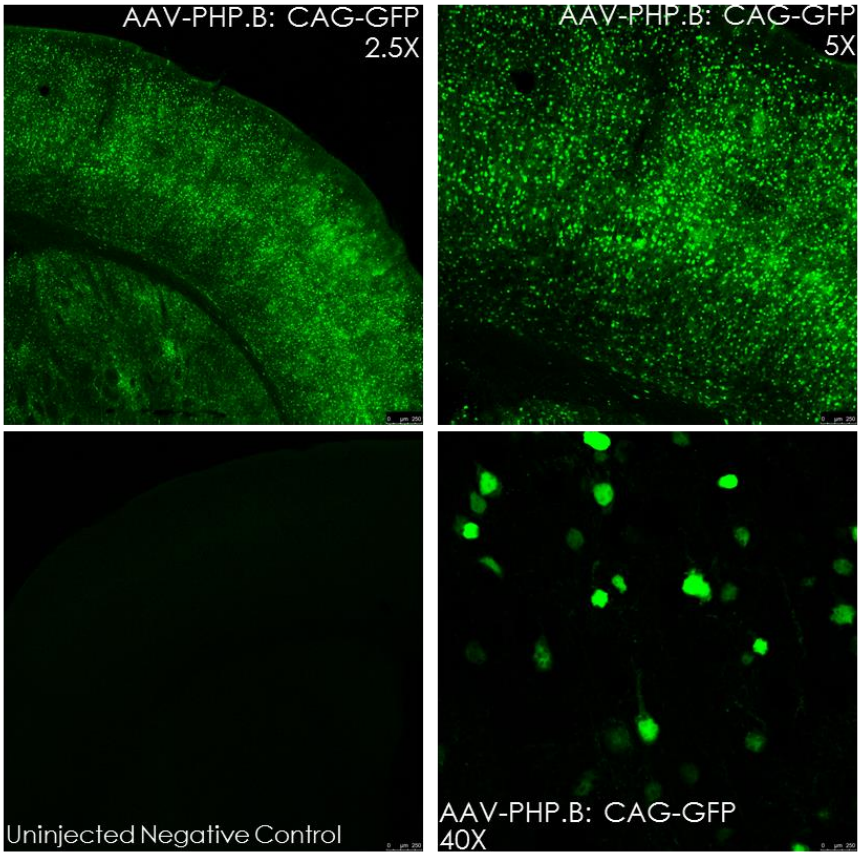

Figure 1: PHP.B-GFP viruses shows high expression 10 days after retro-orbital injection in C57 mice. C57 mice were given retro-orbital injections of PHP.B-GFP. Tissue was collected 10 days later and immunohistochemistry performed against GFP. Mice exhibit widespread expression of GFP in both the striatum and cortex.

Figure 3.2

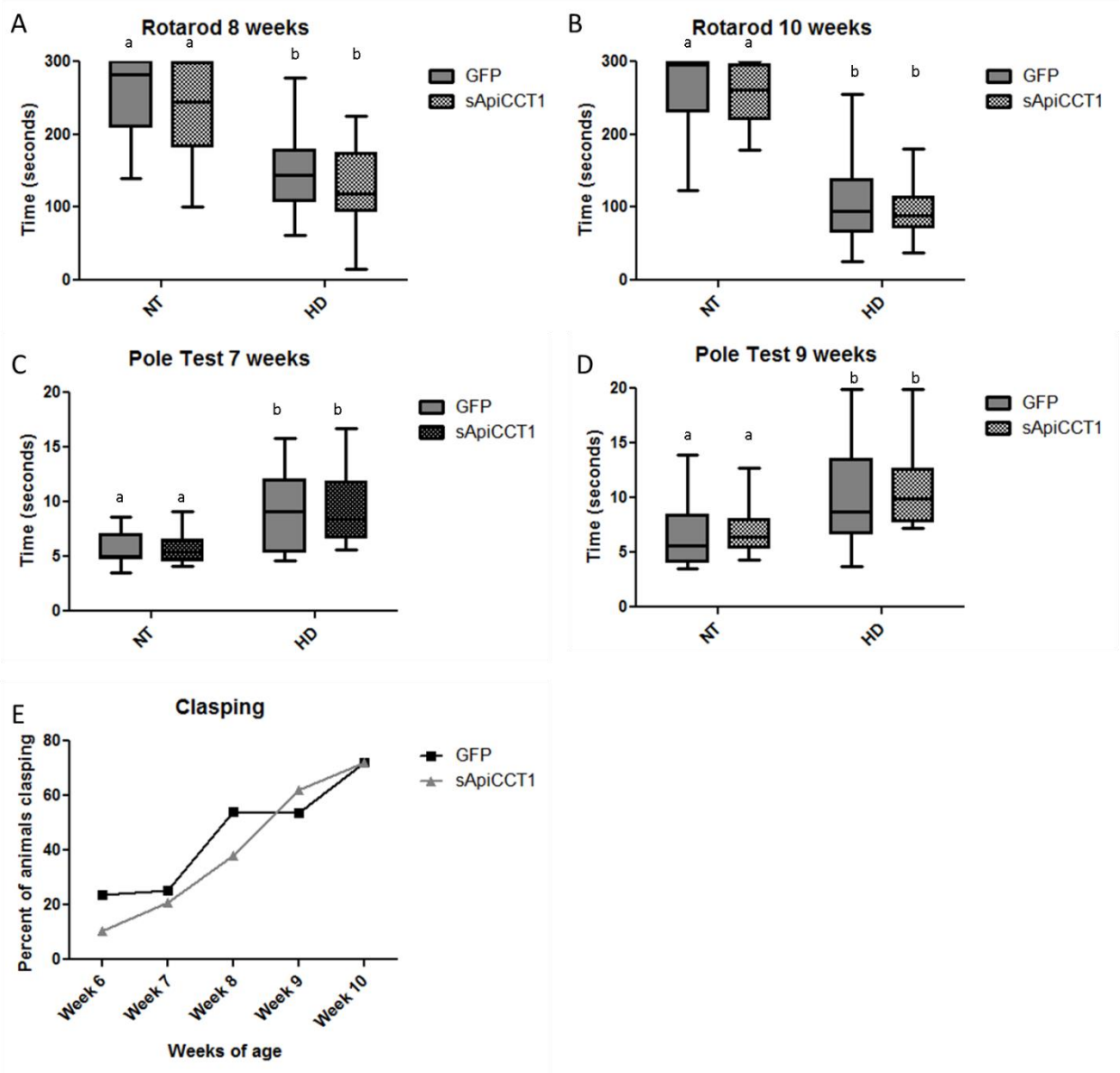

Figure 2: PHP.B-sApiCCT1 injected mice do not show improvements in behavioral outcomes. Mice were given retroorbital injections of PHP.B-sApiCCT1 or PHP.B-GFP at 5 weeks of age and behavioral outcomes analyzed. (A-B) Rotarod shows no treatment effect at either 8 or 10 weeks of age. (C) Pole test shows no treatment effect at 9 weeks of age. (D) Treatment with PHP.B-sApiCCT1 does not improve clasping behavior. Significance bars denote genotype effects in behavior.

Figure 3.3

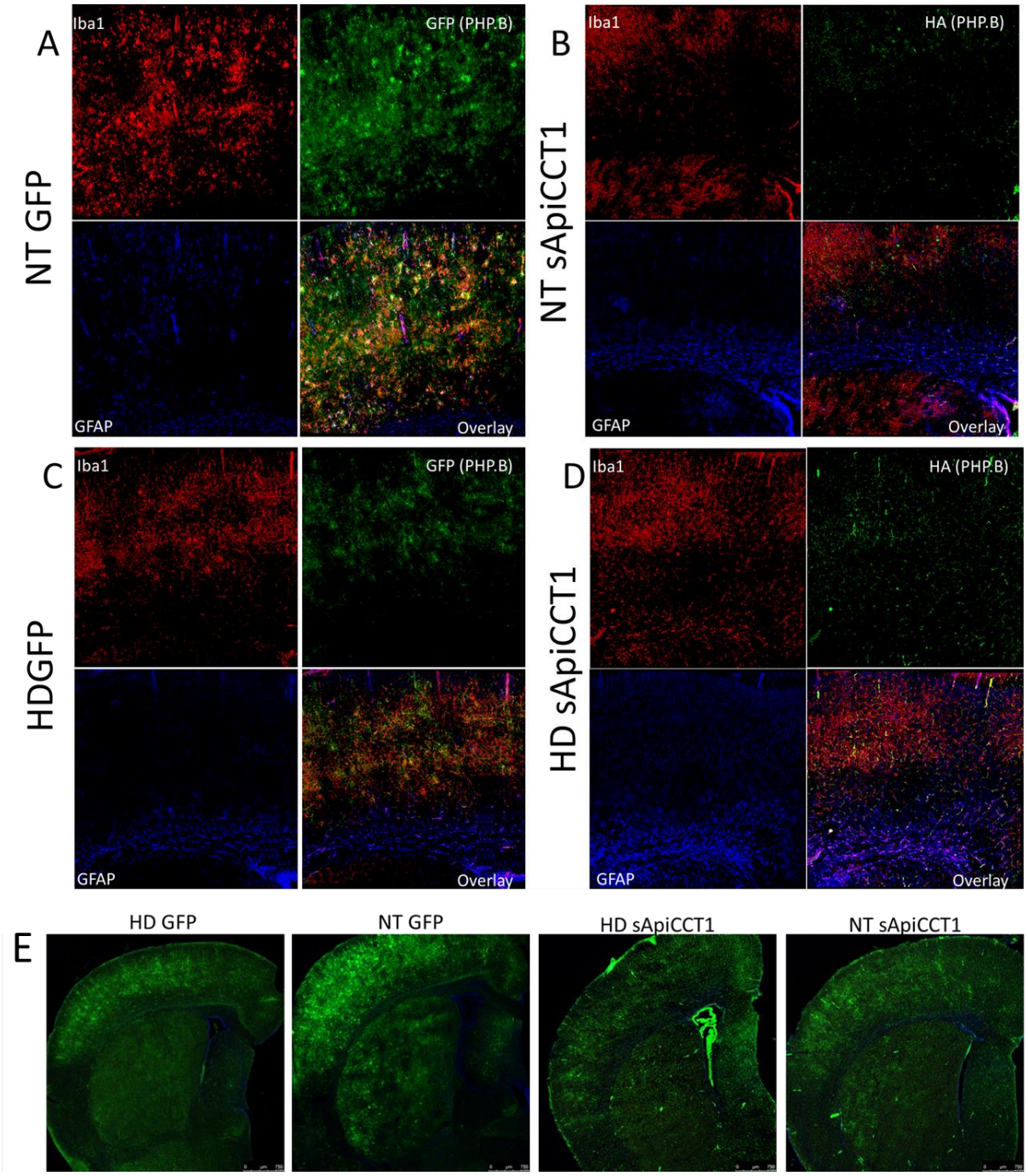

Figure 3: Activated microglia are found near areas of high virus expression. Brains were sectioned and stained with anti-Iba1 (red, microglia), anti-GFAP (blue, astrocytes), and anti-GFP or anti-HA (green, treatment). (A-D) 10X image of the cortex. There appear to be microglia activation surrounding the areas with high virus expression. All animals show some activation of microglia, with panel (A) showing the most microglial activation and also the highest viral expression.

Figure 3.4

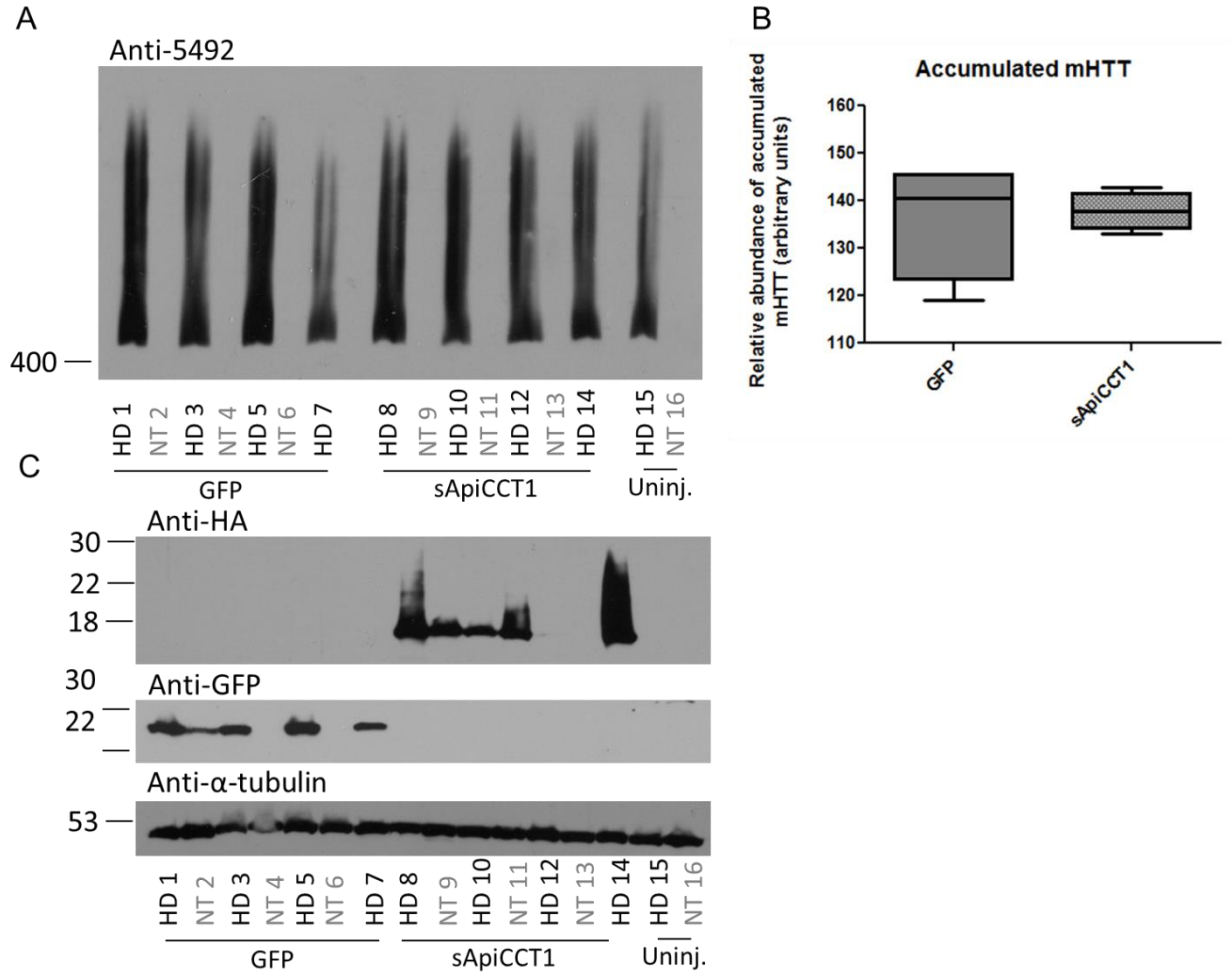

Figure 4: PHP.B-sApiCCT1 does not ameliorate mHTT accumulation in striatal tissue from treated R6/2 mice. (A) Western blot analysis of striatal tissue from animals treated with system PHP.B-sApiCCT1. Whole cell lysate were analyzed by AGE to assess mHTT accumulation and PAGE to confirm viral expression. Retro-orbital injection of PHP.B-sApiCCT1 does not reduce mHTT accumulation (p=0.54). (B) Quantitation of AGE western blot. (C) Virus is expressed in most animals, with the exception of four animals who do not have detectable virus.

Figure 3.5

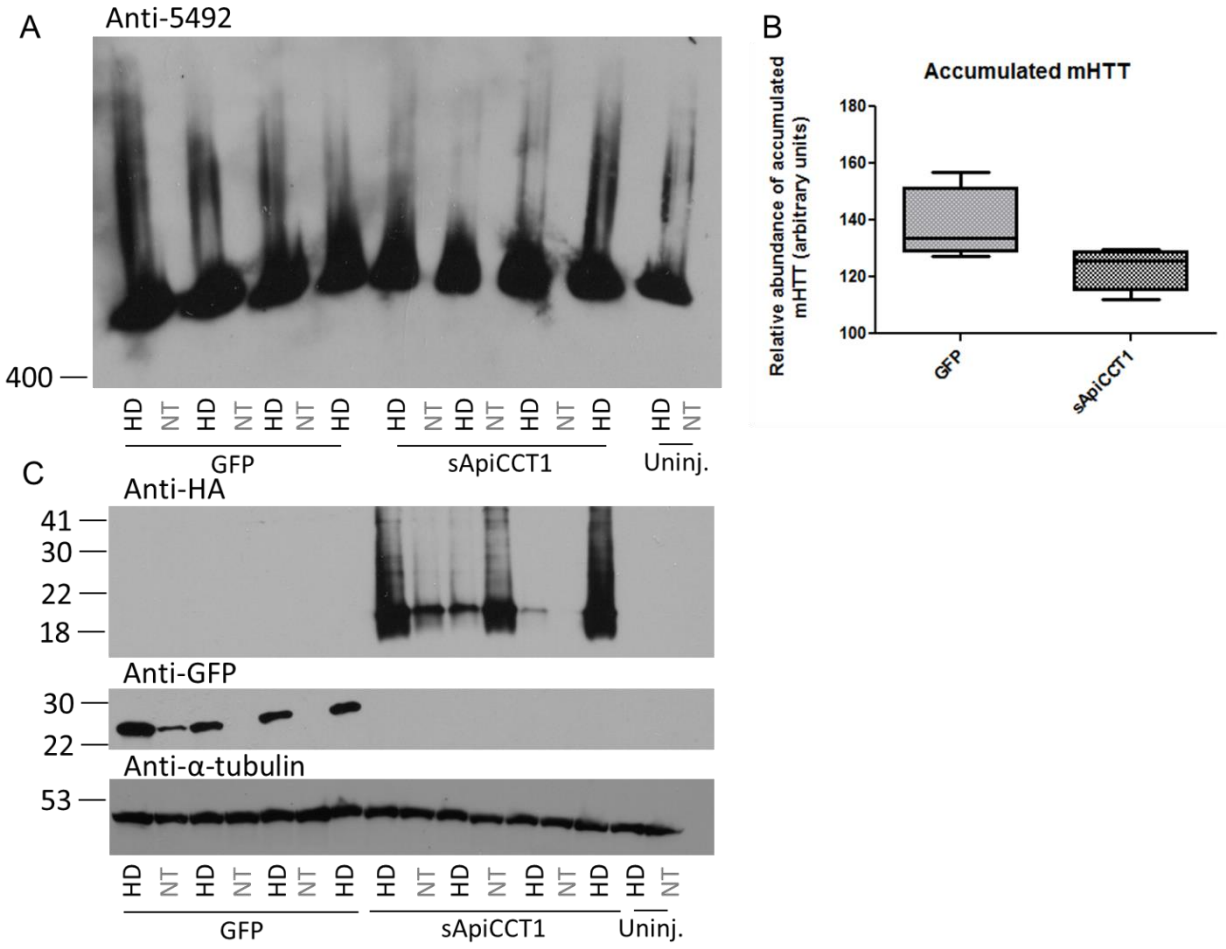

Figure 5: PHP.B-sApiCCT1 does not ameliorate mHTT accumulation in cortex. (A) Western blot analysis of cortical tissue from animals treated with system PHP.B-sApiCCT1. Retro-orbital injection of PHP.B-sApiCCT1 does not reduce mHTT accumulation. (B) Quantitation of AGE western blot. Shows a slight reduction in oligomeric mHTT; however, this effect is not significant (p=0.09). (C) Virus is expressed in most animals, with the exception of a few NT animals .

Figure 3.6

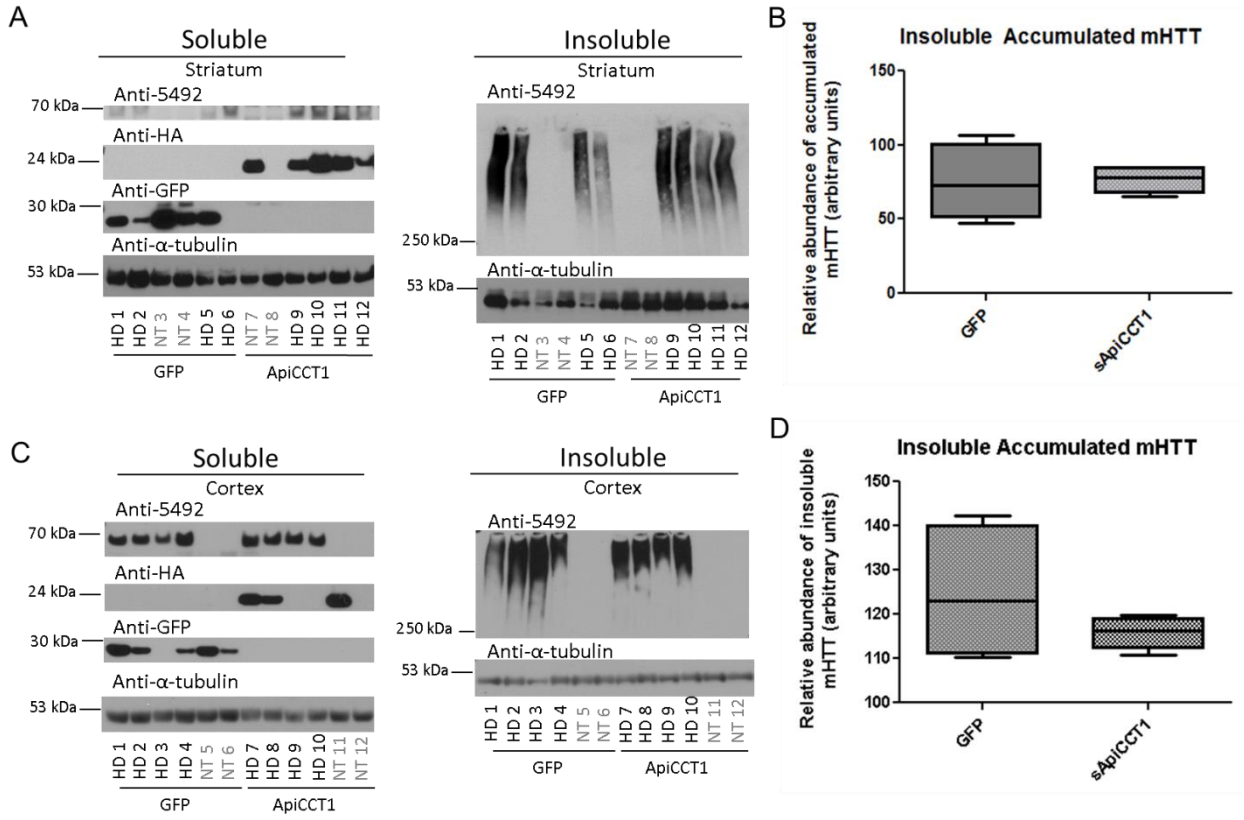

Figure 6: PHP.B-sApiCCT1 does not alter insoluble mHTT accumulation. Western blot analysis of striatal (A, B) and cortical (C, D) mouse tissue separated into detergent-insoluble and detergent-soluble fractions. AAV2/1-sApiCCT1 does not change the amount of insoluble mHTT in either striatum (A, B) or cortex (C, D). (B, D) Quantitation reveals no significant change in insoluble mHTT in either striatum or cortex.

Figure 3.7

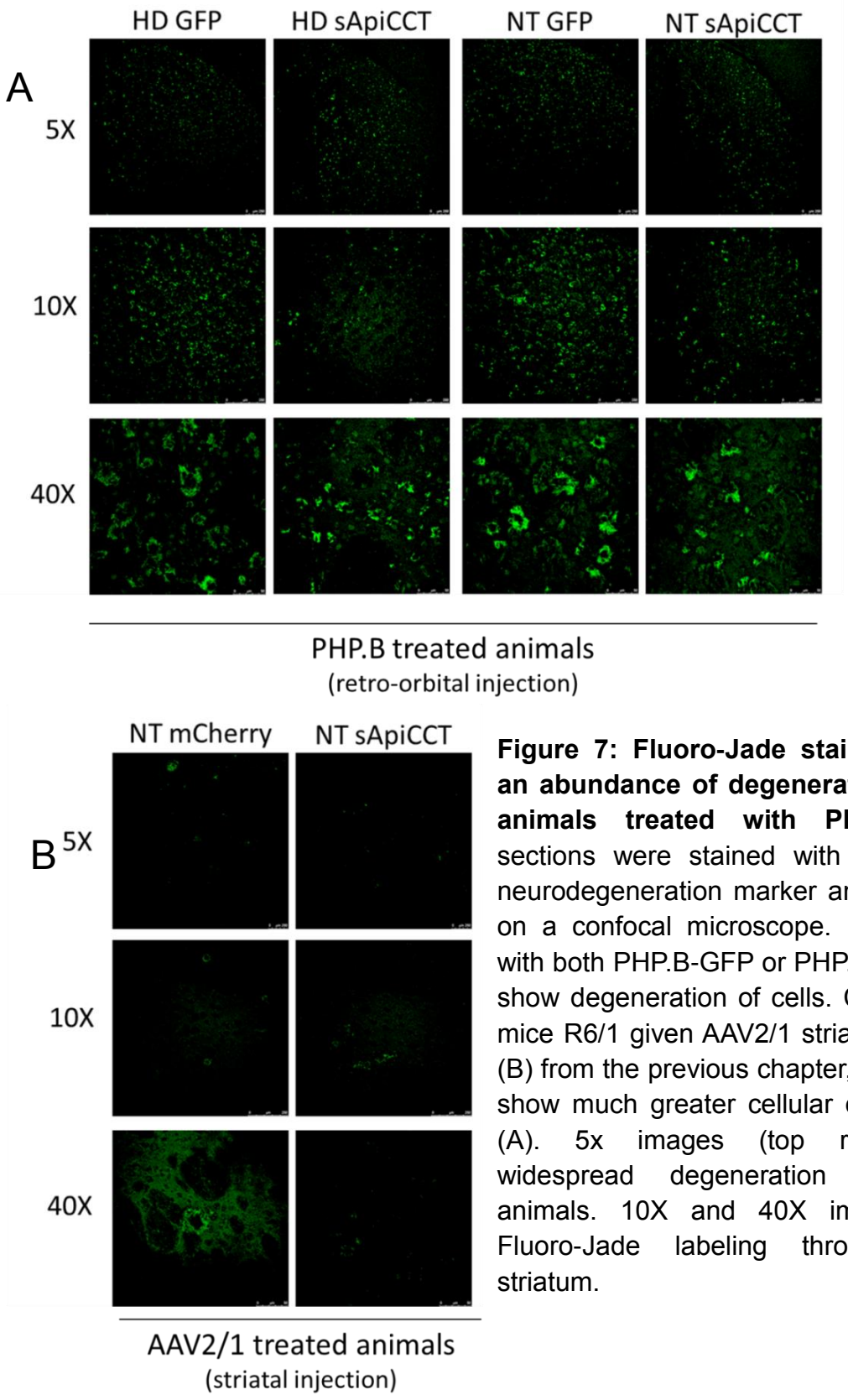

Figure 7: Fluoro-Jade staining shows an abundance of degenerating cells in animals treated with PHP.B. Brain sections were stained with Fluoro-Jade neurodegeneration marker and visualized on a confocal microscope. Mice treated with both PHP.B-GFP or PHP.B-sApiCCT1 show degeneration of cells. Compared to mice R6/1 given AAV2/1 striatal injections (B) from the previous chapter, PHP.B mice show much greater cellular degeneration (A). 5x images (top row) shows widespread degeneration in treated animals. 10X and 40X images show Fluoro-Jade labeling throughout the striatum.

CHAPTER 4

Mouse stem cell-mediated delivery of secreted ApiCCT1 reduces oligomeric mHTT in HD mice

Summary

Stem cell transplantation is a potentially promising approach to treat neurodegenerative disease, providing neuroprotection and rescuing disease phenotypes. Stem cells can be engineered to overexpress therapeutic targets, offering a novel delivery method and potential combination therapy. In the present study, we provide a proof of concept for utilizing mouse neural stem cells (mNSCs) engineered to secrete ApiCCT1, an established modifier of mHTT accumulation. We find that HD mice treated with mNSC-sApiCCT1 show reduced oligomeric mHTT compared to vehicle or mNSC-treated mice; however, we there were no improvements in motor phenotypes measured compared to mNSC alone.

Introduction

Stem cells offer a unique and powerful approach to treat neurodegenerative diseases. The first clinical trials supporting use of stem cells came from fetal tissue transplants, which contain stem and progenitor cells [161]. Transplantation of fetal neural tissue shows moderate clinical improvements in both Parkinson's disease (PD) and Huntington's disease (HD) patients [91, 114, 115, 162, 163]. Furthermore, researchers have shown efficacy for stem cell-based therapies in cell and animal models for a number of neurodegenerative diseases, including Alzheimer's disease (AD) [110, 111], PD [164] and HD [112]. In AD mouse models, transplantation of either mouse or human neural stem cells (NSCs) can improve cognition, enhance synaptic plasticity, and improve neuronal loss [110, 165, 166]. Similarly, striatal transplantation of mouse NSCs (mNSCs) or human neural progenitor cells (hNPCs) in a PD mouse model improves performance on cognitive and motor behavioral tasks [113, 162]. Our lab finds that striatal transplantation of mouse or human NSCs can each provide neuroprotection in

HD mice, ameliorating motor deficits, decreasing aberrant protein accumulation while increasing production of BDNF [manuscript submitted on human NSC transplantation].

The above studies suggest that neuroprotective effects of stem cell transplantation in neurodegenerative diseases may be at least in part mediated by an increase in neurotrophic factors, including BDNF (unpublished data) [110, 113]. While neurotrophic support rescues disease phenotypes and provides neuroprotection, it may be improved upon by combining stem cell transplantation with a therapy to directly target the disease-causing mHTT protein.

Transplantation of cells overexpressing therapeutic proteins has been studied by multiple groups; however, most research has focused on overexpression of neurotrophic factors [167]. The Svendsen group [168] showed that mouse neural progenitor cells (mNPCs) engineered to overexpress glial-derived neurotrophic factors (GDNF) improve behavioral outcomes and neuronal survival compared to control mNPCs when transplanted into HD mice [168]. Here, we provide a proof of concept for transplantation of mNSCs engineered to secrete the apical domain of the first subunit of CCT (ApiCCT1). Previous studies in this dissertation indicate that ApiCCT1 can modulate mHTT accumulation *in vivo*, however studies have been confounded by multiple factors, including potential immune responses from virus expression. We find that hNSC transplantation reduces microglial activation in at least one HD mouse model, another indication that stem cells may be a better choice for delivering sApiCCT1 compared to virus. Combining the neuroprotective effect of mNSCs with the ability of ApiCCT1 to directly target mHTT may produce a powerful combination therapy. Data from chapter 2 of this dissertation suggests that secreted ApiCCT1 (sApiCCT1)

can enter neighboring cells *in vivo,* indicating that secretion of ApiCCT1 from transplanted cells could modulate phenotypes in host tissue. In this study, we find that transplantation of mNSCs secreting ApiCCT1 reduces mHTT accumulation in HD mice. However, we were not able to detect an improvement in motor outcomes compared to mNSCs alone, mostly likely due to the relatively small cohort size. This study serves as a proof of concept for a combination therapy utilizing ApiCCT1 secreting stem cells; however, more research is needed to optimize expression and examine the effect of these cells on HD pathology.

Results

Secreted ApiCCT1 from mouse neural stem cells (mNSC-sApiCCT1) enters mouse primary cortical neurons (PCNs) and can reduce oligomeric mHTT accumulation. To evaluate the efficacy of a stem cell-based approach, mouse neural stem cells (mNSCs) were engineered to constitutively express secreted ApiCCT1 (sApiCCT1) and tested *in vitro* and *in vivo*. Pooled mNSC-GFP cells were stably selected for human His-tagged sApiCCT1 or ApiCCT1 (Fig. 1A). A chicken β-Actin promoter coupled with CMV early enhancer (CAG or CAGG) promoter was chosen for its high expression in multiple cell types, an important consideration as NSCs differentiate to multiple cell types after transplantation [169, 170]. To confirm secretion of ApiCCT1 from cells, conditioned media was collected from cells grown for 48 hours, and a Nickle column used to pull down His tagged ApiCCT1. ApiCCT1 was confirmed in cells expressing ApiCCT1 with a secretion signal, but not untransfected or unsecreted controls (Fig 1B). Cells were co-cultured with PCNs that were transfected with 97QP. ApiCCT1 does appear to get into

cells in co-culture; however, the expression is very low. Even with low uptake, cells co-cultured with ApiCCT1 show a reduction in oligomeric mHTT (Fig 1D). Whole cell lysates were analyzed by Agarose gel electrophoresis (AGE), which resolves fibrillary oligomeric mHTT [1, 63]. AGE followed by western blot suggests that even at a low concentration, ApiCCT1 prevents accumulation of mHTT in PCNs. This is an indication that mNSCs could potentially be used as a delivery vehicle for sApiCCT1.

mNSC transplantation improves behavioral phenotypes in R6/2 mice; however, no additional improvements are seen with mNSC-sApiCCT1. Mice were transplanted with mNSC-sApiCCT1, mNSCs, or vehicle control (100,000 cells per hemisphere). The six groups injected are as follows: (1) Vehicle treated non-transgenic (NT) (n= 5 males). (2) NT treated with mNSC-GFP (n=7 males). (3) NT treated with mNSC-GFP-sApiCCT1 (n=7 males). (4) Vehicle treated HD (n= 5 males). (5) HD treated with mNSC-GFP (n= 7 males). (4) HD treated with mNSC-GFP-sApiCCT1 (n= 5 males).

Animals were subject to behavioral assays beginning at 6 weeks of age. Mice transplanted with either mNSCs or mNSCs-sApiCCT1 showed significant improvements in pole test compared to vehicle (Fig. 2A). However, mice transplanted with mNSC-sApiCCT1 did not show an improvement above mNSCs alone. Similarly, mNSC transplated mice show a moderate improvement in rotarod performance at 8 weeks, but this result is not significant (Fig. 2B), potentially due to the low number of animals tested (n=7) or the rapid progression of the R6/2 mouse model. Because mNSCs alone are neuroprotective and result in behavioral improvements, it may not be possible to detect an improvement in motor behavior with the addition of sApiCCT1 in this mouse model. mNSC-sApiCCT1 transplanted animals do show improvements in clasping behavior,

with both mNSC and mNSC-sApiCCT1 treated animals showing improvements at 2 weeks after transplantation, and only mNSC-sApiCCT1 showing improvements at 3 weeks after transplantation (Fig. 2 C,D). This result may be an indication that sApiCCT1 is delaying progression of disease; however, more extensive behavioral testing is needed to confirm this.

Mice given mNSC-sApiCCT1 transplantations show reduced mHTT accumulation. ApiCCT1 can cross the cell membrane and localize to the cytoplasmic and nuclear compartments [63, 64]. Therefore, we hypothesize that secretion of ApiCCT1 by mNSCs could modulate HD phenotypes in host tissue. To test this, whole cell lysates were analyzed by AGE followed by western blot. We found a significant reduction in oligomeric mHTT in animals transplanted with mNSC-sApiCCT1 compared to both vehicle and mNSC alone (Fig 3A). This indicates that the neurotrophic support offered by mNSCs may not be as robust as that of mNSCs expressing sApiCCT1, which provide a robust decrease in mHTT accumulation.

Transplantation of mNSC-sApiCCT1 reduces seeding potential of R6/2 mouse striatal lysates. Recent studies suggest that mHTT may propogate via a prion-like mechanism [171, 172] and polyQ oligomers and CSF from BACHD mice can seed aggregation in cell models [173]. Tan, et al. [173] have established an assay to measure the seeding potential of various substances, including homogenized mouse tissue. To test the seeding potential of tissue from mice treated with mNSC-sApiCCT1, striatal lysates were analyzed with in a cell-free seeding assay as previously described [173]. Briefly, PC12 cells were induced to express low amounts of mHttex1-GFP and lysed. PC12 lysates were treated with mNSC-sApiCCT1 tissue lysates and incubated at RT for

16 hours. Aggregation was then measured by filter retardation assay. Results indicate that tissue from mice treated with mNSC-sApiCCT1 has a reduced seeding potential compared to vehicle control (Fig. 4, red box). This is further confirmation that mNSC-sApiCCT1 modulate mHTT accumulation.

Discussion

Taken together, these data provide a proof of concept that a strategy to secrete ApiCCT1 may offer an improvement above mNSC transplantation alone by delivery of an agent that can additionally target the mHTT protein itself. We did not detect a change in motor phenotypes above mNSC transplant alone. However, this may result from the fact that mNSC transplantation alone maximally improved behavioral phenotypes in R6/2 or that expression of ApiCCT1 was not sufficient given that we used a pool of randomly integrated cells. We did find a significant reduction in oligomeric mHTT in animals transplanted with mNSC-sApiCCT1 compared to mNSCs alone and a reduction in seeding potential in animals transplanted with mNSC-sApiCCT1 compared to vehicle-treated animals. However, more research is needed to determine which species are modulated by mNSC-sApiCCT1, whether these cells improve long-term behavioral outcomes in HD mice compared to mNSC transplantation, and which cell type is best to deliver ApiCCT1.

The benefit of sApiCCT1 may lie in prevention of disease progression, particularly prevention of acquisition of disease in transplanted stem cells, which was not tested in the present study. An important finding in clinical transplantation studies from PD and

HD patients is that transplanted tissue can develop disease phenotypes [91, 114], Autopsy analysis of three HD patients who received fetal transplants showed that transplants may develop disease-like pathology years after engraftment within a patient's host brain [114]. Further research by the same group identified mHTT aggregates within transplanted tissue, characterized the spread of mHTT from the host tissue to the genetically normal material, and found that mHTT is primarily localized to the extracellular matrix in transplanted tissue [116]. This finding could be explained by a prion-like transmission of pathology. Several studies have shown that mHTT exhibits a prion-like mechanism and that mHTT aggregates can be taken up by cells [174-176]. It is therefore possible that stem cells may eventually develop intracellular aggregates and other HD pathological features when transplanted in an HD brain. In this dissertation, we describe a novel modifier of mHTT accumulation, ApiCCT1. ApiCCT1 appears to prevent mHTT accumulation in the present study and may have the potential to prevent development of pathology in transplanted stem cells. We were not able to detect a change in motor outcomes, therefore we may need to test this approach in 1) a slower progressing mouse model of HD, either R6/1 or a full length model or 2) select clonal populations of highest expressing NSCs to detect an improvement in behavioral and biochemical phenotypes above mNSC transplantation alone.

MATERIALS AND METHODS

Cell Culture and Biochemical Analysis

mNSC's stably expressing GFP were generously provided by Dr. Blurton-Jones' group [110]. mNSCs were transfected with constructs expressing His-tagged sApiCCT1 with puromyocin resistance under an IRES element (Fig. 1A). Pools of stably expressing cells were selected with puromyocin. Constructs expressing sApiCCT1 under a CAGG promoter and containing puromycin resistance under IRES were generated. GFP-mNSCs were transfected with this construct and stably selected for sApiCCT1 expression. Primary cortical neurons (PCNs) were isolated from embryonic day 17 FVB mice as previously described [62]. Cortical neurons were plated at 13×10^6 cells per dish, in poly-L-lysine (Sigma) coated 10cm dish (Corning) in Neurobasal medium supplemented with B27, N2, 2 mM glutamax, and streptomycin/amphotericin B (Life Technologies). PCNs were co-cultured with mNSCs using co-culture inserts (Millipore) for 5 to 7 days. Cells were harvested and lysed in RIPA and protein quantified using Lowry protein assay. Whole cell lysates were analyzed by both PAGE and AGE. SDS-AGE followed by Western blot analysis was performed a previously described [1, 62, 63, 140, 141]. Samples were analyzed with 15% Criterion Bis-Tris polyacrylamide gel (Bio-Rad), followed by western blot. Blots were quantified using ImageJ software.

mNSC transplantation

mNSCs were transplanted into the striatum of 5-week-old R6/2 mice (100,000 cells per hemisphere). Cells were transplanted using a stereotax apparatus (coordinates 0.01mm caudal to bregma, 0.2mm right/left lateral, 0.345 pocket to 0.325mm ventral to pial surface). Mice were anesthetized with isofluorane, placed in stereotax, and injected with $12X10^9$ genome copies of virus in each hemisphere with a Hamilton syringe. The needle was left in place for 2 minutes before slowly removing and the incision was sutured.

Mouse Behavior and Tissue Biochemistry

Behavioral outcomes were analyzed using rotarod, pole test, and clasping. At 9 weeks of age (4 weeks after injection), mice were sacrificed by Euthasol followed by transcardinal perfusion. Cortex and striatum were microdissected from one hemisphere and flash frozen for biochemical analysis. The other hemisphere was fixed in paraformaldehyde overnight, transferred to 30% sucrose solution, and sectioned using a microtome. Brain tissue was lysed in modified RIPA (radio immune precipitation) buffer containing 10mM Tris, pH7.2, 158mM NaCl, 1mM EDTA, 0.1% SDS, 1% Triton X-100, 1% sodium deoxycholate, and 1x Complete protease inhibitors (Roche) as described previously [62] and analyzed with AGE followed by western blot.

Cell Free Seeding Assay

Tissue lysates from animals treated with mNSC-sApiCCT1 or vehicle-treated animals were analyzed in a cell free seeding assay as previously described [173].

CHAPTER 4

FIGURES

Figure 4.1

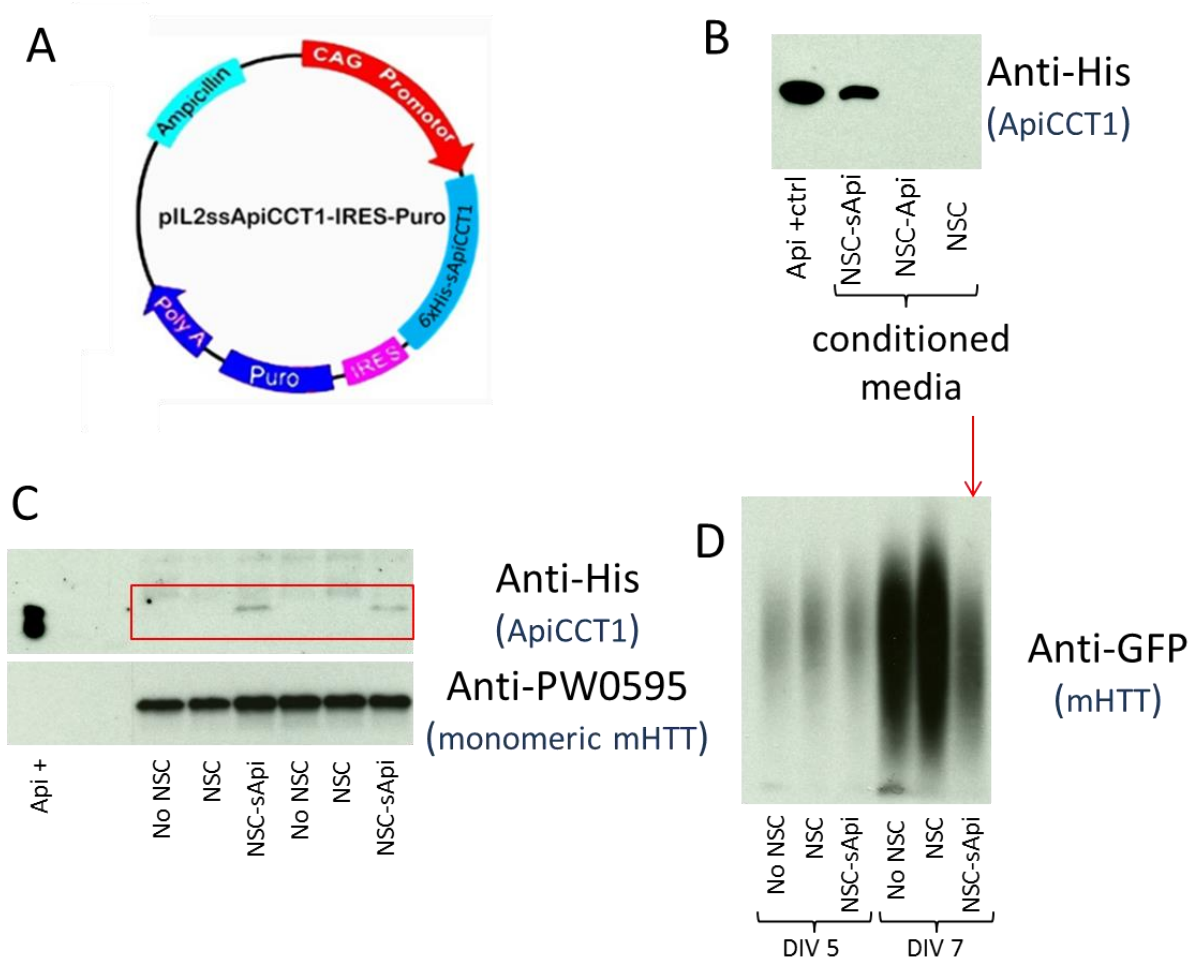

Figure 1. Secreted ApiCCT1 from mouse neural stem cells (mNSC-sApiCCT1) enters mouse primary cortical neurons (PCNs) and can reduce oligomeric mHTT accumulation in co-culture. (A) Schematic representation of construct used to develop line of mNSCs stably expressing sApiCCT1. (B) Secretion was confirmed using a Ni-NTA column to purify His-tagged ApiCCT1 from conditioned media. (C) Secreted ApiCCT1 enters PCNs when co-cultured with mNSC-sApiCCT1. (D) SDS-AGE analysis shows a reduction in oligomeric mHTT in PCNs co-cultured with mNSC-sApiCCT1 at DIV 7.

Figure 4.2

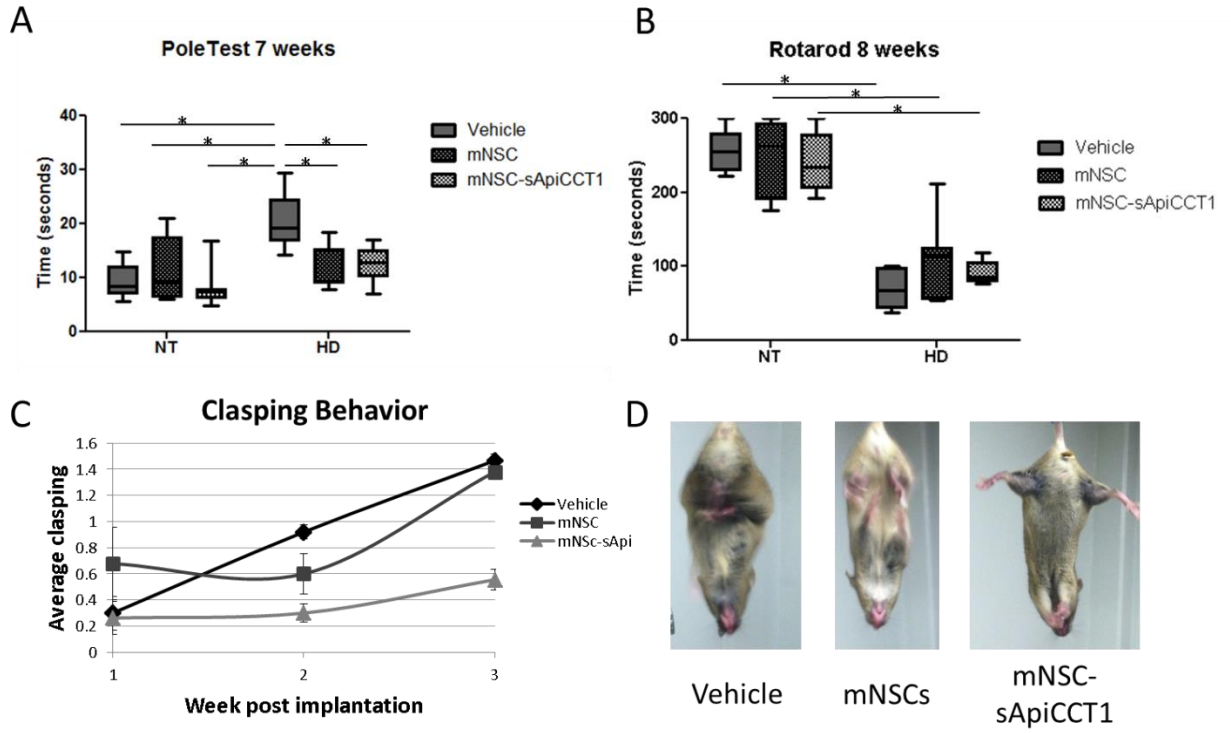

Figure 2. mNSC delivery produces behavioral improvements 4 weeks after transplantation. 5 week old R6/2 were transplanted with mNSC-sApiCCT1, mNSCs alone, or vehicle in striatum. Tissue was harvested 4 weeks later, at 9 weeks of age. (A) mNSC-sApiCCT1 transplanted mice show improvements in a pole test at 7 weeks of age compared to vehicle, but is not statistically different from mNSCs alone. (B) No significant improvement is seen in rotarod in either group at 8 weeks of age. (C,D) mNSC-sApiCCT1 mice show reduced clasping behavior, a measure of disease progression, compared to vehicle and mNSC alone. *p<0.05

Figure 4. 3

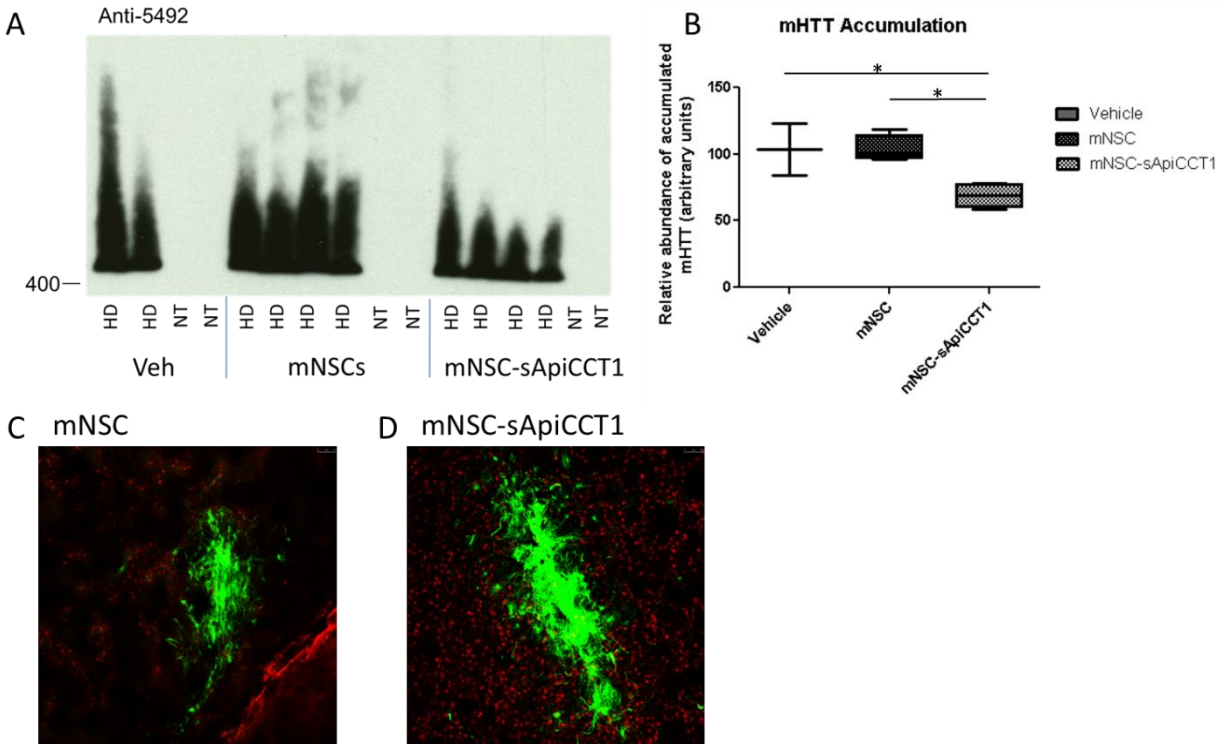

Figure 3. mNSC-sApiCCT1 delivery reduces fibrillar mHTT oligomers *in vivo* 4 weeks after transplantation. 5-week-old R6/2 were transplanted with mNSC-sApiCCT1, mNSCs alone, or vehicle in striatum. Tissue was harvested 4 weeks later, at 9 weeks of age. (A-B) SDS-AGE reveals a significant reduction in oligomeric mHTT in striatum of animals transplanted with mNSC-sApiCCT1 compared to mNSCs alone and vehicle control. (C, D) Immunohistochemistry confirms expression of cells in the striatum. Tissue is stained with anti-EM48 (red) and anti-GFP (green). *p<0.05

Figure 4.4

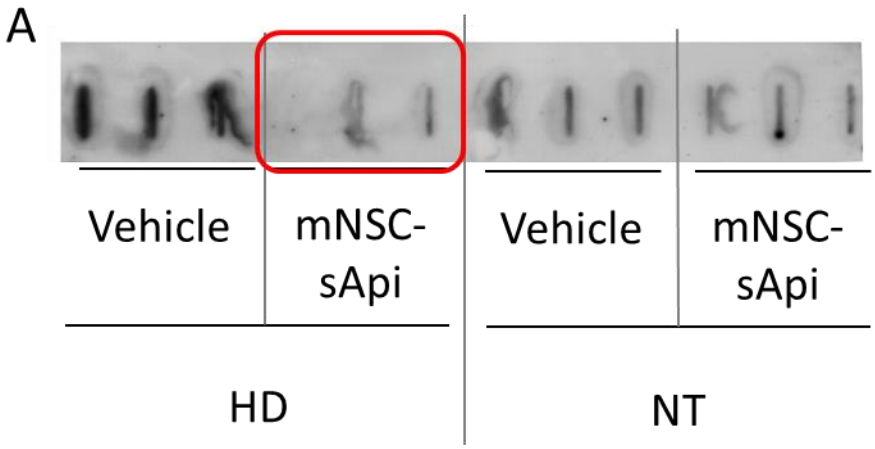

Figure 4. Transplantation of mNSC-sApiCCT1 reduces seeding potential of R6/2 mouse striatal lysates. Cell lysates from mice treated with mNSC-sApiCCT1 or vehicle were analyzed in a cell free seeding assay. mNSC-sApiCCT1-treated mice show reduced seeding potential compared to vehicle control (red box).

Chapter 5

CONCLUDING REMARKS

In this dissertation, we sought to evaluate delivery approaches for a potential disease-modifying therapy for Huntington's disease. Huntington's disease is a devastating genetic neurodegenerative disease for which no disease-modifying therapies currently exist. The therapeutic target tested here is a fragment of a chaperone protein that corresponds to the apical domain of the first subunit of the chaperonin CCT (ApiCCT1). ApiCCT1 has been well-characterized to ameliorate mutant Huntingtin (mHTT)-mediated phenotypes *in vitro* [63, 93, 100, 105], but whether these effects of ApiCCT1 will translate *in vivo* is not yet clear. The studies presented here show that delivery of ApiCCT1 is feasible *in vivo*; however, interpretation of efficacy is preliminary, with confounding factors due to differences in stress responses.

In the first aim of this dissertation, we tested local delivery of ApiCCT1 in the striatum. We reported results for two studies. The first indicates that AAV2/1-mediated striatal delivery of secreted ApiCCT1 (sApiCCT1) can modulate mHTT accumulation, but was not powered for behavioral efficacy. The second study testing AAV2-1-mediated delivery of sApiCCT1 in a larger cohort showed little to no modulation of mHTT accumulation with some behavioral improvements. This study may have been confounded by external stress-inducing factors and additional immune responses to viral injection. Therefore, we cannot conclusively assess *in vivo* efficacy of sApiCCT1, while providing important data suggesting that sApiCCT1 can modulate molecular readouts. The data indicate, however that sApiCCT1 is not sufficient to overcome additional stressors in R6/1 mice.

One study finds that AAV2/1-sApiCCT1 can reduce oligomeric mHTT but not visible mHTT. Another study finds a significant reduction in low MW, soluble accumulated

mHTT, but no other accumulated species. This may indicate that AAV2/1-sApiCCT1 preferentially modulates mHTT smaller, oligomeric mHTT, but not insoluble or visible accumulated mHTT. Given that *in vitro* results show CCT interaction with both monomeric and large mHTT fibrils, this finding was somewhat surprising. However, it is possible that ApiCCT1 influences mHTT differently in an *in vivo* context. We are delivering this virus when R6/1 mice are 5 weeks of age. While visible inclusions are not found at that age [3], it is likely that mHTT is beginning to accumulate within neurons. If ApiCCT1 binds to fibrils and monomeric mHTT, but not oligomeric mHTT, and if we introduce ApiCCT1 in a context where oligomeric mHTT is already present, then ApiCCT1 may not prevent that oligomeric mHTT from forming fibrils. However, if ApiCCT1 is able to bind monomeric mHTT as previous studies suggest, then ApiCCT1 would prevent formation of new oligomeric mHTT. Therefore, it is possible that the effect we see is due to the ability of ApiCCT1 to prevent new formation of mHTT accumulation rather than an effect on already established mHTT aggregation. Future studies should test whether ApiCCT1 prevents or reverses mHTT accumulation by delivering sApiCCT1 at different stages of disease progression *in vivo.*

In the second aim, we tested global delivery of sApiCCT1. However, confounding factors again prevented comprehensive testing of this hypothesis. PHP.B-sApiCCT1 did not modify any markers of disease progression in R6/2 HD mice. Further, mice injected with PHP.B virus exhibited degeneration as indicated by widespread staining with Fluoro-Jade, a marker of degenerating cells.

While the PHP.B virus offers a high rate of neuronal transduction, PHP.B-mediated global delivery of sApiCCT1 did not ameliorate HD phenotypes in R6/2 mice. This could

be due to a number of factors including unusually high virus expression, the rapidly progressing animal model of choice, external stressors, the choice of control virus expressing a fluorescent protein versus vehicle control, the choice of promoter expressing sApiCCT1, or the capsid protein mutation that allows PHP.B to efficiently transduce the CNS. Further studies are needed to differentiate between these factors and evaluate global sApiCCT1 delivery.

Together, chapters 2 and 3 describe studies where viral delivery of sApiCCT1 was not sufficient to rescue HD phenotypes. While we cannot conclusively determine *in vivo* efficacy of ApiCCT1, these studies indicate that ApiCCT1 was not able to overcome exogenous stressors. Namely, AAV2/1-mediated delivery was confounded by an increase in ER stress and both studies were confounded by increased microglial activation and the lack of an ideal control for comparisons to untreated HD animals. Under these viral delivery conditions, sApiCCT1 was not sufficient to rescue HD phenotypes.

In the third aim, we provide a proof-of-principle supporting the use of mNSCs as a delivery mechanism for sApiCCT1 in R6/2 HD mice. Mice transplanted with mNSC-sApiCCT1 showed reduced oligomeric mHTT compared to vehicle or mNSCs only. Importantly, one of the potential drawbacks of mNSC transplantation is that transplanted cells could potentially develop HD phenotypes. Although we did not detect a change in behavioral phenotypes compared to mNSCs alone, this approach may provide value above mNSCs alone as 1) sApiCCT1 may provide a disease-modifying component to stem cell treatments by reducing mHTT accumulation and 2) could prevent acquisition

of mHTT-associated phenotypes in the transplanted cells themselves caused by protein propagation or “seeding” mechanisms.

Future Directions

CCT mechanism of action: *mHTT protein levels and clearance*

Previous results show that ApiCCT1 prevents aggregation in a range of cell models and previous results from our lab suggest there may be a reduction in the total amount of mHTT [63, 93, 100, 105], suggesting that ApiCCT1 prevents aggregation and may enable degradation of mHTT. ApiCCT1 binding to mHTT could thus have two effects, the first of which is to prevent aberrant interaction with other proteins, including HTT itself, thus preventing aggregation and maintaining more mHTT in the monomeric form. Secondly, this shift to monomeric mHTT may enable mHTT to be cleared more readily by the cell. Because mHTT is directly linked to dysfunction of protein clearance pathways, preventing mHTT accumulation and aggregation may restore the protein clearing ability of the cell, thus further ameliorating mHTT-mediated toxicity. Future studies should include precise quantitative analysis of total mHTT levels, including aggregation species-specific analysis. Newly developed time-resolved fluorescence energy transfer (TR-FRET) assays are capable of quantifying endogenous mHTT levels in mouse cells and can be used to precisely monitor levels of mHTT *in vivo* [177]. Such techniques will allow us to determine if ApiCCT1 is reducing mHTT levels *in vivo*. However, it is also possible that the interaction of ApiCCT1 with HTT could also prevent the normal function of HTT that may be dependent upon the N17 domain, including

HTT's function as a scaffold for autophagy [101], and have significant impact particularly for systemic delivery.

CCT mechanism of action: *Cell penetration*

One of the notable features of apiCCT1 is its ability to penetrate both the plasma and nuclear membranes. It is unclear what mechanism allows ApiCCT1 to function as a cell penetrating peptide (CPP). However, the majority of CPPs rely on positively charged amino acids (primarily arginine and lysine). ApiCCT1 contains a domain that is similar to other well-characterized protein transduction domains, containing an arginine and lysine rich region (sequence: MGVRRCKKEDLRR) [63]. It is unclear whether this domain is responsible for the ability of ApiCCT1 to penetrate the cell membrane. Further, this transduction domain can enable a CPP to penetrate the cell membrane through either endocytosis or direct translocation. Often the attachment of large cargo to a CPP can alter the method of transduction, favoring endocytosis over direct translocation [178]. Our lab and collaborators find that GFP-tagged ApiCCT1 is not able to cross the cell membrane, suggesting that ApiCCT1 is likely not entering the cell via endocytosis. Direct translocation occurs via two proposed models, the carpet model and the barrel-stave model, which rely on positively charged amino acids within the protein transduction domain [179]. Future studies should focus on mutation of this potential protein transduction domain to determine if specific amino acids are responsible for facilitating necessary for translocation.

mNSC delivery of sApiCCT1

Data in this dissertation provides a proof of concept for mNSCs as a delivery vehicle for sApiCCT1. The mNSCs used in this study showed relatively low expression of sApiCCT1 (Chapter 4, Fig. 4), however even with this caveat, we found that mNSC-sApiCCT1 can modulate mHTT accumulation and reduce seeding potential of R6/2 striatal lysates. However, we were not able to measure a change in motor outcomes. We may be better able to characterize stem cell-mediated delivery of sApiCCT1 in a mouse model with slower disease onset or by selecting for higher levels of sApiCCT1 in clonal lines selected for high expression. Future research should focus on validating this delivery approach with stem cells expressing sApiCCT1 at higher levels. Our lab is currently generating a line of human NSCs (hNSCs) engineered to express sApiCCT1 using genome editing to insert sApiCCT1 into a safe harbor location and optimize expression of sApiCCT1. hNSCs offer an advantage to mNSCs in that they are more compatible for use in human patients and offer enhanced neuroprotective effects compared to mNSCs (unpublished results) in R6/2 mice.

Global delivery of sApiCCT1

PHP.B-mediated systemic delivery of sApiCCT1 did not rescue HD phenotypes. It is unclear whether this is due to the specific virus used, the choice of promoter to express sApiCCT1, the mouse model chosen, or global expression of sApiCCT1. Future research should first focus on fully characterizing the immune and stress response to PHP.B systemic delivery to determine if this is a useful approach for therapeutic delivery. Studies are underway in our lab to answer this question.

Further studies to test global expression of sApiCCT1 can utilize multiple approaches for broad based viral expression. We can add a synapsin promoter to the gene of interest in an AAV9-based package, including PHP.B, for neuronal specific expression. There is some precedent for this, with multiple groups utilizing synapsin promoters for CNS specificity [180, 181].

Therapeutic Implications and Approaches

ApiCCT1 has been characterized and validated as a therapeutic target in multiple cell models, including N2A [93], PC12 [63], and PCNs [64]. Data from our studies were complicated by confounding factors; however, our overall the data suggests that sApiCCT1 expression is not sufficient to rescue HD phenotypes under certain conditions. The results suggest that viral delivery may not provide an optimal delivery method for ApiCCT1.

There are countless methods to deliver proteins *in vivo*. In chapter 2, we tested direct delivery of purified protein in a pilot study, which appeared to be tolerated and protective; however, this approach may be difficult with the need for continuous delivery. In chapter 4, we tested viral and stem cell-mediated delivery. Stem cells offer a promising delivery vehicle as this would provide a combination therapy and release a regulated level of sApiCCT1 to other cells while providing neuroprotection to the transplanted cells themselves, as demonstrated for cells in culture. Research from our lab and others is focused on studying stem cells in the context of delivering therapeutic proteins *in vivo* [111], and this approach has substantial promise for translation to therapies in the clinic.

Another well-characterized and highly advantageous approach to deliver ApiCCT1 is nanoparticles. Polymeric nanoparticles, small colloidal particles, can be used to encapsulate proteins for delivery to various tissues in the body. In particular, nanoparticles can be utilized for nasal delivery to reach the brain [182, 183]. ApiCCT1 could feasibly be encapsulated in a polymeric nanoparticle and easily delivered to HD patients. This would circumvent the risks surrounding invasive and surgical procedures. While nanoparticles have the potential to elicit an undesirable immune response [184], this response may be avoided through various approaches including immunosuppression and engineering nanoparticles to avoid immune system recognition [185].

Furthermore, exosomes could also be used as a potential method for delivery of sApiCCT1. Exosomes, a type of endogenous nanoparticles, are membrane-based vesicles and offer an advantage over other types of nanoparticles, such as liposomes and polymeric nanoparticles, as exosomes are found to be non-immunogenic [186] and non-toxic [187]. A review of siRNA delivery approaches finds that exosome-mediated delivery of siRNA exhibits fewer drawbacks compared to viral, lipid nanoparticle, and polymeric nanoparticle delivery [188]. Further, a study published earlier this year establishes a method to package exogenous proteins within exosomes for delivery to the brain [189]. Therefore, exosome-mediated delivery sApiCCT1 is feasible and may be a better approach to assess *in vivo* efficacy of sApiCCT1 as we could avoid the aberrant immune response seen with the viral delivery descried in chapters 2 and 3 of this dissertation.

In this dissertation, we provide evidence that secretion of ApiCCT1 in the striatum of HD mice can ameliorate mHTT pathology and motor phenotypes. Overall, data from this dissertation and previous studies supports ApiCCT1 as a therapeutic target for the treatment of Huntington's disease; however, delivery methods need to be optimized. This dissertation also raises other questions for future studies, including investigating the mechanism of action of ApiCCT1. Here, we suggest that future studies examine whether ApiCCT1 prevents mHTT accumulation *in vivo* by delivering sApiCCT1 at various stages of disease progression. We also recommend that global delivery of sApiCCT1 is evaluated using alternative approaches, including nanoparticles, exosomes, PHP.B virus with neuronal-specific promoter, or traditional AAV9, as the PHP.B virus used in these studies yielded unexpected histological changes. Lastly, we suggest testing stem cell-mediated delivery of sApiCCT1 in R6/1 or full length models of HD to fully characterize the effect of mNSC-sApiCCT1 as a combination therapy for Huntington's disease.

References:

1. Sontag, E.M., et al., *Detection of Mutant Huntingtin Aggregation Conformers and Modulation of SDS-Soluble Fibrillar Oligomers by Small Molecules.* J Huntingtons Dis, 2012. **1**(1): p. 119-32.

2. Balchin, D., M. Hayer-Hartl, and F.U. Hartl, *In vivo aspects of protein folding and quality control.* Science, 2016. **353**(6294): p. aac4354.

3. Crook, Z.R. and D. Housman, *Huntington's Disease: Can Mice Lead the Way to Treatment?* Neuron, 2011. **69**(3): p. 423-435.

4. Group, T.H.s.D.C.R., *A novel gene containing a trinucleotide repeat that is expanded and unstable on Huntington's disease chromosomes. .* Cell, 1993. **72**(6): p. 971-83.

5. Zuccato, C., M. Valenza, and E. Cattaneo, *Molecular mechanisms and potential therapeutical targets in Huntington's disease.* Physiol Rev, 2010. **90**(3): p. 905-81.

6. Rubinsztein, D.C., et al., *Phenotypic characterization of individuals with 30-40 CAG repeats in the Huntington disease (HD) gene reveals HD cases with 36 repeats and apparently normal elderly individuals with 36-39 repeats.* Am J Hum Genet, 1996. **59**(1): p. 16-22.

7. Potter, N.T., E.B. Spector, and T.W. Prior, *Technical Standards and Guidelines for Huntington Disease Testing.* Genet Med, 2004. **6**(1): p. 61-65.

8. Bates, G.P., *History of genetic disease: the molecular genetics of Huntington disease - a history.* Nat Rev Genet, 2005. **6**(10): p. 766-73.

9. Gusella, J.F., et al., *A polymorphic DNA marker genetically linked to Huntington's disease.* Nature, 1983. **306**(5940): p. 234-238.

10. Morrison, P.J., *Prevalence estimates of Huntington disease in Caucasian populations are gross underestimates.* Mov Disord, 2012. **27**(13): p. 1707-8; author reply 1708-9.

11. Pringsheim, T., et al., *The incidence and prevalence of Huntington's disease: a systematic review and meta-analysis.* Mov Disord, 2012. **27**(9): p. 1083-91.

12. Quarrell, O., et al., *The Prevalence of Juvenile Huntington's Disease: A Review of the Literature and Meta-Analysis.* PLoS Curr, 2012. **4**: p. e4f8606b742ef3.

13. Myers, R.H., *Huntington's disease genetics.* NeuroRx, 2004. **1**(2): p. 255-62.

14. Tabrizi, S.J., et al., *Biological and clinical manifestations of Huntington's disease in the longitudinal TRACK-HD study: cross-sectional analysis of baseline data.* Lancet Neurol, 2009. **8**(9): p. 791-801.

15. Gusella, J.F. and M.E. MacDonald, *Huntington's disease.* Semin Cell Biol, 1995. **6**(1): p. 21-8.

16. Aylward, E.H., et al., *Longitudinal change in regional brain volumes in prodromal Huntington disease.* J Neurol Neurosurg Psychiatry, 2011. **82**(4): p. 405-10.

17. Turner, L.M., et al., *Striatal morphology correlates with frontostriatal electrophysiological motor processing in Huntington's disease: an IMAGE-HD study.* Brain Behav, 2016. **6**(12): p. e00511.

18. Niccolini, F. and M. Politis, *Neuroimaging in Huntington's disease.* World J Radiol, 2014. **6**(6): p. 301-12.

19. Duff, K., et al., *Mild cognitive impairment in prediagnosed Huntington disease.* Neurology, 2010. **75**(6): p. 500-7.

20. Paulsen, J.S., et al., *Critical periods of suicide risk in Huntington's disease.* Am J Psychiatry, 2005. **162**(4): p. 725-31.

21. Dayalu, P. and R.L. Albin, *Huntington disease: pathogenesis and treatment.* Neurol Clin, 2015. **33**(1): p. 101-14.

22. Guay, D.R.P., *Tetrabenazine, a monoamine-depleting drug used in the treatment of hyperkinetic movement disorders.* The American Journal of Geriatric Pharmacotherapy, 2010. **8**(4): p. 331-373.

23. Coppen, E.M. and R.A. Roos, *Current Pharmacological Approaches to Reduce Chorea in Huntington's Disease.* Drugs, 2017. **77**(1): p. 29-46.

24. Davies, S.W., et al., *Formation of neuronal intranuclear inclusions underlies the neurological dysfunction in mice transgenic for the HD mutation.* Cell, 1997. **90**(3): p. 537-48.

25. DiFiglia, M., et al., *Aggregation of huntingtin in neuronal intranuclear inclusions and dystrophic neurites in brain.* Science, 1997. **277**(5334): p. 1990-3.

26. Bhattacharyya, A.M., A.K. Thakur, and R. Wetzel, *polyglutamine aggregation nucleation: thermodynamics of a highly unfavorable protein folding reaction.* Proc Natl Acad Sci U S A, 2005. **102**(43): p. 15400-5.

27. Eisenberg, D. and M. Jucker, *The amyloid state of proteins in human diseases.* Cell, 2012. **148**(6): p. 1188-203.

28. Knowles, T.P., M. Vendruscolo, and C.M. Dobson, *The amyloid state and its association with protein misfolding diseases.* Nat Rev Mol Cell Biol, 2014. **15**(6): p. 384-96.

29. Darrow, M.C., et al., *Structural Mechanisms of Mutant Huntingtin Aggregation Suppression by the Synthetic Chaperonin-like CCT5 Complex Explained by Cryoelectron Tomography.* J Biol Chem, 2015. **290**(28): p. 17451-61.

30. Arrasate, M., et al., *Inclusion body formation reduces levels of mutant huntingtin and the risk of neuronal death.* Nature, 2004. **431**(7010): p. 805-10.

31. Yamada, M., et al., *CAG repeat disorder models and human neuropathology: similarities and differences.* Acta Neuropathol, 2008. **115**(1): p. 71-86.

32. Scherzinger, E., et al., *Self-assembly of polyglutamine-containing huntingtin fragments into amyloid-like fibrils: implications for Huntington's disease pathology.* Proc Natl Acad Sci U S A, 1999. **96**(8): p. 4604-9.

33. Hodgson, J.G., et al., *A YAC mouse model for Huntington's disease with full-length mutant huntingtin, cytoplasmic toxicity, and selective striatal neurodegeneration.* Neuron, 1999. **23**(1): p. 181-92.

34. Takahashi, T., et al., *Soluble polyglutamine oligomers formed prior to inclusion body formation are cytotoxic.* Hum Mol Genet, 2008. **17**(3): p. 345-56.

35. Leitman, J., F. Ulrich Hartl, and G.Z. Lederkremer, *Soluble forms of polyQ-expanded huntingtin rather than large aggregates cause endoplasmic reticulum stress.* Nat Commun, 2013. **4**: p. 2753.

36. Hoffner, G. and P. Djian, *Monomeric, oligomeric and polymeric proteins in huntington disease and other diseases of polyglutamine expansion.* Brain Sci, 2014. **4**(1): p. 91-122.

37. Nucifora, L.G., et al., *Identification of novel potentially toxic oligomers formed in vitro from mammalian-derived expanded huntingtin exon-1 protein.* J Biol Chem, 2012. **287**(19): p. 16017-28.

38. Kim, Y.E., et al., *Molecular chaperone functions in protein folding and proteostasis.* Annu Rev Biochem, 2013. **82**: p. 323-55.

39. Kim, Y.E., et al., *Soluble Oligomers of PolyQ-Expanded Huntingtin Target a Multiplicity of Key Cellular Factors.* Mol Cell, 2016. **63**(6): p. 951-64.

40. Haass, C. and D.J. Selkoe, *Soluble protein oligomers in neurodegeneration: lessons from the Alzheimer's amyloid beta-peptide.* Nat Rev Mol Cell Biol, 2007. **8**(2): p. 101-12.

41. Gatchel, J.R. and H.Y. Zoghbi, *Diseases of Unstable Repeat Expansion: Mechanisms and Common Principles.* Nat Rev Genet, 2005. **6**(10): p. 743-755.

42. Becher, M.W., et al., *Intranuclear neuronal inclusions in Huntington's disease and dentatorubral and pallidoluysian atrophy: correlation between the density of inclusions and IT15 CAG triplet repeat length.* Neurobiol Dis, 1998. **4**(6): p. 387-97.

43. Zoghbi, H.Y. and H.T. Orr, *Glutamine repeats and neurodegeneration.* Annu Rev Neurosci, 2000. **23**: p. 217-47.

44. Meriin, A.B. and M.Y. Sherman, *Role of molecular chaperones in neurodegenerative disorders.* Int J Hyperthermia, 2005. **21**(5): p. 403-19.

45. Kordower, J.H. and P. Brundin, *Lewy body pathology in long-term fetal nigral transplants: is parkinson's disease transmitted from one neural system to another[quest].* Neuropsychopharmacology, 0000. **34**(1): p. 254-254.

46. Goedert, M., et al., *100 years of Lewy pathology.* Nat Rev Neurol, 2013. **9**(1): p. 13-24.

47. Olanow, C.W. and S.B. Prusiner, *Is Parkinson's disease a prion disorder?* Proceedings of the National Academy of Sciences, 2009. **106**(31): p. 12571-12572.

48. Soto, C., *Transmissible Proteins: Expanding the Prion Heresy.* Cell. **149**(5): p. 968-977.

49. Zhang, X., et al., *A potent small molecule inhibits polyglutamine aggregation in Huntington's disease neurons and suppresses neurodegeneration in vivo.* Proc Natl Acad Sci U S A, 2005. **102**(3): p. 892-7.

50. Yamamoto, A., J.J. Lucas, and R. Hen, *Reversal of neuropathology and motor dysfunction in a conditional model of Huntington's disease.* Cell, 2000. **101**(1): p. 57-66.

51. Ochaba, J., et al., *PIAS1 Regulates Mutant Huntingtin Accumulation and Huntington's Disease-Associated Phenotypes In Vivo.* Neuron, 2016. **90**(3): p. 507-20.

52. Sanchez, I., C. Mahlke, and J. Yuan, *Pivotal role of oligomerization in expanded polyglutamine neurodegenerative disorders.* Nature, 2003. **421**(6921): p. 373-9.

53. Aronin, N. and M. DiFiglia, *Huntingtin-lowering strategies in Huntington's disease: antisense oligonucleotides, small RNAs, and gene editing.* Mov Disord, 2014. **29**(11): p. 1455-61.

54. Kordasiewicz, H.B., et al., *Sustained therapeutic reversal of Huntington's disease by transient repression of huntingtin synthesis.* Neuron, 2012. **74**(6): p. 1031-44.

55. Carroll, J.B., et al., *Potent and selective antisense oligonucleotides targeting single-nucleotide polymorphisms in the Huntington disease gene / allele-specific silencing of mutant huntingtin.* Mol Ther, 2011. **19**(12): p. 2178-85.

56. Yu, D., et al., *Single-stranded RNAs use RNAi to potently and allele-selectively inhibit mutant huntingtin expression.* Cell, 2012. **150**(5): p. 895-908.

57. Watts, J.K. and D.R. Corey, *Silencing disease genes in the laboratory and the clinic.* J Pathol, 2012. **226**(2): p. 365-79.

58. Sathasivam, K., et al., *Aberrant splicing of HTT generates the pathogenic exon 1 protein in Huntington disease.* Proc Natl Acad Sci U S A, 2013. **110**(6): p. 2366-70.

59. Schlachetzki, J.C., S.W. Saliba, and A.C. Oliveira, *Studying neurodegenerative diseases in culture models.* Rev Bras Psiquiatr, 2013. **35 Suppl 2**: p. S92-100.

60. Cisbani, G. and F. Cicchetti, *An in vitro perspective on the molecular mechanisms underlying mutant huntingtin protein toxicity.* Cell Death Dis, 2012. **3**: p. e382.

61. Apostol, B.L., et al., *A cell-based assay for aggregation inhibitors as therapeutics of polyglutamine-repeat disease and validation in Drosophila.* Proc Natl Acad Sci U S A, 2003. **100**(10): p. 5950-5.

62. Sontag, E.M., et al., *Methylene blue modulates huntingtin aggregation intermediates and is protective in Huntington's disease models.* J Neurosci, 2012. **32**(32): p. 11109-19.

63. Sontag, E.M., et al., *Exogenous delivery of chaperonin subunit fragment ApiCCT1 modulates mutant Huntingtin cellular phenotypes.* Proc Natl Acad Sci U S A, 2013. **110**(8): p. 3077-82.

64. Zhao, X., et al., *TRiC subunits enhance BDNF axonal transport and rescue striatal atrophy in Huntington's disease.* Proc Natl Acad Sci U S A, 2016. **113**(38): p. E5655-64.

65. The Hd iPsc Consortium, *Induced Pluripotent Stem Cells from Patients with Huntington's Disease Show CAG-Repeat-Expansion-Associated Phenotypes.* Cell Stem Cell, 2012. **11**(2): p. 264-278.

66. Lim, R.G., et al., *Huntington's Disease iPSC-Derived Brain Microvascular Endothelial Cells Reveal WNT-Mediated Angiogenic and Blood-Brain Barrier Deficits.* Cell Rep, 2017. **19**(7): p. 1365-1377.

67. Takahashi, K. and S. Yamanaka, *Induction of pluripotent stem cells from mouse embryonic and adult fibroblast cultures by defined factors.* Cell, 2006. **126**(4): p. 663-76.

68. Kim, C., *iPSC technology--Powerful hand for disease modeling and therapeutic screen.* BMB Rep, 2015. **48**(5): p. 256-65.

69. *Developmental alterations in Huntington's disease neural cells and pharmacological rescue in cells and mice.* Nat Neurosci, 2017. **20**(5): p. 648-660.

70. *Induced pluripotent stem cells from patients with Huntington's disease show CAG-repeat-expansion-associated phenotypes.* Cell Stem Cell, 2012. **11**(2): p. 264-78.

71. Li, J., N. Popovic, and P. Brundin, *The use of the R6 transgenic mouse models of Huntington's disease in attempts to develop novel therapeutic strategies.* NeuroRx, 2005. **2**(3): p. 447-464.

72. Menalled, L.B., et al., *Genetic deletion of transglutaminase 2 does not rescue the phenotypic deficits observed in R6/2 and zQ175 mouse models of Huntington's disease.* PLOS ONE, 2014. **9**(6): p. e99520.

73. Luthi-Carter, R., et al., *Decreased expression of striatal signaling genes in a mouse model of Huntington's disease.* Hum Mol Genet, 2000. **9**(9): p. 1259-71.

74. Choi, M.L., et al., *Dopaminergic manipulations and its effects on neurogenesis and motor function in a transgenic mouse model of Huntington's disease.* Neurobiol Dis, 2014. **66**: p. 19-27.

75. Li, J.Y., N. Popovic, and P. Brundin, *The use of the R6 transgenic mouse models of Huntington's disease in attempts to develop novel therapeutic strategies.* NeuroRx, 2005. **2**(3): p. 447-64.

76. Gray, M., et al., *Full-length human mutant huntingtin with a stable polyglutamine repeat can elicit progressive and selective neuropathogenesis in BACHD mice.* J Neurosci, 2008. **28**(24): p. 6182-95.

77. Warrick, J.M., et al., *Suppression of polyglutamine-mediated neurodegeneration in Drosophila by the molecular chaperone HSP70.* Nat Genet, 1999. **23**(4): p. 425-428.

78. Cummings, C.J., et al., *Over-expression of inducible HSP70 chaperone suppresses neuropathology and improves motor function in SCA1 mice.* Hum Mol Genet, 2001. **10**(14): p. 1511-1518.

79. Yang, S., et al., *Age-dependent decrease in chaperone activity impairs MANF expression, leading to Purkinje cell degeneration in inducible SCA17 mice.* Neuron, 2014. **81**(2): p. 349-65.

80. Murshid, A., T. Eguchi, and S.K. Calderwood, *Stress proteins in aging and life span.* Int J Hyperthermia, 2013. **29**(5): p. 442-7.

81. Hay, D.G., et al., *Progressive decrease in chaperone protein levels in a mouse model of Huntington's disease and induction of stress proteins as a therapeutic approach.* Hum Mol Genet, 2004. **13**(13): p. 1389-405.

82. Sittler, A., et al., *Geldanamycin activates a heat shock response and inhibits huntingtin aggregation in a cell culture model of Huntington's disease.* Hum Mol Genet, 2001. **10**(12): p. 1307-15.

83. Jana, N.R., et al., *Polyglutamine length-dependent interaction of Hsp40 and Hsp70 family chaperones with truncated N-terminal huntingtin: their role in suppression of aggregation and cellular toxicity.* Hum Mol Genet, 2000. **9**(13): p. 2009-18.

84. Bailey, C.K., et al., *Molecular chaperones enhance the degradation of expanded polyglutamine repeat androgen receptor in a cellular model of spinal and bulbar muscular atrophy.* Hum Mol Genet, 2002. **11**(5): p. 515-23.

85. Kobayashi, Y., et al., *Chaperones Hsp70 and Hsp40 suppress aggregate formation and apoptosis in cultured neuronal cells expressing truncated androgen receptor protein with expanded polyglutamine tract.* J Biol Chem, 2000. **275**(12): p. 8772-8.

86. Stenoien, D.L., et al., *Polyglutamine-expanded androgen receptors form aggregates that sequester heat shock proteins, proteasome components and SRC-1, and are suppressed by the HDJ-2 chaperone.* Hum Mol Genet, 1999. **8**(5): p. 731-41.

87. Chai, Y., et al., *Analysis of the role of heat shock protein (Hsp) molecular chaperones in polyglutamine disease.* J Neurosci, 1999. **19**(23): p. 10338-47.

88. Cummings, C.J., et al., *Chaperone suppression of aggregation and altered subcellular proteasome localization imply protein misfolding in SCA1.* Nat Genet, 1998. **19**(2): p. 148-54.

89. Zhou, H., S.H. Li, and X.J. Li, *Chaperone suppression of cellular toxicity of huntingtin is independent of polyglutamine aggregation.* J Biol Chem, 2001. **276**(51): p. 48417-24.

90. Kitamura, A., et al., *Cytosolic chaperonin prevents polyglutamine toxicity with altering the aggregation state.* Nat Cell Biol, 2006. **8**(10): p. 1163-70.

91. Braak, H. and K. Del Tredici, *Assessing fetal nerve cell grafts in Parkinson's disease.* Nat Med, 2008. **14**(5): p. 483-485.

92. Adachi, H., et al., *Heat shock protein 70 chaperone overexpression ameliorates phenotypes of the spinal and bulbar muscular atrophy transgenic mouse model by*

reducing nuclear-localized mutant androgen receptor protein. J Neurosci, 2003. **23**(6): p. 2203-11.

93. Tam, S., et al., *The chaperonin TRiC blocks a huntingtin sequence element that promotes the conformational switch to aggregation.* Nat Struct Mol Biol, 2009. **16**(12): p. 1279-85.

94. Spiess, C., et al., *Mechanism of the eukaryotic chaperonin: protein folding in the chamber of secrets.* Trends Cell Biol, 2004. **14**(11): p. 598-604.

95. Saibil, H.R. and N.A. Ranson, *The chaperonin folding machine.* Trends Biochem Sci, 2002. **27**(12): p. 627-32.

96. Booth, C.R., et al., *Mechanism of lid closure in the eukaryotic chaperonin TRiC/CCT.* Nat Struct Mol Biol, 2008. **15**(7): p. 746-53.

97. Zhuravleva, A. and S.E. Radford, *How TriC folds tricky proteins.* Cell, 2014. **159**(6): p. 1251-2.

98. Meyer, A.S., et al., *Closing the folding chamber of the eukaryotic chaperonin requires the transition state of ATP hydrolysis.* Cell, 2003. **113**(3): p. 369-81.

99. Yam, A.Y., et al., *Defining the TRiC/CCT interactome links chaperonin function to stabilization of newly made proteins with complex topologies.* Nat Struct Mol Biol, 2008. **15**(12): p. 1255-62.

100. Shahmoradian, S.H., et al., *TRiC's tricks inhibit huntingtin aggregation.* Elife, 2013. **2**: p. e00710.

101. Pavel, M., et al., *CCT complex restricts neuropathogenic protein aggregation via autophagy.* Nat Commun, 2016. **7**: p. 13821.

102. Koyuncu, S., et al., *Proteostasis of Huntingtin in Health and Disease.* Int J Mol Sci, 2017. **18**(7).

103. Nollen, E.A.A., et al., *Genome-wide RNA interference screen identifies previously undescribed regulators of polyglutamine aggregation.* Proc Natl Acad Sci U S A, 2004. **101**(17): p. 6403-6408.

104. Behrends, C., et al., *Chaperonin TRiC promotes the assembly of polyQ expansion proteins into nontoxic oligomers.* Mol Cell, 2006. **23**(6): p. 887-97.

105. Tam, S., et al., *The chaperonin TRiC controls polyglutamine aggregation and toxicity through subunit-specific interactions.* Nat Cell Biol, 2006. **8**(10): p. 1155-62.

106. Shen, K. and J. Frydman, *The interplay between the chaperonin TRiC and N-terminal region of Huntingtin mediates Huntington's Disease aggregation and pathogenesis*, in *Protein Quality Control in Neurodegenerative Diseases*, R.I. Morimoto and Y. Christen, Editors. 2013, Springer Berlin Heidelberg. p. 121-132.

107. Zheng, Z., et al., *An N-terminal nuclear export signal regulates trafficking and aggregation of Huntingtin (Htt) protein exon 1.* J Biol Chem, 2013. **288**(9): p. 6063-71.

108. Bates, G., *Huntingtin aggregation and toxicity in Huntington's disease.* Lancet, 2003. **361**(9369): p. 1642-4.

109. Stern, B., et al., *Improving mammalian cell factories: The selection of signal peptide has a major impact on recombinant protein synthesis and secretion in mammalian cells.* Trends Cell Mol Biol, 2007. **2**: p. 1-17.

110. Blurton-Jones, M., et al., *Neural stem cells improve cognition via BDNF in a transgenic model of Alzheimer disease.* Proceedings of the National Academy of Sciences, 2009. **106**(32): p. 13594-13599.

111. Kitiyanant, N., et al., *BDNF-, IGF-1- and GDNF-secreting human neural progenitor cells rescue amyloid beta-induced toxicity in cultured rat septal neurons.* Neurochem Res, 2012. **37**(1): p. 143-52.

112. McBride, J.L., et al., *Human neural stem cell transplants improve motor function in a rat model of Huntington's disease.* The Journal of Comparative Neurology, 2004. **475**(2): p. 211-219.

113. Goldberg, N.R., et al., *Neural Stem Cells Rescue Cognitive and Motor Dysfunction in a Transgenic Model of Dementia with Lewy Bodies through a BDNF-Dependent Mechanism.* Stem Cell Reports, 2015. **5**(5): p. 791-804.

114. Cicchetti, F., et al., *Neural transplants in patients with Huntington's disease undergo disease-like neuronal degeneration.* Proc Natl Acad Sci U S A, 2009. **106**(30): p. 12483-8.

115. Reuter, I., et al., *Long-term clinical and positron emission tomography outcome of fetal striatal transplantation in Huntington's disease.* J Neurol Neurosurg Psychiatry, 2008. **79**(8): p. 948-51.

116. Cicchetti, F., et al., *Mutant huntingtin is present in neuronal grafts in Huntington disease patients.* Ann Neurol, 2014. **76**(1): p. 31-42.

117. Bates, G., *Huntingtin aggregation and toxicity in Huntington's disease.* The Lancet, 2003. **361**(9369): p. 1642-1644.

118. Gutekunst, C.A., et al., *Nuclear and neuropil aggregates in Huntington's disease: relationship to neuropathology.* J Neurosci, 1999. **19**(7): p. 2522-34.

119. Zhang, L., Q. Leng, and A.J. Mixson, *Alteration in the IL-2 signal peptide affects secretion of proteins in vitro and in vivo.* J Gene Med, 2005. **7**(3): p. 354-65.

120. Westerink, R.H. and A.G. Ewing, *The PC12 cell as model for neurosecretion.* Acta Physiol (Oxf), 2008. **192**(2): p. 273-85.

121. Mangiarini, L., et al., *Exon 1 of the HD gene with an expanded CAG repeat is sufficient to cause a progressive neurological phenotype in transgenic mice.* Cell, 1996. **87**(3): p. 493-506.

122. Caughey, B. and P.T. Lansbury, *Protofibrils, pores, fibrils, and neurodegeneration: separating the responsible protein aggregates from the innocent bystanders.* Annu Rev Neurosci, 2003. **26**: p. 267-98.

123. Naver, B., et al., *Molecular and behavioral analysis of the r6/1 huntington's disease transgenic mouse.* Neuroscience, 2003. **122**(4): p. 1049-1057.

124. Carter, R.J., J. Morton, and S.B. Dunnett, *Motor coordination and balance in rodents.* Curr Protoc Neurosci, 2001. **Chapter 8**: p. Unit 8 12.

125. Hickey, M.A., et al., *Extensive early motor and non-motor behavioral deficits are followed by striatal neuronal loss in knock-in Huntington's disease mice.* Neuroscience, 2008. **157**(1): p. 280-95.

126. McFarland, N.R., et al., *Comparison of transduction efficiency of recombinant AAV serotypes 1, 2, 5, and 8 in the rat nigrostriatal system.* J Neurochem, 2009. **109**(3): p. 838-45.

127. Mullen, R.J., C.R. Buck, and A.M. Smith, *NeuN, a neuronal specific nuclear protein in vertebrates.* Development, 1992. **116**(1): p. 201-11.

128. Sofroniew, M.V. and H.V. Vinters, *Astrocytes: biology and pathology.* Acta Neuropathol, 2010. **119**(1): p. 7-35.

129. O'Rourke, J.G., et al., *SUMO-2 and PIAS1 modulate insoluble mutant huntingtin protein accumulation.* Cell Rep, 2013. **4**(2): p. 362-75.

130. Ochaba, J., et al., *Potential function for the Huntingtin protein as a scaffold for selective autophagy.* Proceedings of the National Academy of Sciences, 2014.

131. Cao, T., et al., *Morphological and genetic activation of microglia after diffuse traumatic brain injury in the rat.* Neuroscience, 2012. **225**: p. 65-75.

132. Eisch, A.J., L.C. Schmued, and J.F. Marshall, *Characterizing cortical neuron injury with fluoro-jade labeling after a neurotoxic regimen of methamphetamine.* Synapse, 1998. **30**(3): p. 329-333.

133. Lee, H., et al., *IRE1 plays an essential role in ER stress-mediated aggregation of mutant huntingtin via the inhibition of autophagy flux.* Hum Mol Genet, 2012. **21**(1): p. 101-14.

134. Oslowski, C.M. and F. Urano, *Measuring ER stress and the unfolded protein response using mammalian tissue culture system.* Methods Enzymol, 2011. **490**: p. 71-92.

135. Scheper, W. and J.J. Hoozemans, *The unfolded protein response in neurodegenerative diseases: a neuropathological perspective.* Acta Neuropathol, 2015. **130**(3): p. 315-31.

136. Duennwald, M.L. and S. Lindquist, *Impaired ERAD and ER stress are early and specific events in polyglutamine toxicity.* Genes Dev, 2008. **22**(23): p. 3308-19.

137. Vidal, R., et al., *Converging pathways in the occurrence of endoplasmic reticulum (ER) stress in Huntington's disease.* Curr Mol Med, 2011. **11**(1): p. 1-12.

138. Noh, J.Y., et al., *SCAMP5 links endoplasmic reticulum stress to the accumulation of expanded polyglutamine protein aggregates via endocytosis inhibition.* J Biol Chem, 2009. **284**(17): p. 11318-25.

139. Loos, M., et al., *Within-strain variation in behavior differs consistently between common inbred strains of mice.* Mamm Genome, 2015. **26**(7-8): p. 348-54.

140. Legleiter, J., et al., *Mutant huntingtin fragments form oligomers in a polyglutamine length-dependent manner in vitro and in vivo.* J Biol Chem, 2010. **285**(19): p. 14777-90.

141. Weiss, A., et al., *Sensitive biochemical aggregate detection reveals aggregation onset before symptom development in cellular and murine models of Huntington's disease.* J Neurochem, 2008. **104**(3): p. 846-58.

142. Deverman, B.E., et al., *Cre-dependent selection yields AAV variants for widespread gene transfer to the adult brain.* Nat Biotechnol, 2016. **34**(2): p. 204-9.

143. Arrasate, M. and S. Finkbeiner, *Protein aggregates in Huntington's disease.* Exp Neurol, 2012. **238**(1): p. 1-11.

144. Gu, X., et al., *Pathological cell-cell interactions are necessary for striatal pathogenesis in a conditional mouse model of Huntington's disease.* Mol Neurodegener, 2007. **2**: p. 8.

145. Wang, N., et al., *Neuronal targets for reducing mutant huntingtin expression to ameliorate disease in a mouse model of Huntington's disease.* Nat Med, 2014. **20**(5): p. 536-41.

146. Pulicherla, N., et al., *Engineering liver-detargeted AAV9 vectors for cardiac and musculoskeletal gene transfer.* Mol Ther, 2011. **19**(6): p. 1070-8.

147. Sonntag, F., K. Schmidt, and J.A. Kleinschmidt, *A viral assembly factor promotes AAV2 capsid formation in the nucleolus.* Proc Natl Acad Sci U S A, 2010. **107**(22): p. 10220-5.

148. DiMattia, M.A., et al., *Structural insight into the unique properties of adeno-associated virus serotype 9.* J Virol, 2012. **86**(12): p. 6947-58.

149. Ding, W., et al., *Intracellular trafficking of adeno-associated viral vectors.* Gene Ther, 2005. **12**(11): p. 873-80.

150. Aschauer, D.F., S. Kreuz, and S. Rumpel, *Analysis of Transduction Efficiency, Tropism and Axonal Transport of AAV Serotypes 1, 2, 5, 6, 8 and 9 in the Mouse Brain.* PLOS ONE, 2013. **8**(9): p. e76310.

151. Yardeni, T., et al., *Retro-orbital injections in mice.* Lab Anim (NY), 2011. **40**(5): p. 155-60.

152. Schuster, D.J., et al., *Biodistribution of adeno-associated virus serotype 9 (AAV9) vector after intrathecal and intravenous delivery in mouse.* Front Neuroanat, 2014. **8**: p. 42.

153. Howard, D.B., et al., *Tropism and toxicity of adeno-associated viral vector serotypes 1, 2, 5, 6, 7, 8, and 9 in rat neurons and glia in vitro.* Virology, 2008. **372**(1): p. 24-34.

154. Squitieri, F., et al., *Abnormal morphology of peripheral cell tissues from patients with Huntington disease.* J Neural Transm (Vienna), 2010. **117**(1): p. 77-83.

155. Turner, C., J.M. Cooper, and A.H.V. Schapira, *Clinical correlates of mitochondrial function in Huntington's disease muscle.* Movement Disorders, 2007. **22**(12): p. 1715-1721.

156. Maywood, E.S., et al., *Disruption of peripheral circadian timekeeping in a mouse model of Huntington's disease and its restoration by temporally scheduled feeding.* J Neurosci, 2010. **30**(30): p. 10199-204.

157. Moffitt, H., et al., *Formation of polyglutamine inclusions in a wide range of non-CNS tissues in the HdhQ150 knock-in mouse model of Huntington's disease.* PLOS ONE, 2009. **4**(11): p. e8025.

158. Lodi, R., et al., *Abnormal in vivo skeletal muscle energy metabolism in Huntington's disease and dentatorubropallidoluysian atrophy.* Ann Neurol, 2000. **48**(1): p. 72-6.

159. Lalic, N.M., et al., *Glucose homeostasis in Huntington disease: abnormalities in insulin sensitivity and early-phase insulin secretion.* Arch Neurol, 2008. **65**(4): p. 476-80.

160. Panov, A.V., et al., *Early mitochondrial calcium defects in Huntington's disease are a direct effect of polyglutamines.* Nat Neurosci, 2002. **5**(8): p. 731-6.

161. Ishii, T. and K. Eto, *Fetal stem cell transplantation: Past, present, and future.* World J Stem Cells, 2014. **6**(4): p. 404-20.

162. Goldberg, N.R.S., et al., *Human Neural Progenitor Transplantation Rescues Behavior and Reduces alpha-Synuclein in a Transgenic Model of Dementia with Lewy Bodies.* Stem Cells Transl Med, 2017. **6**(6): p. 1477-1490.

163. Rosser, A.E. and A.C. Bachoud-Levi, *Clinical trials of neural transplantation in Huntington's disease.* Prog Brain Res, 2012. **200**: p. 345-71.

164. Zuo, F.X., et al., *Transplantation of Human Neural Stem Cells in a Parkinsonian Model Exerts Neuroprotection via Regulation of the Host Microenvironment.* Int J Mol Sci, 2015. **16**(11): p. 26473-92.

165. Chen, W.W. and M. Blurton-Jones, *Concise review: Can stem cells be used to treat or model Alzheimer's disease?* Stem Cells, 2012. **30**(12): p. 2612-8.

166. Ager, R.R., et al., *Human neural stem cells improve cognition and promote synaptic growth in two complementary transgenic models of Alzheimer's disease and neuronal loss.* Hippocampus, 2015. **25**(7): p. 813-26.

167. Crane, A.T., J. Rossignol, and G.L. Dunbar, *Use of Genetically Altered Stem Cells for the Treatment of Huntington's Disease.* Brain Sci, 2014. **4**(1): p. 202-19.

168. Ebert, A.D., et al., *Ex vivo delivery of GDNF maintains motor function and prevents neuronal loss in a transgenic mouse model of Huntington's disease.* Exp Neurol, 2010. **224**(1): p. 155-62.

169. Qin, J.Y., et al., *Systematic comparison of constitutive promoters and the doxycycline-inducible promoter.* PLoS ONE, 2010. **5**(5): p. e10611.

170. Yamasaki, T.R., et al., *Neural stem cells improve memory in an inducible mouse model of neuronal loss.* J Neurosci, 2007. **27**(44): p. 11925-33.

171. Jeon, I., et al., *Human-to-mouse prion-like propagation of mutant huntingtin protein.* Acta Neuropathol, 2016. **132**(4): p. 577-92.

172. Pecho-Vrieseling, E., et al., *Transneuronal propagation of mutant huntingtin contributes to non-cell autonomous pathology in neurons.* Nat Neurosci, 2014. **17**(8): p. 1064-72.

173. Tan, Z., et al., *Huntington's disease cerebrospinal fluid seeds aggregation of mutant huntingtin.* Mol Psychiatry, 2015. **20**(11): p. 1286-93.

174. Yang, W., et al., *Aggregated polyglutamine peptides delivered to nuclei are toxic to mammalian cells.* Hum Mol Genet, 2002. **11**(23): p. 2905-17.

175. Ren, P.H., et al., *Cytoplasmic penetration and persistent infection of mammalian cells by polyglutamine aggregates.* Nat Cell Biol, 2009. **11**(2): p. 219-25.

176. Pearce, M.M., et al., *Prion-like transmission of neuronal huntingtin aggregates to phagocytic glia in the Drosophila brain.* Nat Commun, 2015. **6**: p. 6768.

177. Liang, Y., et al., *TR-FRET Assays for Endogenous Huntingtin Protein Level in Mouse Cells.* J Huntingtons Dis, 2014. **3**(3): p. 253-9.

178. Koren, E. and V.P. Torchilin, *Cell-penetrating peptides: breaking through to the other side.* Trends Mol Med, 2012. **18**(7): p. 385-93.

179. Shaw, P.A., et al., *Comparison of protein transduction domains in mediating cell delivery of a secreted CRE protein.* Biochemistry, 2008. **47**(4): p. 1157-66.

180. Lukashchuk, V., et al., *AAV9-mediated central nervous system-targeted gene delivery via cisterna magna route in mice.* Mol Ther Methods Clin Dev, 2016. **3**: p. 15055.

181. Jackson, K.L., et al., *Better Targeting, Better Efficiency for Wide-Scale Neuronal Transduction with the Synapsin Promoter and AAV-PHP.B.* Front Mol Neurosci, 2016. **9**: p. 116.

182. Patel, A., et al., *Recent advances in protein and Peptide drug delivery: a special emphasis on polymeric nanoparticles.* Protein Pept Lett, 2014. **21**(11): p. 1102-20.

183. Saraiva, C., et al., *Nanoparticle-mediated brain drug delivery: Overcoming blood-brain barrier to treat neurodegenerative diseases.* J Control Release, 2016. **235**: p. 34-47.

184. Kononenko, V., M. Narat, and D. Drobne, *Nanoparticle interaction with the immune system.* Arh Hig Rada Toksikol, 2015. **66**(2): p. 97-108.

185. Zolnik, B.S., et al., *Nanoparticles and the immune system.* Endocrinology, 2010. **151**(2): p. 458-65.

186. Ha, D., N. Yang, and V. Nadithe, *Exosomes as therapeutic drug carriers and delivery vehicles across biological membranes: current perspectives and future challenges.* Acta Pharm Sin B, 2016. **6**(4): p. 287-96.

187. Sun, D., et al., *Exosomes are endogenous nanoparticles that can deliver biological information between cells.* Adv Drug Deliv Rev, 2013. **65**(3): p. 342-7.

188. van den Boorn, J.G., et al., *SiRNA delivery with exosome nanoparticles.* Nat Biotechnol, 2011. **29**(4): p. 325-6.

189. Sterzenbach, U., et al., *Engineered Exosomes as Vehicles for Biologically Active Proteins.* Mol Ther, 2017. **25**(6): p. 1269-1278.